THE UNIVERSITY OF MANITOBA

CRACKING BEHAVIOR OF REINFORCED CONCRETE MEMBERS SUBJECTED TO TENSILE MEMBRANE FORCES

by

M. EL-SHAHAWI

A THESIS

SUBMITTED TO THE FACULTY OF GRADUATE STUDIES

IN PARTIAL FULFILLMENT OF THE REQUIREMENTS FOR THE DEGREE

OF MASTER OF SCIENCE

DEPARTMENT OF CIVIL ENGINEERING

WINNIPEG, MANITOBA, CANADA

OCTOBER 1981

CRACKING BEHAVIOR OF REINFORCED CONCRETE MEMBERS SUBJECTED TO TENSILE MEMBRANE FORCES

BY

M. EL-SHAHAWI

A thesis submitted to the Faculty of Graduate Studies of
the University of Manitoba in partial fulfillment of the requirements
of the degree of

MASTER OF SCIENCE

ABSTRACT

In order to gain a better understanding of the cracking behavior in containment vessels, eighteen concrete wall segments reinforced in two directions with deformed bars was loaded in tension. The segments varied in amount of concrete cover, bar diameter, reinforcement ratio, and thickness. As loading progressed, strains, crack widths, and crack spacings were measured.

It was observed that the mechanism of through-cracking was dependent upon the width of the member. For smaller widths, through cracks tended to form from a single surface crack. For larger widths, several surface cracks would join to form a single through-crack.

The observed values of the final crack-spacing have been compared with the values based on equations presented by other researchers. Based on this comparison a simplified and refined technique to estimate the crack spacing and crack width is presented.

ACKNOWLEDGEMENTS

The author wishes to gratefully acknowledge and thank Dr. Sami Rizkalla for initiating this investigation and for providing much-needed guidance and support throughout.

Much appreciation is given to Messrs. Ed. Lemke, Brian Turnbull, Moray McVey, John Clark, and Dick Wiebe, whose continual assistance made possible the completion of the testing programme. Also, the author wishes to thank Professor J. Glanville and Professor N. Bassim, for the help and guidance during the revision of this work. Financial assistance for this investigation provided by the National Science and Engineering Research Council is gratefully acknowledged. Finally, I wish to thank Mrs. Valerie Ring for typing the original manuscript.

TABLE OF CONTENTS

CHAPTER PAGE

LIST OF TABLES

LIST OF FIGURES

NUMBER		PAGE

NOTATION AND TERMINOLOGY

a - bar spacing

A_c - average area of concrete having a centroid identical to that of the steel reinforcement divided by the number of bars

A_s - cross-sectional area of reinforcing bars

C - minimun concrete cover to the surface of the steel bar (measured perpendicular to the surface)

C_1 - empirical constant

d_b - diameter of the steel bar

E_c - modulus of elasticity of concrete

E_s - modulus of elasticity of steel

f_t - induced tensile stress in concrete

f'_t - tensile strength of concrete

f_{s1} - stress in reinforcement prior to cracking

$f_{s1,cr}$ - stress in reinforcement immediately prior to cracking

f_{s2} - stress in reinforcement at a crack

$f_{s2,cr}$ - stress in reinforcement at a crack immediately after cracking

f_{tx} - tensile stress in concrete at a distance x from the crack surface

f_{sx} - stress in reinforcement at a distance x from the crack surface

f_{sp} - split tensile strength of the concrete

f_{cx} - the concrete compression stress at any point x

f_{tc} - maximum tensile stress in the concrete

ℓ_o - "almost lost bond" length of bar at a given crack

ℓ_t - transfer length

ℓ_{m1} - proposed "almost lost bond" length of bar at a crack based on Beeby's expression

ℓ_{m2} - proposed "almost lost bond" length of bar at a crack based on Leonhardt's expression

L - total length over which strain and crack width measurements were made

$K_1, K_2, K_3 \ldots K_8$ - empirical constants

N - number of through-the-wall cracks at a given load

n - modular ratio - E_s/E_c

P - axial load

P_{cr} - cracking load

P_s - axial load at the stabilized crack pattern

S - spacing of cracks at any stage

S_m - average crack spacing

S_b - average crack spacing based on Beeby's Equation

S_L - average crack spacing based on Leonhardt's Equation

S_{exp} - average crack spacing based on test results

S_{bm} - modified average crack spacing based on Beeby's Equation

S_{Lm} - modified crack spacing based on Leonhardt's Equation

t - concrete thickness

W_m - average crack width

W_{mb} - average crack width based on Beeby's Equation

W_{mL} - average crack width based on Leonhardt's Equation

W_s - maximum crack width

$\Delta f_{s\ max}$ - maximum reduction in steel stress between two cracks

ΔL_s - total elongation of steel between two cracks

ΔL_c - total elongation of concrete between two cracks

ε_{cm} - average strain in the concrete

ε_{cr} - strain just before cracking

ε_{cx} - concrete strain at point x

ε_m - average gross strain measured over a gauge length which includes several cracks

ε_{mb} - average gross strain based on Beeby's Equation

ε_{mL} - average gross strain based on Leonhardt's Equation

ε_{s2} - steel strain at a crack

ε_{sx} - steel strain at point x

p - reinforcement ratio, A_s/A_c

μ - concrete bond strength

μ_{max} - maximum bond stress

μ_x - concrete bond stress at a distance x from the crack surface

CHAPTER 1

INTRODUCTION

1.1 General Introduction

There are many instances where reinforced concrete components of structures are subjected to membrane tensile forces, such as walls of liquid tanks, walls of nuclear reactor containment structures, and silos.

In general, reinforced concrete belongs to the type of structures which are assumed to be cracked under service conditions. This assumption is due to the fact that plain concrete has a comparatively small fracture strain in tension and therefore will crack at low stresses, which in turn will affect the general response and usefulness of the structure.

There are many research reports on crack behavior in reinforced concrete members. However, most of the experimental work has tended to concentrate on the behavior of members reinforced in one direction only. Very little work is available on crack behavior of members reinforced in two directions,which represent most of the construction details of any structure.

Internationally, there is remarkably little agreement on design methods for predicting crack width and spacing. If formulae from different national codes are compared, it is in many cases very difficult to discern any common ground between them. This lack of agreement goes beyond the form of the equation used to predict crack width and spacing and introduces the needs for further research.

In general, the cracking phenomenon is quite complex and depends upon, among other things, the loading state, the concrete strength, diameter of bars, the reinforcement ratio and the concrete cover. At the same time, most of the previous reports present tests on concrete segments reinforced in two directions and loaded in tension in one direction.

The tested segments in this study generally represent an element cut from any structure subjected to pure membrane tensile forces. Different design and construction details were considered to study the effect of the various parameters believed to affect the cracking behavior for such structures.

1.2 Objectives of this Report

The objectives of this investigation can be summarized as follows:

1) to review the development of the different theories dealing with formation and prediction of cracks in reinforced concrete members subjected to pure tension;

2) to determine experimentally the effects of different parameters which are felt to have a significant effect on crack patterns, such as member thickness, reinforcement ratio and concrete cover;

3) to study the cracking behavior of reinforced concrete member subjected to pure tension in the presence of transverse reinforcement.

4) to compare the experimental data with those obtained by other researchers; and

5) to propose a simplified and refined technique to estimate the number and width of cracks.

1.3 Scope of Investigation

Eighteen concrete segments reinforced in two directions with deformed steel bars were tested. The segments were 5", 7" and 10" thick, and 30" long. All segments were subjected to uniaxial tensile load and loaded beyond the yield strain of the steel. The segments were designed to provide data on the effect of the concrete cover, member thickness, bar diameter and reinforcement steel ratio on the cracking behavior.

This report analyses the crack behavior of the segments and presents methods to predict the crack spacings and widths. Chapter 2 gives an overview of the published developments of all the theories dealing with cracks in reinforced concrete due to pure tension. Description, fabrication, material properties, and instrumentation of the segments are summarized in Chapter 3. The cracking data for the segment tests is presented in Chapter 4. Test results were compared with existing theories and a proposed simplified method for predicting crack widths and spacing are presented in Chapter 5. Conclusions, recommendations and required research work are presented in Chapter 6.

CHAPTER 2

LITERATURE REVIEW

2.1 Introduction

Many experimental and analytical research projects have been conducted to study the phenomenon of cracking in reinforced concrete members. Most of the results reported are highly variable and dependent on the testing conditions. So far there is no universal accepted theory or equation for the prediction of crack widths and spacing.

This chapter will review and discuss the different theories dealing with the initiation and progression of cracks in reinforced concrete members subjected to pure axial tensile forces.

2.2 Formation of Cracks

When a reinforced concrete member is subjected to an axial tension load, the concrete and steel can be assumed to act as an integral unit, provided that the induced stresses in the concrete are less than its tensile strength f'_t, Figure 2.1(a).

The tensile strength of the concrete varies along the length of the bar as shown by the top line in Figure 2.1(b).At points located some distance from the ends of the bar the concrete stress will be uniform at f_t as shown by the shaded area in Figure 2.1(b). The steel stress will be nf_t where n is the modular ratio, E_s/E_c. The first crack will occur when the tensile stress f_t reaches the tensile strength of the concrete in the weakest part of the bar. At the location of the crack, the entire load is resisted by the reinforcement crossing the crack. The stress distribution in the concrete will then be as shown in Figure 2.1(c). Within the transfer length ℓ_t the concrete stress will be less than f'_t.

Because the first crack occurred where the concrete was weakest, the load must be increased before another crack can form. This crack will form at the next point where the applied load stress, f_t, reaches the tensile strength f'_t. This point will not be closer than ℓ_t to the first crack as shown in Figure 2.1(c). Cracks will continue to form until the spacing between all cracks is less than or equal to $2\ell_t$. After this occurs, the tensile stress between the cracks will not reach f'_t [2,11,13].

As a result of this sequence of crack development, the final crack pattern will consist of cracks with average spacing, s_m, in the range

$$\ell_t \leq S_m \leq 2\ell_t \quad . \qquad \text{..............} \qquad (2.1)$$

This extreme variability in crack spacing leads to an equally extreme variability in crack widths.

Once the cracking has reached a final pattern (stabilized state) the average crack width, W_m, can be calculated as the product of the average crack spacing, S_m, multiplied by the average strain, ε_m, minus the average strain in the concrete at the level at which cracks are being measured, ε_{cm}, thus

$$W_m = S_m(\varepsilon_m - \varepsilon_{cm}) \quad . \qquad \text{..............} \qquad (2.2)$$

Since the strain in the concrete will tend to be small, it is frequently ignored, giving

$$W_m = S_m \, \varepsilon_m \quad . \qquad \text{..............} \qquad (2.3)$$

Immediately prior to cracking, the stress in the steel, $f_{s1,cr}$, can be computed from the transformed area as

$$f_{s1,cr} = \frac{P_{cr}}{A_s(1+\frac{1}{pn})} , \qquad \text{..............} \qquad (2.4)$$

where p is the reinforcement ratio, n is the modular ratio. The subscript 1 refers to the uncracked state.

The steel stress can be rewritten also as

$$f_{s1,cr} = E_s \varepsilon_{cr} , \qquad \text{..............} \qquad (2.5)$$

where ε_{cr} is the concrete strain immediately prior to cracking.

Once the crack has formed in a tension member, the entire load is carried by the reinforcement crossing the crack, giving a stress at the crack of

$$f_{s2} = \frac{P}{A_s} . \qquad \text{..............} \qquad (2.6)$$

The subscript 2 refers to cracked state. Thus immediately after cracking, the stress is

$$f_{s2,cr} = \frac{P_{cr}}{A_s} . \qquad \text{..............} \qquad (2.7)$$

A comparison of Equation (2.4) and (2.7) shows that the steel stress at a crack will increase suddenly and sharply when the crack forms as shown in Figure 2.2[11]. Thus the steel stress after cracking is $(1+\frac{1}{pn})$ times the stress before cracking. This jump in steel stress tends to destroy the bond between the concrete and the adjacent steel bar. For deformed bars, this loss or weakening of the bond will occur due to internal cracks extending into the concrete from each deformation lug as shown in Figure 2.3[9].

2.3 Crack Propagation

As the stresses in concrete increase beyond its tensile strength at any section, a discontinuity will be initiated near the reinforcement bar at this section. As a result of this discontinuity, the concrete stresses and strain will be altered, causing loss of bond between the reinforcing bars and the concrete. By increasing the magnitude of the applied load, the discontinuity will propagate to initiate a visible local crack. As the applied stresses continue to increase, these local cracks will propagate to form a crack through the concrete thickness.

After the formation of the first crack, the stresses around the crack edge will be lower than the concrete strength. Further crack growth could occur only when the applied load increases the concrete stresses to its tensile strength. This increase of stresses will initiate another discontinuity and form a new crack following the same path described before.

2.4 Cracking Mechanisms

The mechanism of cracking of axially loaded reinforced concrete members is suggested in many studies to depend on the bond between the concrete and steel [2,9,11,15]. Consider the axially loaded tension member in Figure 2.4. The first two cracks will form at random locations where the uniform applied stresses exceed the concrete strength. Slip occurs between the concrete and steel at the crack locations. At the cracks, the concrete is free from stress and the reinforcing alone carries the external loads. Tensile stress is present in the concrete between the cracks as shown in Figure 2.4(b). The magnitude and distribution of bond stress between the cracks determine the distribution of tensile stress in the steel and concrete between the cracks as shown in Figure 2.4(c).

The classical mechanism for cracking of reinforced concrete members is based on the assumption that the tensile stresses in concrete are uniform and the bond stresses exist along the reinforcement. The analysis of the limiting crack spacing and maximum crack width is based on the condition that the uniform tensile stress in the concrete does not again exceed the tensile strength.

The distance S between existing cracks shown in Figure 2.4 is assumed to be twice the limiting minimum crack spacing. At a distance x from the crack surface, f_{tx} represents the tensile stress in the concrete due to the force that has been transmitted by the bond stresses.

$$f_{tx} = \frac{\pi d_b}{A_c} \int_0^x \mu_x \, dx \quad , \qquad \ldots\ldots\ldots\ldots\ldots \quad (2.8)$$

where A_c is the concrete area, and μ_x is the bond stress at a distance x from the crack, and d_b is the diameter of the steel bar.

The steel stress f_{sx} at the same section in terms of the applied force P can be expressed as

$$f_{sx} = \frac{P}{A_s} - f_{tx} \quad , \qquad \ldots\ldots\ldots\ldots\ldots \quad (2.9)$$

where A_s is the reinforcement steel area.

The tensile stress in the concrete will reach its maximum value at x = S/2 at which a new crack will be formed. At this location the bond stress is almost zero for a considerable portion of the member located between cracks and the tensile concrete stress is constant.

As cracking progresses, the spacing of the cracks becomes smaller, reaching its limiting value. The maximum stress in the unbroken portion of the concrete as the minimum spacing approaches its tensile strength f'_t which could be obtained from Equation (2.8) by substituting for x = S/2,

$$f_t = \frac{\pi d_b}{A_c} \int_o^{S/2} \mu_x \, d_x \; . \qquad \ldots\ldots\ldots\ldots\ldots \quad (2.10)$$

Many assumptions have been made concerning the distribution of bond stress by various investigators [11]. If the bond stress at any distance x from a crack is assumed to be a function of the maximum bond stress μ and of $\phi = x/S$, then a general solution may be found for Equation (2.10) as follows:

$$\mu_x = \mu f(x/S) = \mu f(\phi)$$

then

$$\int_o^{S/2} \mu_x \, dx = \mu S \int_o^{1/2} f(\phi) d\phi = \mu S K_b \; . \qquad \ldots\ldots\ldots\ldots \quad (2.11)$$

By substituting Equation (2.11) into (2.10) and solving for the length S, one can obtain:

$$S = \frac{\pi A_c \, d_b \, f'_t}{K_b \mu} \; . \qquad \ldots\ldots\ldots\ldots\ldots \quad (2.12)$$

where K_b is function of the surface characteristics of the reinforcement steel. The values of K_b is 0.5 for smooth bars and 1.0 for deformed bars.

When the length S is just sufficient to form a new crack, the minimum spacing S/2 is obtained. Any distance less than S is not sufficient to form a new crack, thus the observed limiting crack spacing will range from S/2 to S.

2.4.1 Bond Slip Theories

One of the earliest approaches for cracking phenomena in reinforced concrete members was conducted by Saligar (1936). He assumed that the width and spacing of cracks are principally controlled by the bond failure between the concrete and the reinforcement steel.

Saligar [15] assumed that the force P, transferred by bond in a given length ℓ_t is:

$$P = K_1 \mu_{max} (\pi d_b) \ell_t \ , \qquad \ldots\ldots\ldots\ldots\ldots \quad (2.13)$$

where the average bond stress is expressed as a constant K_1 times the maximum bond stress μ_{max}. The surface area over which this acts is the perimeter πd_b times the transfer length. The transfer length ℓ_t is the length required to raise the concrete stress to the tensile strength f'_t. Thus

$$P = A_c \ f'_t$$

and

$$A_c \ f'_t = K_1 \mu_{max} (\pi d_b) \ell_t \ . \qquad \ldots\ldots\ldots\ldots\ldots \quad (2.14)$$

Substituting the reinforcement ratio $p = \dfrac{\pi d_b^2/4}{A_c}$ and replacing $1/4K_1$ with K_2 gives

$$\ell_t = K_2 \frac{d_b}{p} \frac{f'_t}{\mu_{max}} \ . \qquad \ldots\ldots\ldots\ldots\ldots \quad (2.15)$$

If it is assumed that μ_{max} is related to f'_t , since bond failure involves splitting of the concrete,

$$\ell_t = K_3 \frac{d_b}{p} \ . \qquad \ldots\ldots\ldots\ldots \quad (2.16)$$

Thus the average crack spacing S_m can be expressed

$$S_m = K_4 \frac{d_b}{p} \ , \qquad \ldots\ldots\ldots\ldots \quad (2.17)$$

where K_4 is obtained experimentally. This calculation assumes that plane sections remain plane in the concrete, during and after loading.

The total change in length from halfway between two cracks to halfway between the next two cracks is equal to the elongation of the steel ΔL_s

$$\Delta L_s = \int_0^S \varepsilon_{sx}\, dx \; , \qquad \text{.............. (2.18)}$$

where ε_{sx} = the steel strain at any point x

$= f_{sx}/E_s$.

This change in length is partially accounted for by the crack width W and partially by the elongation of the concrete ΔL_c

$$\Delta L_c = \int_0^S \varepsilon_{cx}\, dx \; . \qquad \text{.............. (2.19)}$$

where ε_{cx} = the concrete strain at any point

$= f_{cx}/E_c$.

Thus,

$$W = \Delta L_s - \Delta L_c$$

or

$$W = \int_0^S (\varepsilon_{sx} - \varepsilon_{cx})\, dx \; . \qquad \text{.............. (2.20)}$$

From Figure 2.4, equilibrium requires that:

$$\Delta f_s\, A_s = f_{tc}\, A_c$$

or

$$f_{tc} = \Delta f_s \cdot p \; . \qquad \text{.............. (2.21)}$$

where f_{tc} is the maximum tensile stress in the concrete, thus the concrete elongation ΔL_c can be expressed as:

$$\Delta L_c = \frac{f_{tc}}{E_c} \cdot S \cdot C_1 \; , \qquad \text{.............. (2.22)}$$

where C_1 is a constant relating the area of the concrete stress diagram in Figure 2.4.

$$C_1 = 2/3 \text{ for parabolic diagram}$$

$$= 1/2 \text{ for triangular diagram}$$

Similarly

$$\Delta L_s = \frac{f_{s2} \cdot S}{E_s} - \frac{\Delta f_s \cdot S \cdot C_1}{E_s} , \quad \ldots\ldots\ldots\ldots\ldots \quad (2.23)$$

and the crack width is:

$$W = \frac{f_{s2} \cdot S}{E_s} - \frac{\Delta f_s \cdot S \cdot C_1}{E_s} - \frac{p \cdot \Delta f_s \cdot S \cdot C_1 \cdot n}{E_s}$$

or

$$W = \frac{S}{E_s}[f_{s2} - \Delta f_s \; C_1(1 + pn)] \; . \quad \ldots\ldots\ldots\ldots\ldots \quad (2.24)$$

The major unknowns here are Δf_s,S and C_1. Reis et al. [13] review a number of attempts to solve this expression.

2.4.2 Redistribution of Concrete Stress

Broms has proposed a cracking mechanism based on an elasticity analysis of concrete stresses [4,5].

When a tension member was subjected to axial tension force as shown in Figure 2.5(a), the crack spacing at the level of the reinforcement was observed to decrease rapidly with increasing applied load. After the axial stress in the reinforcement had reached a certain critical value, the spacing of the visible cracks remained approximately constant. The resulting minimum crack spacing can be predicted from the stress redistribution that takes place at the formation of tensile cracks. This redistribution can be calculated analytically by assuming that:

a) The concrete surrounding the reinforcement behaves as a reasonably elastic material;

b) The tensile force which is transferred gradually from the reinforcement to the concrete can be replaced by a line load.

High calculated values of the axial tensile stress will be present within an area located inside a circle between two adjacent pre-existing cracks. Outside this stress circle, very small tensile stresses will be present as illustrated in Figure 2.5(b). When the maximum tensile stress within any stress circle exceeds the tensile crack strength of the concrete, a new tensile crack develops. This tensile crack will spread laterally until the average tensile stress at the root of the crack decreases to a value smaller than the tensile strength of the concrete. For a member reinforced with a single reinforcing bar, the length of this new tensile crack will be governed by the diameter of the circle inscribed between two adjacent pre-existing cracks, and thus, by the crack spacing. If the diameter of the inscribed circle is equal to or larger than the total width of the member as shown in Figure 2.6(a), then the new crack will traverse the total section of the member. Such a crack is defined as a primary crack. If the diameter of the inscribed circle is less than the total width as shown in Figure 2.6(b), then the new crack (which forms halfway between two existing primary cracks) will extend over only part of the total member width. This crack is defined as a secondary crack. Therefore, as cracking proceeds, the length of subsequent cracks will decrease in proportion to the crack spacing as shown in Figure 2.6(c). The length of the new cracks which develop in a member reinforced with several bars will depend on the spacing of the individual bars and on the primary crack spacing. In the case when the primary crack spacing is larger than the spacing of the reinforcement, Figure 2.7(a), the individual stress circles corresponding to each reinforcing bar overlap, and as a result, the tensile cracks which develop at each individual bar join into a single crack which extends over part or all of the width of the member. The new tensile crack will extend to the unloaded vertical sides of the member (and will become a primary crack) if the stress circle corresponding to the bar is located closest to the side of the member, Figure 2.7 (b). This condition occurs when primary crack spacing is larger than twice the thickness of the side cover. When the primary crack spacing is less than twice the concrete cover, Figure 2.7(b). then the new tensile crack will not reach the surface of the member and will become a secondary crack. The preceding analysis suggests that the absolute minimum visible crack spacing will be equal to the distance from the surface to the center of the bar located closest to the surface of the member. Thus, it is suggested that the theoretical minimum crack spacing will be equal to the thickness of the concrete cover measured from the center of the reinforcing bar located closest to the considered face. Broms suggests that the crack spacing will vary between the theoretical minimum crack spacing and twice this value with average minimum spacing equal to 1½ time the concrete cover as defined above. Thus the average crack spacing S_m is given by

$$S_m = K_5 C \; . \qquad \text{...........} \qquad (2.25)$$

where K_5 ranges from 1 to 2 as given in Equation (2.1).

2.4.3 Localized Bond Failure

A very different theory of crack spacing was advanced by Y. Goto et al. [9]. Goto assumed no slip of the bars. Internal cracks will be formed behind the ribs of the deformable steel bars as shown in Figure 2.3

They concluded that the formation of these internal cracks is considerably influenced by the surface of the reinforcement bars. After the formation of these internal cracks, the axial tensile force on the concrete is carried by the uncracked shell of the concrete section. The small concrete teeth will resist the interlocking forces by flexural resistance. This resistance decreases with increasing the length of these small bond cracks. As one or two of the bar lugs lose their resisting strength, almost no bond length will extend equally each way from the crack as shown in Figure 2.3. This length is defined by Leonhardt as "almost lost bond" length [11].

2.4.4 Localized Bond Slip Theories

This theory represents realistically the actual behavior of cracks in reinforced concrete members. It combines most of the previously discussed theories. There is definitely some movement of the bar relative to the concrete, due to slip or the internal cracks. At the same time, it is also true that the bond will spread out roughly within a 45 degree cone and become uniform where this cone reaches the edges of the prism as was suggested by Broms [4] and shown in Figure 2.8.

Ferry-Borges [7] expressed the minimum crack spacing as the sum of Equations (2.17) and (2.25) with the appropriate constants:

$$S_m = K_4 C + K_5 \frac{d_b}{p} . \qquad \text{..............} \qquad (2.26)$$

Welch and Janjua [17] assumed the crack spacing was the sum of the unbonded length adjacent to the crack due to internal cracking, plus the transfer length, ℓ_t, which was taken equal to C. Allowing for variations in the spacing of the cracks, they expressed the crack minimum spacing for deformed bars as:

$$S_m = 1.5C + 5d_b \; . \qquad \ldots\ldots\ldots\ldots\ldots \qquad (2.27)$$

Leonhardt in 1976 [11] showed that when the concrete stress, due to the applied load, reaches the tensile strength the concrete starts to crack and the tensile force which was carried by the concrete must suddenly be taken over by the reinforcing bars, causing a jump of stresses in the steel, see Figure 2.2. The magnitude of this stress increase is given by:

$$\Delta f_s = \frac{f_t}{p} \; , \qquad \ldots\ldots\ldots\ldots\ldots \qquad (2.28)$$

where Δf_s, is the change in steel stress and p is the reinforcement ratio. If this sudden increase in steel stress is large enough, some bond-slip can occur and the crack formation is likely to be a combination of bond-slip and internal cracking.

Based on experimental results, Leonhardt assumes the length of the almost lost bond region ℓ_o as:

$$\begin{aligned} \ell_o &= \frac{f_{s2,cr}}{6500} d_b (f_{s2,cr} \text{ in psi}) \\ &= \frac{f_{s2,cr}}{45} d_b (f_{s2,cr} \text{ in N/mm}^2) \; , \end{aligned} \qquad \ldots\ldots\ldots\ldots \qquad (2.29)$$

where d_b is the diameter of the reinforcement and $f_{s2,cr}$ is the stress in the steel at the crack immediately after cracking. To account for the bond-slip, Figure 2.9 shows that the bond stress μ must have a peak close to the crack on both sides of the crack. The curve shape decreases following an e-function, to the point where the tensile strains of steel and concrete are equal again. This length of active bond stress is called the transfer length ℓ_t and is given by:

$$\ell_t = K_6(C,a) + 0.1 \left(\frac{d_b}{p}\right) \; , \qquad \ldots\ldots\ldots\ldots\ldots \qquad (2.30)$$

where $K_6(C,a)$ is representing spreading-out length considering cover (C) and bar spacing (a). It is the length in which stresses spread out from the crack. It may be assumed:

$$K_6(C,a) = 1.2\ C \text{ for } a \leq 2C$$

or

$$K_6(C,a) = 1.2\ (C + \frac{a-2C}{4}) \text{ for } a \leq 2C$$

with

$$a < 14d_b\ .$$

By increasing the load new cracks will be initiated up to a certain load stage at which the number of cracks does not increase. This is the so-called stabilized crack pattern with some cracks having the minimum possible value for the average crack spacing, S_m, which is given by:

$$S_m = \frac{1}{2}\ \ell_o + \ell_t\ , \qquad \ldots\ldots\ldots\ldots\ldots \qquad (2.31)$$

and the average crack width W_m is given by:

$$W_m = \ell_o\ \varepsilon_{s2} + \ell_t\ \varepsilon_m\ , \qquad \ldots\ldots\ldots\ldots\ldots \qquad (2.32)$$

where ε_{s2} is the steel strain due to f_{s2} in the cracked section, ε_m is the average gross strain, measured over the cracks regarding concrete contribution within the transfer length, which can be found by tests only.

Similarly, Beeby suggests a value for the minimum crack spacing given by:

$$S_m = 1.33\ C + 0.08\ \frac{d_b}{p}\ . \qquad \ldots\ldots\ldots\ldots\ldots \qquad (2.33)$$

Beeby [2,3] showed that the mechanism of internal failure in the cases of two specimens reinforced with plain and deformed bars are different, being primarily slip where plain bars are used and primarily internal cracking where deformed bars are used. This difference in behavior makes little effect to the crack widths in general. However, it seems likely that there is some minimum effective steel percentage below which plain bars will lead to much larger cracks. Studies by Base [1] and others indicate that the type of reinforcement used did not significantly affect the measured crack spacing; for plain bars the value of S_m will be about 20 percent larger than those for deformed bars, with correspondingly larger crack widths.

The crack widths based on the bond slip theories differ primarily in the way in which ε_m are defined.

Welch and Janjua [17] proposed an equation for computing the mean strains given by:

$$\varepsilon_m = \frac{f_{s2} - 3 \text{ ksi}}{E_s} \quad \ldots\ldots\ldots\ldots\ldots \quad (2.34)$$

The term 3 ksi is approximately equal to $\frac{nf'_t}{2}$ and is approximately the average stress in the concrete stress diagram in Figure 2.4.

For a member loaded in axial tension Beeby [1] predicted the average crack width with S_m given by Equation (2.33) and a term for ε_m given as:

$$\varepsilon_m = \varepsilon_{s2} - K_7 \frac{f'_t \, f_{s2,cr}}{E_s \, f_{s2} \, p} \quad \ldots\ldots\ldots\ldots\ldots \quad (2.35)$$

And

$$W_m = S_m \, \varepsilon_m \quad \ldots\ldots\ldots\ldots\ldots \quad (2.36)$$

Leonhardt [11] has presented a detailed procedure for computing the mean strains. Figure 2.9 is a load deformation diagram for an axially loaded reinforced concrete prism. The steel alone would develop strains ε_{m2} corresponding to the dashed line. The average gross strain over the entire length is ε_m. The difference between ε_m and ε_{s2} is referred to as concrete tension "stiffening". If the cracking strain of the concrete ε_{cr} is ignored as being very small, ε_m can be approximated by:

$$\varepsilon_m = \varepsilon_{s2} \, [1 - (\frac{f_{s2,cr}}{f_{s2}})^2] \; . \qquad \ldots\ldots\ldots\ldots\ldots \qquad (2.37)$$

2.4.5 Empirical Relationships

The following are some other research projects which were conducted to study the behavior of cracks in reinforced concrete members.

2.4.5.1 Kaar and Mattock [10]

The study indicated that the bar spacing and concrete area around the reinforcement steel represents two major variables in cracking behavior in reinforced concrete members. They proposed two empirical formulae for the maximum crack width W_s at the level of reinforcement as follows:

$$W_s = 0.067 \, \sqrt{A_c} \, f_{s2} \qquad \ldots\ldots\ldots\ldots\ldots \qquad (2.38)$$

$$W_s = 0.115 \, \sqrt[4]{A_c} \, f_{s2} \qquad \ldots\ldots\ldots\ldots\ldots \qquad (2.39)$$

where A_c is the average area of concrete having a centroid identical to that of the steel reinforcement divided by the number of bars.

2.4.5.2 Gergely and Lutz [8]

Gergely and Lutz statistically studied all available beam test results and concluded:

a) Steel stress was the most important variable;

b) Other important variables are the effective area around the bar, A_c, and the side or bottom cover, C;

c) The bar diameter d_b was not a major variable.

Based on their statistical analysis, they proposed:

W_s (at level of steel)

$$= 0.091 \sqrt[3]{(C + \frac{d_b}{2})\, A_c}\, (f_{s2} - 5 \text{ ksi}) \times 10^{-3} \text{in.} \quad \ldots\ldots\ldots \quad (2.40)$$

2.4.5.3 Studies by Base [1]

Early studies by Base in England concluded:

a) Different types of reinforcement did not show much difference among the measured crack widths; those having plain bars showed about 20 percent wider average crack widths than those reinforced with deformed bars. This difference was smaller than the ratio of the bond strengths of plain and deformed bars.

b) Other variables being constant, changes in bar diameter did not show any effect on cracking.

c) Spacing and widths of cracks were found to be directly proportional to the distance of the surface to the nearest longitudinal bar.

d) Crack width was also proportional to the measured surface strain at the level where the cracks were measured.

Thus the suggested relation was:

$$W_m = K_8 \; C \; \varepsilon_m \quad \ldots\ldots\ldots\ldots\ldots \quad (2.41)$$

where W_m = the average crack width, ε_m = the gross surface strain at the level where crack width is required, C = the distance of the point where crack width is measured to the surface of the nearest longitudinal bar, and K_8 is a constant. For deformed bars, K_8 = 1.67 for average crack width.

2.5 Effect of Transverse Reinforcement on Crack Behavior

Most of the experimental programs to date have used specimens reinforced in one direction only. In practice, however, most concrete structures are reinforced in at least two directions. A number of investigators have observed a strong correlation between the spacing of reinforcement parallel to the cracks and the spacing of the cracks themselves.

Beeby concluded that transverse bars such as stirrups in beams have some influence on crack spacing, but that this influence is only effective where the stirrup spacing and the expected crack spacing are similar.

Nawy [12] has shown a strong relationship between crack spacing and the spacing of perpendicular bars.

Preliminary results from tests recently conducted (not yet published) at the Cement and Concrete Association on large elements subjected to pure tension, indicate that there is a tendency for cracks to form in the vicinity of the transverse bars. However, the actual number of major cracks, and hence their width, has been largely unaffected by them.

Recently, the results obtained by Dr. Regan at the Polytechnic of central London on concrete gravity platforms shows that the transverse steel had a dominant influence on the distribution and size of the cracks.

It is very clear that there are cases where the transverse steel can dominate the phenomenon of cracks in reinforced concrete; however, to pin down the exact conditions under which this occurs, further research is required. Research to this end is currently in progress at the University of Manitoba.

CHAPTER 3

EXPERIMENTAL PROGRAM

3.1 Introduction

The purpose of the segment tests was to obtain data on load-deformation response, crack initiation, and propagation that is representative of that which could occur in concrete structures reinforced in two directions, and subjected to axial tensile stresses.

The segments were reinforced in two directions and subjected to axial tensile forces in one direction. The load transfer to the segments was accomplished by pulling on the reinforcing bars which were extended beyond the edges of the segments.

One of the main objectives of this study is to develop analytical techniques which would permit the prediction of crack response of a reinforced concrete structure subjected to pure tensile stresses. Various parameters were considered in the test program to permit general evaluation of the analytical technique.

In most of the existing theory for predicting the crack width and crack spacing in reinforced concrete, the major parameters are the concrete cover over the reinforcing bars, bar diameters and the bar spacing. To ascertain the effects of these quantities, the bar size and spacing and concrete thickness, as well as concrete cover, were varied. The percentage of reinforcement used in the segments was chosen so that a full crack pattern can be developed before yielding of the reinforcement transmitting the load to the concrete.

3.2 Major Variables in the Test Program

A total of 18 reinforced concrete segments are included in this test program. All specimens were reinforced in two directions with deformed bars. Transverse reinforcement was provided by M10 bars spaced at at 3" centre to centre on both faces. Longitudinal reinforcement was spaced at 3" centre to centre and extended 11" beyond each end of the specimen as shown in Figure 3.1.

The summary of the major variables for each segment is given in Table (3.1). These parameters were varied as follows:

Concrete cover:	- 1/2" and 3/4"
Bar diameter:	- 0.375" (#3 bar) to 0.75" (#6 bar)
Reinforcement ratio:	- 0.0145 to 0.0295
Specimen width:	- 5" to 10"

In Table (3.1) each specimen was labelled as follows:

The first letter referred to the nature of the applied forces. In this testing program, all segments were subjected to axial tension loads and the letter "T" was used. The middle mark number referred to the width and reinforcement ratio of the specimen. Finally, the last letter referred to the concrete cover thickness. The letter "A" represented 1/2" of concrete cover, while "B" represented 3/4".

3.3 Fabrication of Test Specimens

Wooden forms were used to fabricate all the test segments. Because of the uniqueness of the specimen configuration, it was required to modify the formwork for each segment. The initial design of the formwork is shown in Figure 3.2. This form was used to cast specimens T1A and T1B. The plywood form was constructed to fit around segment edges. Eight circular holes were drilled in the form at the specimen's short ends to allow the longitudinal reinforcement to extend outside the formwork. Prior to concreting, two coats of water resistant sealant and varnish were applied to prevent swelling and permit re-use of the forms. In describing the segments in this report, the word "face" refers to the 30" x 12" surfaces. The word "edge" refers to surface through which the reinforcement extends. After casting the first two specimens, the forms were reoriented to sit on edge, rather than on a face, Figure 3.3, to obtain two parallel smooth faces. To simplify removal of the forms, inner surfaces were coated with form oil before casting. C-clamps were used to prevent bowing of the sides due to the lateral pressures exerted by the freshly-poured concrete.

To achieve the proper alignment of the reinforcement protruded beyond the formwork, rubber stoppers were used to seal the end holes, (see Figure 3.4).These rubber stoppers prevented leakage during casting and simplified the disassembly of the form. To drill the rubber stoppers to the right bar diameters, they were cooled to a temperature of 200°F in an alcohol solution.

Since the load-deformation response of concrete in tension is one of the objectives in this study, the steel strain was also measured using mechanical strain gauges. Prior to casting, 1/4" diameter plugs were welded to the reinforcing bars. These plugs were just long enough to reach the surface of the forms and were enclosed in a rubber tube with 1/2" outside diameter. After the concrete had hardened this tube was removed leaving a 1/8" gap around the plug so that if the reinforcement moved relative to the concrete during testing, the plug would not bear on the concrete. Stainless steel Demic locating discs were mounted on the ends of the plugs.

Prior to concreting, the longitudinal and transverse reinforcements were tied together and mounted in the form, Figure 3.2.

Two types of vibration were used during casting of the specimens. The larger vibrators were used between the two layers of reinforcement, while the smaller vibrator was used between the rebars and the formwork. In addition, the sides of the forms were pounded with a plastic mallet to remove air voids along the form walls. Upon completion of vibration, the concrete in the forms was trowelled smooth.

After casting, the specimens were left to dry in open air for about one hour, then placed in a curing room for 7 days. Following this 7-day curing time, the specimens were removed from the curing room and covered with wet burlap and remained in the "air-dry" stage an additional 21 days before testing.

3.4 Material Properties

3.4.1 Concrete

3.4.1.1 Concrete Mix Data

All concrete used in the wall segment tests had a nominal design strength of 6000 psi and was mixed in the laboratory. The volume of each batch was 3.0 cu. ft., which is the capacity of the mixer, and contained the following quantities:

Water	- 35 lbs.
Cement (type 1 Porland Cement)	- 70 lbs.

Sand	-	141 lbs.
3/8" gravel	-	186 lbs.
Water cement ratio by weight	-	0.50

Only one batch was required to cast a segment and the accompanying test cylinders. The water/cement ratio had originally been set at 0.54 for specimens T1A and T1B. However, 8" slump was observed. Thus, the water/cement ratio was reduced to 0.5 for the remaining specimens.

3.4.1.2 Concrete Compressive and Tensile Strength

With each segment, six standard 6" x 12" cylinders were cast to determine concrete strength. These cylinders were cured in the laboratory in the same manner as the segments and were loaded at the same time as the corresponding segment was tested. Three of these cylinders were tested in compression and the remaining three were used in split cylinder tensile tests. The results of these tests are summarized in Table (3.2). Since the compressive cylinder tests were performed at time of the segment test and were cured with the segment, the values of compressive strength, f'_c are not so much a measure of the potential of the concrete mix, but rather of the compressive strength of the concrete in the segment at the time of testing.

3.4.2 Reinforcing Steel

The reinforcement used in the segment tests consisted of hot rolled deformed bars conforming to CSA G30.12-72. All bars of the same size come from the same heat at the time of rolling. For each specimen, reinforcement for each side was cut from a single length of rebar. The remainder from each length was tested in tension to determine yield stress, ultimate stress, and modulus of elasticity. The samples were tested in a

60,000 lb. Baldwin universal testing machine. All specimens showed the typical ductile behavior and well defined yield point. The results of these tests are summarized in Table (3.3).

Several tests were performed on one set of reinforcement to determine whether the 1/4" studs welded to the rebar had any effect on the tensile strength. The effect, if any, was negligible.

3.5 Testing Apparatus and Procedure:

3.5.1 Loading Apparatus

During testing of the segments, the loads were applied using a 600,000 lb. capacity universal testing machine. Load was transmitted between the rams and the specimen using specially designed end fittings as shown in Figure 3.5. A closeup view of the end fitting is given in Figure 3.6. Load was transmitted to each reinforcing bar by a threaded bar welded to the rebar and screwed onto the load cells attached to the end fitting. The end fitting was very rigid to achieve uniformity of loads from the machine to each load cell. It was constructed out of four one-inch steel plates, as shown in Figure 3.6. Heavy steel plates were used as brackets to support the load cells. The brackets were also provided with a set of adjusting bolts to align the specimen in the testing machine, (see Figure 3.6). The load cell was built by attaching four electric resistance strain gauges to a high strength bolt. The bolt head was machined to support a threaded socket, as shown in Figure 3.7. Each reinforcing bar extending from the two sides of the segment was welded to a threaded bar which was threaded to the load cell socket. After testing, the segment was removed by sawing approximately 1/4" off the threaded bar. The hole in each threaded bar was re-drilled to match the larger-sized reinforcing bars for the other specimens.

The load cell socket was used to adjust the load transferred to each reinforcing bar to provide uniformity of forces applied to the segment. The load cell bolt nut was also machined to act as a universal joint and provide proper seating.

3.5.2 Testing Procedure

A typical test for one segment took approximately three days to set up in the loading apparatus, one day to perform actual tests and half a day to dismantle. Set-up included aligning the segment in the machine, attaching instrumentation and connecting and adjusting the reinforcing bars to loading devices.

The protruding ends of each reinforcing bar were welded to a threaded end bar which later could be threaded to the individual load cell. The specimen was lifted into place with the aid of a pivoting clamp mounted in a hydraulic jack. Once the specimen was in position, the top and then the bottom load cells were screwed onto the threaded ends. The bottom cells remained loose so that the specimen was essentially suspended from the top. At this time, two plumb bobs were hung from the sides of each specimen. The adjustable bolts in the end fitting were used to provide proper alignment of the specimen and match the centre-line of the specimen with the plumb bob.

An initial load of 1000 lbs. was used to provide proper seating of the load cells. The load was then increased by increments of 1600 lbs. which is equivalent to 200 lbs. in each reinforcing bar. The uniformity of loads in each reinforcing bar was achieved by tightening and loosening the socket of the load cells. The procedure was repeated until the loads were within 10 percent of the initial theoretical distribution of the load, in each bar.

Frequently the specimen was mounted, aligned, and balanced the day before the actual testing. If this was the case, some final adjustment was usually required just prior to testing.

After balancing of the loads, testing of the specimen started by applying an initial load of 3000 lbs. to insure proper seating of the segment. This load was considered the "zero" load condition for the test. The test began by obtaining initial readings of all load, strain, and deformation gauges. The load was then applied in increments of 5000 lbs. which was deemed to be appropriate to produce sufficient data. A complete test generally took from eight to ten hours with each load level requiring from thirty to forty minutes. The majority of this time was spent marking cracks and measuring their widths, in addition to reading the mechanical strain gauges.

At each load increment, the load was held constant while the mechanical strain gauges were taken and recorded. The loads in each rebar were recorded by the data acquisition system. When the first crack appeared, an additional set of load and strain readings were taken. As well, crack widths were measured using a microscope, both along the centre-line of the specimen and directly above one of the middle rebars. Width of all subsequent cracks were measured for each increment. The crack patterns were marked and numbered at the end of each increment, so that the cracking sequence could be photographed for future reference. Testing was terminated when the load approached the predicted ultimate point,in order to avoid damage to the instrumentation. The specimen was then unloaded and the final crack pattern was noted.

3.6 Instrumentation and Data Processing

3.6.1 Introduction

For each segment, approximately sixty measurements were recorded at each load level. These measurements were of such quantities as loads, strains, elongations and crack widths. The loads and LVDT (linear variable differential transformer) readings were taken electronically using the data acquisition system in the laboratory. The other readings, such as mechanical strain gauges and crack widths, were read and recorded manually, but immediately following a test these readings were input to computer files for reduction and processing. This section contains a description of the measuring devices and their locations, along with a brief discussion of preliminary reduction of the data.

3.6.2 Data Acquisition System

The data logging equipment in the laboratory provides excitation to the electric resistance strain gauges and LVDT's, and converts the outputs to voltage readings in digital format. These data logging devices were monitored by means of a Hewlett-Packard D.A.S. 9825 data acquisition unit. This unit has a central processor core the size of 14 K words and has been expanded recently to 64 K words.

In general, the system will take the reading from each channel, convert it to digital signal and record the result on a magnetic cassette tape cartridge for future use.

3.6.3 Measurement of Applied Loads

The vertical load applied to the segment by the Baldwin machine was measured by differential pressure transducers contained in the machine.

The load cells were used to measure the forces in each of the reinforcing bars. Following each test the forces applied to the segment as measured by the Baldwin machine was compared to those obtained by summing up the forces in the reinforcing bars. In every case, the two measurements agreed to within 2 percent.

3.6.4 Measurement of Strains

Values of strain were obtained using both LVDT's and hand-held mechanical gauges. The location of the LVDT's and the Demic points for the mechanical strain gauges are given in Figure 3.8. The LVDT readings were read and stored using the Hewlett-Packard data acquisition system. Readings from the mechanical gauges are the change in length between two targets.

Concrete strains were obtained using special machined stainless steel discs glued to the concrete surface at 8" spacings. The steel strain were obtained by gluing the same discs on the end of the plugs as described in (3.3). The mechanical gauge was manufactured by W.K. Mays & Sons, United Kingdom, Model No. 1255, and has a dial sensitive to 0.0001 in. For the remainder of this report, values of strain obtained with the mechanical extensometer are referred to as Demic readings. Since the distance between Demic points was initially 8 inches, the strain for a particular reading was obtained by dividing the change in length as measured by the dial gauge, ΔL, by this length.

To obtain a representative strain in the concrete from the Demic readings for load greater than that required to cause cracking, it is necessary to use the average value, instead of the individual ones.

3.6.5 Crack Measurements

Two lines were marked on the segment surface to measure the cracks. One line was located directly over a reinforcing bar and the other midway between two adjacent bars. The width of all cracks crossing these lines was measured using a 50-power microscope. The eyepiece of the microscope contained a reticule with 0.02 mm divisions. The microscope was mounted on a frame attached to the lower crosshead of the testing machine, (see Figure 3.9). The microscope frame was equipped with two variable electric drill motors which could rapidly move the microscope horizontally and vertically. Hand cranks were used for the finer adjustments.

In all cases, initial cracking occurred during the application of a load increment. The presence of cracks following a given load increment was determined by examining the surface using an illuminated 5-power magnifying glass.

CHAPTER 4

TEST RESULTS

4.1 Organization of Presentation of Results

This chapter summarizes the observation and test results for each of the 18 segments considered in this report.

A summary of the major variables for each segment is given in Table (3.1). Tabulations and plots of measured loads, strains and crack width for all the other specimens are given in Appendix A, which is printed as Vol. II of this report.

To illustrate the use of Appendix A, it is proposed to use segment T3A in this chapter as an example for the typical test data obtained for all other segments presented in Appendix A. Thus, the test data for segment T3A will be examined in detail in Section 4.3. The plots showing the relationships between load, strains obtained using mechanical gauges, LVDT's and crack width are given in Appendix B, which is printed as Vol. III. The code numbering of the tables in Appendix A will follow the same code numbering presented for segment T3A. The code number of each table consists of five digits, the first three digits corresponding to the number of the segment and the last two digits to the table number. For example, T3A.T1 is the first table for segment T3A. This system is extended to the numbering of the figures in Appendix B by replacing the fourth digit, T, with P, which refers to the plot number. All strains reported are average strains based on readings taken in the middle 24" portion of the specimen. The reasons for this and the methods of averaging are presented in Section 4.2. The development of cracks during testing was generally observed between increments of applied loading and recorded on a separate sheet for each specimen. Also, photographs were taken for each load increment for further comparison.

During testing, an initial preload equal to 5% of the predicted yield load was applied to facilitate alignment of the system and then further loading was applied. The loads reported in this chapter and in the various figures and tables include this preload.

4.2 Crack Spacing and Crack Width Measurement

4.2.1 Method and Location of Measurement

To remove effects of the load transfer zone from the strain data, average strains were computed for the centre 24" region of face A of each specimen. The location of the cracks crossing the two vertical lines on face A were plotted. The cracks were numbered to show the sequence of formation. The technique used in reducing the crack width and crack spacing data is illustrated below using Figure 4.1 as an example.

Strain measurements were made in the 24" region between Demic points. The crack width and spacing reported are referred to this space.

For cracks near the end of the measuring zone, such as crack (7) in Figure 4.1, only a portion of the crack width was assumed to result from strains in the measuring zone. It was assumed that strains occurring in the zone extending from halfway between cracks (7) and (8) to halfway between cracks (7) and (5) would contribute to the width of crack (7). This total width is x inches of which x_1 inches falls within the length over which strain was measured. Therefore, in computing the total width of cracks related to strain in the 24" measuring zones, (x_1/x) times the width of crack (7) was included. Thus, the total width of cracks related to strains was calculated by adding the width of

$$\frac{x_1}{x} W7 + W2 + W3 + W1 + W5 + W6 + \frac{y_1}{y} W4$$

i.e. Total crack width $= \sum_{i=1}^{7} W_i$.

The resulting width will be referred to as the "total crack width" or ΣW.

The term $\Sigma W/L$, where L was the total length considered in computing ΣW (in this case, 24"), is referred to as the "average crack strain" The number of cracks, N, in the measuring zone, in this case, is:

$$N = \frac{x_1}{x} + 5 + \frac{y_1}{y}$$

This number will be referred to as the "total number of cracks". The "average spacing" is computed as L/N. Finally, the average crack width is $\Sigma W/N$.

4.3 Specimen T3A

The summary of the major variables for this specimen is given in Table 3.1. In describing the specimen in this chapter, "face A" refers to the 30" x 12" surface where the microscope was mounted. The word "edge" refers to the surface through which the reinforcement extends.

Two lines were drawn along the centreline of the specimen and directly above one of the middle rebars on face A. Widths of all subsequent cracks were measured along these two lines. During testing, a Hewlett-Packard D.A.S. was used to record the total applied load, the loads in individual load cells, and the gross strain measured by the L.V.D.T.'s. Data were stored during testing on cassette tape cartridges and retrieved later in tabulated form.

After mounting the test specimen, a nominal load of 1,000 lbs. was applied. The load level was then increased by 1,600 lbs., corresponding ideally to 200 lbs. in each bar. The actual load in each bar was monitored by the data acquisition system. Any variation between the actual loads and the "ideal" loads were compensated for by slightly tightening or loosening the load cells to achieve uniformity of load. This procedure was repeated until the actual loads were within 10 percent of the ideal, and the sum of the loads in the top 8 cells was within 5 percent of the sum of bottom cells. The specimen was then considered to be adequately balanced. An initial load of 3,000 lbs. was applied to the specimen to seal the loading apparatus. This load was arbitrarily chosen as the "zero" load. The load was then increased by an increment of 5,000 or 10,000 lbs., deemed appropriate to produce a sufficient quantity of data before yielding of the reinforcement occurred. Strains were measured with two types of apparatus; a hand-held Demic gauge and Linear Variable Displacement Transducers (L.V.D.T.'s).

The L.V.D.T.'s measured the gross strain over the entire length of the specimen. At each increment, the load was held constant while Demic readings were taken and recorded. At the same time, the data acquisition system recorded the total load measured by the loading machine, the rebar loads measured by the load cells, and the gross strains measured by the L.V.D.T.'s.

At a load of 28.40 kips the first cracks were observed and an additional set of load and strain readings were taken. Crack widths were measured using the microscope, both along the centreline of the specimen and directly above one of the middle rebars. The crack patterns were marked and numbered at the end of each increment so that the cracking sequence could be photographed for future reference, see Figure T3A.P1. This procedure was repeated for each increment and continued until the load approached the predicted yield point. The load increment was then halved, in order to gain a better understanding of the cracking behavior as yielding of the rebars occurred.The specimen was then unloaded and photographs were taken of the final crack pattern. As mentioned in Section 4.1, data for specimen T3A are presented in tabulated form in Tables T3A.T1 through T3A.T6.

Table T3A.T1 summarizes the major variables for segment T3A. The initial load, first crack load and the yield load, which was obtained from the test, are presented in the last line of this table. Table T3A.T2 shows the concrete strain on both lines at face A of the specimen based on readings recorded by hand-held mechanical gauge during each load increment. Table T3A.T3 shows the average concrete strain based on readings recorded by hand-held mechanical strain gauge on two lines, one on the rebar and one between rebars. The average of the strain for these two lines is also given in column 4. The average concrete strain based on L.V.D.T. readings on two sides of the specimen is given in columns 5 and 6, while the average of these two sides are presented in the last column.

Table T3A.T4 shows the steel strain on two lines located over the inside rebars based on readings recorded by hand-held mechanical gauges during each load increment. Table T3A.T5 shows the average steel strain on two lines. The average of the strain for these two lines is also given in Column 4.

Table T3A.T6 shows the total crack width measured on two lines in face A which were located on rebars and between rebars as explained in Chapter 3; the fourth column of the table represents the average total crack width for both lines. Columns 5 and 6 shows the average crack width on each line and column 7 gives the average crack width for both lines.

Figures T3A.P2 and T3A.P3 shows plots for load vs concrete strains for specimen T3A. Typically, the section (top, middle, or bottom) in which the first crack appeared underwent slightly larger strains throughout the loading. Figure T3A.P4 compares concrete strains measured by Demics mounted directly above and between the longitudinal reinforcement. The average strains are virtually identical. Figure T3A.P5 and T3A.P6, on the other hand, compare steel strains measured along each of the two central rebars. In general, strains measured at different locations along the rebar remained equal. Figure T3A.P7 shows a plot of the average steel strain along one line in comparison with those along the other line. Again, the two values are virtually identical, indicating a balanced loading at the ends of the specimen. Figure T3A.P8 shows load vs gross strain as measured by each L.V.D.T. Once again there was good correlation between the strains on the two sides of the specimen. This indicates that the specimen was aligned properly with little or no eccentricity.

Finally, Figures T3A.P9 and T3A.P10 compare the gross strain to the average steel strain, and the average concrete strain respectively. The correlation between each pair of values is reasonably good. However, the gross strain at any load level is consistently lower than either the average steel or average concrete strain. This observation was typical for each specimen. This can be explained as follows:

Theoretically, the stress in the centre at each end of the specimen is essentially zero, increasing to some uniform value towards the centre of the specimen. Therefore, the average strain at the ends should be lower in comparison to the strains in the central portion. The distance over which the load is transferred to the concrete is known as the transfer length. Since the gauge length of the L.V.D.T.'s includes the entire transfer length, while the Demic gauge lengths do not, it seems reasonable that the strains measured by the L.V.D.T.'s should be consistently lower, as was the case.

Each load-strain curve has a similar characteristic shape. Before the first crack occurs, the relationship ls linear. At cracking, however, the sudden redistribution in stress results in a discontinuity in the load-strain curve, which is clearly indicated by the gradual decrease of the slope of the load-strain relation figures T3A.P2 through T3A.P10. This implies that the jump in steel stress Δf_s becomes less and less for each successive crack formation.

CHAPTER 5

DISCUSSION OF RESULTS

5.1 Introduction

Various procedures for computing crack width and spacing were presented in Chapter 2. In general, these theories indicate that the average crack width can be computed if the average spacing and average strains are known. These two quantities are discussed in Sections 5.2 and 5.3. The overall procedure used to calculate crack width is given in Section 5.8, where it is compared with test data.

5.2 Crack Spacing and Sequence of Formation

In Section 2.4 several procedures for estimating the crack spacing were discussed. These relate the average spacing to the ratio of bar diameter, d_b, to the reinforcement ratio, p, and the minimum cover to the surface of the bar, C, where the cracks are observed. The two values of the concrete cover considered in this test program were 0.50 inches and 0.75 inches.

A total of 18 specimens reinforced in two directions were tested. The specimens were divided into three groups with different concrete thickness of 5", 7" and 10". The sequence of crack formation for the first two groups with smaller concrete cover was almost the same, but it was different for the group with larger concrete thickness. The development of cracks in specimen T2A, as an example for the first two groups, and specimen T8A as an example for the 10" group, will be described in this section. The crack development in specimen T2A was typical of other specimens from the first two groups. Specimen T2A was axially loaded and at a load of 40 kips the first cracks developed in a horizontal direction. The first through crack was roughly in the middle of the specimen and coincided with the location of the transverse steel bar. The second crack was roughly midway between the bottom edge of the specimen and the first crack and coincided with one of the transverse bars. The third crack was located between the first crack and the top edge of the specimen and coincided with one of the transverse steel bars. As the load increased, new cracks developed between the existing cracks. Figures 5.1 and 5.2 shows the sequence of crack formation for specimen T2A. Horizontal cracks have formed at almost every transverse bar.

Specimen T8A was axially loaded and at a load of 32 kips the first surface cracks developed. As the load increased, more surface cracks developed. The first through crack developed at a load of 96 kips and it was roughly in the middle of the specimen and coincided with the location of a transverse steel bar. The second and third cracks were located on both sides of the first crack. With an increase in the load, the through cracks divided near the surface to form two surface cracks forming what is known as the "fork action" [11]. Figures 5.3 and 5.4 indicate the location of the surface cracks coinciding approximately with the location of the transverse rebars. From the same figures it is apparent that the through cracks in the stabilized crack pattern coincided with the location of every second transverse bar. In summary, this group of specimens tended to have more surface cracks and fewer through cracks than the specimens in the first two groups.

It was observed that for all the specimens the average crack spacing decreases as more cracks form and the final crack pattern in reached at an average gross strain ε_m ranging from 0.0009 to 0.0013. In the analysis that follows, it will be assumed that the crack pattern has reached its final stage when ε_m equals 0.0011.

5.3 Effect of Variables on Crack Spacing

The effect of concrete cover, concrete thickness and percentage of steel on crack width and crack spacing were investigated. As described in Chapter 3, all the specimens were subjected to uniaxial tensile forces and loaded beyond the yield strain of the steel.

Two thicknesses were used for the concrete cover: 0.5 inches and 0.75 inches. For each concrete cover, nine segments were tested. In each group of nine, three subgroups of three segments were tested with individual values for the steel ratios. For each steel ratio subgroup, three different thicknesses of the concrete were investigated using one segment each. These parameters are shown in detail in Table (3.1).

5.3.1 Effect of Concrete Cover

Two groups of nine identical specimens with different concrete cover, C, of 0.5 inches and 0.75 inches were investigated. Table (5.1) compares the average crack spacing at the stabilized crack pattern for the two groups and indicates that concrete cover thickness has only a slight effect on the average crack spacing. Figure 5.5 shows the change in average crack spacing as a function of the average gross strain, ε_m, for two specimen with different concrete cover, which was typical for all the specimens. The figure also indicates that the average spacing decreases as the strain increases and the final crack pattern is reached at gross strain,

ε_m, equal 0.0011. Although this variable has only a little effect on the average crack spacing, the variation of concrete cover in the test program was not sufficient for conclusions regarding the effect of this parameter to be drawn. Further research is required to study the effect of the concrete cover on crack behavior.

5.3.2 Effect of Concrete Thickness

Three groups of specimens with different concrete thicknesses 5", 7" and 10" were tested. Table (5.1) indicates that for specimens having the same percentage of steel, p, and constant concrete cover, C, increasing the concrete thickness, t, results in an increase in the average crack spacing at the stabilized crack pattern. Figure 5.6 shows the change in the average crack spacing as a function of the gross strain, ε_m, for three specimens having the same percentage of steel and concrete cover with different concrete thicknesses, which was typical for all the specimens.

5.3.3 Effect of Steel Ratio (p)

The tested specimens were divided into three groups, each group consisting of six specimens having the same steel ratio, p. Figure 5.7 shows the change in average crack spacing as a function of the average gross strain, ε_m, for three specimens having the same dimension and constant concrete cover. The figure indicates that for constant concrete thickness, t, and constant concrete cover, C, increasing the steel ratio, p, appears to have an insignificant effect on the average crack spacing at the final crack pattern. However, referring to Equations (2.17) and (2.26), the effect of reinforced steel ratio p should be included in a ratio of the bar diameter, d_b/p.

5.3.4 Effect of Transverse Reinforcement

All the 18 specimens were reinforced transversely by #3 bars spaced at 3". There is little certainty as to what effect transverse reinforcement will have on crack width and spacing. However, Beeby suggests that spacers could act as crack inducers and as a result cracks will only form over bars if they were going to form close to that position anyway. The crack spacings at the final pattern for all the 18 specimens are given in Table (5.2).

Table (5.2) clearly shows that for all the specimens with thicknesses of 5" and 7" the average crack spacing was always close to the spacing of the transverse bars. This observation supports Beeby's expectation. However, for a 10" concrete thickness the average crack spacing was almost double the spacing of transverse steel bars.

Further research will be required to study the effect of the transverse steel on the crack behavior. Research is now being undertaken on this question at the University of Manitoba.

5.4 Comparison of Computed and Measured Crack Spacings

The average crack spacing was calculated using two of the expressions discussed in Chapter 2.

Using Beeby's formula, Equation (2.33), and Leonhardt's formula, Equation (2.31), the crack spacings were computed and then compared with the results from the test. This comparison with observed results facilitates an evaluation and suitable modification of existing theories of crack formation.

5.4.1 Comparison of Measured and Computed Crack Spacing Based on Beeby's Expression

Based on Equation (2.33), the average crack spacing at the final crack pattern was calculated and compared with the test results, see Table (5.3). Figure 5.8 illustrates the comparison between the ratio of Beeby's computed values to the experimental results $S_b/S_{exp.}$ as a function of bar diameter divided by steel percentage (d_b/p). The comparison suggests an underestimation of the average crack spacing by Beeby since the average ratio between the computed and measured values is about 70%.

5.4.2 Comparison of Measured and Computed Crack Spacing Based on Leonhardt's Expression

Based on Leonhardt's Equation (2.31) the average crack spacing was calculated and given in Table (5.3), where the ratios between the computed and measured values are shown in the final column. Table (5.4) illustrates the information required for computing the crack spacing values based on Equation (2.31) where

$$f_{s1,cr} = \frac{P_{cr}}{A_c + nA_s}$$

in which P_{cr} = cracking load for the given specimen and,

$$f_{s2,cr} = \frac{P_{cr}}{A_s}$$

and the almost no bond length $\ell_o = \dfrac{f_{s2,cr}\, d_b}{6500}$.

Figure 5.9 clearly indicates that the spacing based on Leonhardt gives values close to the test results, since the average value of the ratio between predicted and measured values is 1.13, from which it may be concluded that the Leonhardt expression provides less discrepancy in the prediction of crack spacings.

5.5 Proposed Modifications of Crack Spacing Prediction

The comparison between the computed and measured crack spacing in Section 5.4 indicates that Beeby's prediction always underestimates the crack spacing. At the same time prediction by Leonhardt usually slightly overestimates the crack spacing. A modification should be made in both expressions in order to achieve easier and more accurate predictions.

5.5.1 Modification Based on Beeby's Equations

It is proposed to modify Beeby's equation by including the almost no bond length, introduced by Leonhardt in order to reduce the discrepancy between the values predicted by Beeby and the observed values. Since Beeby's prediction is always underestimating the crack spacing, an attempt will be made to use the difference between the measured and calculated value to propose an additional term to Beeby's equation.

By subtracting the values of crack spacing predicted by Beeby from the experimental values a length ℓ is obtained equal to 1/2 ℓ_{m1} (see Figure 5.10, Table 5.5). This ℓ_{m1} is an equivalent term to the almost no bond length proposed by Leonhardt, Equation (2.29). Figure 5.11 shows the relation between ℓ_{m1} and the bar diameter, d_b, which relationship leads to an expression for the prediction of ℓ_{m1}.

$$\ell_{m1} = 10.0\ (d_b - 0.28)\ . \quad \ldots\ldots\ldots\ldots\ldots \quad (5.1)$$

This expression in turn leads to a new equation for predicting the crack spacing at the final crack pattern.

$$S_{mb} = 1/2\ \ell_{ml} + \ell_t\ , \quad \ldots\ldots\ldots\ldots\ldots\ldots \quad (5.2)$$

where ℓ_{ml} is the length of the modified almost lost bond length given in Equation (5.1) and ℓ_t is the transfer length proposed by Beeby's

$$\ell_t = 1.33\ C + 0.08\ \frac{d_b}{p}\ . \quad \ldots\ldots\ldots\ldots\ldots\ldots \quad (5.3)$$

Table 5.6 shows the calculation for the average crack spacing S_{mb}, based on the proposed expression (5.2).

5.5.2 Modification Based on Leonhardt's Equation

Although Leonhardt's expression is more appropriate in the present application than Beeby's, some modification is proposed to refine its predictive ability and redefine the ℓ_o expression in terms of the section properties instead of the steel stress level. According to Leonhardt's Equation (2.31),

$$S_m = 1/2\ \ell_o + \ell_t$$

Leonhardt's expression for the almost no bond length is

$$\ell_o = \frac{f_{s2,cr}}{6500}\ d_b\ , \quad (f_{s2,cr}\ \text{in psi})$$

Leonhardt predicted that the value of ℓ_o could vary from 2 to 4 times the bar diameter d_b.

Figure 5.12 shows the average value of ℓ_o/d is 3.13, which agrees with Leonhardt's prediction for ℓ_o. It is also noted that ℓ /d decreases with increasing d_b (bar diameter), which means that the length of the "almost lost" bond in general decreases with increasing bar diameter. An attempt is made using the experimental results to develop a relation which predicts more reliably the "almost lost" bond length. At the same time, this relation is formulated more simply, because it is not a function of stress level in the steel, as used by Leonhardt, but a direct function of the section properties.

From the test results, one can relate the stress after the first crack, $f_{s2,cr}$ to the bar diameter, d_b (see Figure 5.13). Using the least square method, resulting in the following equation for the modified almost last bond length, ℓ_{m2};

$$\ell_{m2} = \frac{1.3}{d_b^{0.2}} \quad \text{..................} \quad (5.3)$$

Equation (5.3) gives a simpler and more reliable method for calculating the length of the "almost lost" bond at the stabilized crack pattern. Thus, the modified expression for the average crack spacing, S_{mL} will be as follows:

$$S_{mL} = 1/2\ \ell_{m2} + \ell_t\ , \quad \text{..................} \quad (5.4)$$

where

$$\ell_t = 1.2\ C + 0.1\ \frac{d_b}{p}$$

and ℓ_{m2} is given in Equation (5.3).

5.6 Comparison of Measured and Computed Crack Spacing Based on the Proposed Modification

The average crack spacing at the stabilized crack pattern for the eighteen specimens were calculated using the proposed Equations (5.2) and (5.4). These predicted spacings are compared with the measured spacing from the test.

5.6.1 Comparison of Measured and Computed Crack Spacing Based on Equation (5.2)

Based on Equation (5.2) the average crack spacing at the stabilized crack pattern were calculated for the 18 specimens and compared with the experimental results.

Figure 5.14 shows the ratio between the predicted crack spacing and the measured values.

The average value of the predicted crack spacing, based on Equation (5.2), is 97% of the average of the measured values, as shown in Figure 5.14. While the result appears good and gives accurate prediction for this particular test program, it is recommended that more extensive programs should be conducted to test the general applicability of the proposed expression, using a wider selection of parameters.

5.6.2 Comparison of Measured and Computed Crack Spacings Based on Equation (5.4)

Based on the proposed Equation (5.4) the average crack spacing at the stabilized crack pattern were calculated for the eighteen specimens, and compared with the experimental results. Table 5.7 shows the ratio between the predicted values and the experimental values.

The average value of the predicted crack spacing based on Equation (5.4) is 1.12 times the average of the measured values, as shown in Figure 5.15.

Based on the previous comparisons between the measured crack spacing values and the values predicted, using Equation (5.2) and (5.4), it is obvious that Equation (5.2) predicts with the same degree of accuracy the average crack spacing at the final crack pattern.

5.7 Comparison of Computed and Measured Crack Widths

The average crack widths at the final crack pattern for all eighteen specimens were calculated using two of the expressions discussed in Chapter 2, based on Leonhardt's Equation (2.32) and Beeby's Equation

(2.36). The calculated values were compared with the measured values.

5.7.1 Comparison of Measured and Computed Crack Width Based on Leonhardt's Expression

The average crack widths for all eighteen specimens were calculated based on Leonhardt's Equation (2.32). The calculated values and the measured values are given in Table 5.8. The average gross strain for each specimen was calculated at the final crack pattern using Leonhardt's expression for ε_m

$$\varepsilon_m = \varepsilon_{s2} \left(1 - \left(\frac{f_{s2,cr}}{f_{s2}}\right)^2\right) ,$$

where the steel strain was calculated using

$$\varepsilon_{s2} = \frac{P_s}{A_s} ,$$

where P_s is the corresponding load at the final crack pattern. The comparison between the calculated values and the measured values are given in the last Column of Table 5.8 as a ratio W_{mL}/W_{exp}. The high values for these ratios, averaging 2.38 as shown in Figure 5.16 suggest very clearly an overestimation of the average crack width resulting from the use of Leonhardt's expression.

5.7.2 Comparison of Measured and Computed Crack Width Based on Beeby's Expression

Similarly the measured crack width at the final crack pattern for all eighteen specimens were compared with the calculated values based on Beeby's Equation (2.36). Table 5.9 illustrates the information required for computing the crack widths values based on Equation (2.36). The average gross strain, ε_m was calculated for each specimen at the final crack pattern using Leonhardt's expression as follows:

$$\varepsilon_m = \varepsilon_{s2} - \frac{f_t' \, f_{s2,cr}}{E_s \, f_{s2} \, p} \quad ,$$

where f_t' was estimated as sixty percent of the split strength of the concrete, f_{sp} [6,14,16].

The calculated crack widths for all eighteen specimens were compared to the measured values as ratio, W_{mb}/W_{exp} and are shown in Table 5.10. These results were also plotted in Figure 5.17 which clearly indicates an average value of 1.16.

Based on these results, one can confidently conclude that Beeby's expression can be used to evaluate adequately the average crack width at the final crack pattern. However, it is important at this stage to indicate that the crack spacing was based on the original Beeby's Equation (2.35) which as previously discussed in Section 5.4.1 always underestimates the measured crack spacing by about 30 percent.

Based on the previous discussion, it is obvious that there is no real necessity to strive after further methodological refinements in the prediction of average crack widths, and that Beeby's method can be recommended strongly.

6. SUMMARY AND CONCLUSIONS

The following observations and conclusions were drawn from the cracking behaviour in the wall segment tests:

1) The initial induced cracks were extended through the concrete segment. The spacing of such cracks is affected primarily by the spacing of the transverse reinforcement steel. For segments with 5" and 7" concrete thicknesses the average crack spacing was approxmately equal to the spacing of the transverse bars. However, for segment with 10" concrete thickness the average crack spacing was almost double the spacing of transverse steel bars.

2) The number of through-the-wall cracks increases as the strain increases. A fully developed pattern of through-the-wall cracks is reached at a strain approximately equal to 0.0011.

3) When the through-the-wall cracking is fully developed, subsequent loading causes surface cracks which penetrate roughly as far as the surface layer of reinforcement.

4) The concrete cover has only a slight effect on the average crack spacing, however, the variation of concrete cover in the test program was not sufficient for conclusions regarding the effect of this parameter to be drawn.

5) Increasing the concrete thickness, t, results in an increase in the average crack spacing at the stabilized crack pattern and more surface cracks.

6) A new expression for the "almost lost bond" length (Equation (5.3)) is proposed, based on the comparison between the measured crack

spacing with those calculated using Leonhardt expression. The proposed expression introduce simpler and more reliable method for calculating the length of the "almost lost bond" at the stabilized crack pattern in terms of the section properties, instead of the steel stress level.

7) Leonhardt's expression (Equation (2.31)) provides less discrepancy in the prediction of the average crack spacing at the final crack pattern.

8) Beeby's expression (Equation (2.33)) underestimates the average crack spacing at the final crack pattern by about 30%.

9) A new expression for predicting the average crack spacing at the final crack pattern (Equation (5.2)) is proposed, based on the comparison between the measured crack spacing with those calculated using Beeby's Equation (2.33). The average value of the predicted crack spacing, based on the new equation, is 97% of the average crack spacing of the measured values, which represent a reliable and accurate prediction for the average crack spacing at the final crack pattern.

10) Leonhardt's prediction for the average crack width at the stabilized crack pattern (Equation (2.32)) is highly conservative, since the ratio between the measured values and those calculated by Loenhardt suggests an overestimation of the average crack width by about more than double.

11) Beeby's expression (Equation (2.36)) for predicting the average crack width at the final crack pattern can be adeuqately used to evaluate the average crack width at the final crack pattern.

REFERENCES

[1] Base, G.D., Read, J.B., Beeby, A.W. and Tavlor, H.P.J., "An Investigation of the Crack Control Characteristics of Various Types of Bar in Reinforced Concrete Beams". Research Report No. 18, Parts I and II, Cement and Concrete Association, London, December 1966.

[2] Beeby, A.W., "The Prediction of Crack Widths in Hardened Concrete", The Structural Engineer, Vol. 57A, No. 1. January 1979, pp. 9-17.

[3] Beeby, A.W., "A Study of Cracking in Reinforced Concrete Members Subjected to Pure Tension". Technical Report 42.468. Cement and Concrete Association, London. June 1972.

[4] Broms, B.B., "Crack Width and Crack Spacing in Reinforced Concrete Members". Journal of American Concrete Institute, Vol. 62, No. 10. October 1965, pp. 1237-1255.

[5] Broms. B.B., "Technique for Investigation of Internal Cracks in Reinforced Concrete Members". Journal of the American Concrete Institute. Vol. 62, No. 1, January 1965.

[6] Dechka, D. and Sigurdson, S., "Crack Prediction in Reinforced Concrete Wall Segments Under Pure Tension". B.Sc. Thesis, Department of Civil Engineering. University of Manitoba. Winnipeg, June 1981.

[7] Ferry-Borges, J. and Lima, J.A., "Crack and Deformation Similitude in Reinforced Concrete". RILEM Bulletin, No. 7, Paris, June 1960. pp. 79-90.

[8] Gereely, P. and Lutz, L.A., "Maximum Crack Width in Reinforced Concrete Flexural Members", Causes, Mechanism, and Control of Cracking in Concrete, SP-20, American Concrete Institute, Detroit, 1968. pp. 87-117.

[9] Goto, Y., "Cracks Formed in Concrete Around Deformed Tension Bars". Journal American Concrete Institute, Proc. Vol. 68, No. 4, April 1971, pp. 244-251.

[10] Kaar, P.H., "An Approach to the Control of Cracking in Reinforced Concrete", Causes, Mechanism and Control of Cracking in Concrete, SP-20, American Concrete Institute, Detroit, 1968, pp. 141-157.

[11] Leonhardt, F., "Crack Control in Concrete Structures". IABSE Surveys. S-4/77, IABSE Periodica 3/1977, International Association for Bridge and Structural Engineering, Zurich, August 1977.

[12] Nawy, E.G. and Blair, K.W., "Further Studies on Flexural Crack Control in Structural Slab Systems", Cracking, Deflection and Ultimate Load of Concrete Slab Systems, SP-30, American Concrete Institute, Detroit, 1971, pp. 1-42.

[13] Reis, E.D. Jr., Mozer, J.D., Bianchini, A.C. and Kesler, C.G., Causes and Control of Cracking in Concrete Reinforced with High Strength Steel Bars - A Review of Research", Engineering Experiment Station Bulletin 479, University of Illinois. Urbana, Illinois, August 1955.

[14] Rizkalla, S.K.. Simmonds. S.H. and MacGregor, J.G., "Cracking of Reinforced and Prestressed Concrete Wall Segments". Structural Engineering Report No. 82, Department of Civil Engineering, University of Alberta. Edmonton, November 1980.

[15] Saligar, R., "High Grade Steel in Reinforced Concrete", Preliminary Publication, 2nd Congress, International Association Bridge and Structural Engineering, Berlin-Munich, 1936, pp. 293-315.

[16] Simmonds, S.H.. Rizkalla. S.H. and MacGregor, J.G.. "Tests of Wall Segments from Reactor Containments". Structural Engineering Report No. 81, Department of Civil Engineering, University of Alberta, Edmonton, November 1979.

[17] Welch, G.B. and Janjua, M.A.. "Width and Spacing of Tensile Cracks in Reinforced Concrete". UNICIV Report No. R-76, School of Civil Engineering, University of New South Wales, Kensington, NSW, Australia, December 1971.

CONCRETE COVER (C) in	STEEL RATIO (p)	CONCRETE THICKNESS (t) in	SPECIMEN NUMBER	X-SECTION AREA in^2	REINF. BAR SIZE	A_s in^2
0.5	0.0147	5.0	T1A	60.0	#3	0.88
		7.0	T4A	84.0	M10	1.24
		10.0	T7A	110.0	#4	1.60
	0.0207	5.0	T2A	60.0	M10	1.24
		7.0	T5A	77.0	#4	1.60
		10.0	T8A	120.0	M15	2.48
	0.0294	5.0	T3A	55.0	#4	1.60
		7.0	T6A	84.0	M15	2.48
		10.0	T9A	120.0	#6	3.52
0.75	0.0147	5.0	T1B	60.0	#3	0.88
		7.0	T4B	84.0	M10	1.24
		10.0	T7B	110.0	#4	1.60
	0.0207	5.0	T2B	60.0	M10	1.24
		7.0	T5B	77.0	#4	1.60
		10.0	T8B	120.0	M15	2.48
	0.0294	5.0	T3B	55.0	#4	1.60
		7.0	T6B	84.0	M15	2.48
		10.0	T9B	120.0	#6	3.52

TABLE 3.1 OVERVIEW OF VARIABLES CONSIDERED IN SEGMENT TESTS

SPECIMEN NUMBER	COMP. STRENGTH f' (psi)	SPLIT TENSILE STRENGTH, f_{sp} (psi)	$f_t/\sqrt{f'_c}$	MODULUS OF ELASTICITY $E_c \times 10^3$ psi
T1A	7600	610	6.997	4650
T1B	7480	610	7.053	4530
T2A	8510	610	6.612	4720
T2B	7360	630	7.343	4800
T3A	7330	560	6.540	4970
T3B	7220	610	7.178	4640
T4A	8380	660	7.209	4930
T4B	7320	680	7.947	4930
T5A	7280	480	5.672	4550
T5B	7260	550	6.454	4680
T6A	8080	690	7.588	5070
T6B	8510	700	7.588	5020
T7A	7440	570	6.608	4590
T7B	7320	720	8.415	4600
T8A	8900	750	7.949	5170
T8B	8910	720	7.627	5070
T9A	8750	710	7.590	4990
T9B	8410	700	7.633	5160

TABLE 3.2 CONCRETE COMPRESSIVE AND TENSILE STRENGTH

SPECIMEN NUMBER	BAR SIZE d_b	YIELD STRENGTH f_{sy} (psi)	ULTIMATE STRENGTH f_{su} (psi)	MAXIMUM ELONGATION %	MODULUS OF ELASTICITY E_s (ksi)
T1A	#3	61800	87400	23.5	33400
T1B	#3	63150	88200	22.8	29750
T2A	M10	52500	78950	18.5	26000
T2B	M10	52950	79600	20.5	26400
T3A	#4	54300	88100	17.0	26900
T3B	#4	54500	89050	17.3	29950
T4A	M10	52300	79200	17.5	25050
T4B	M10	53050	79100	18.3	26600
T5A	#4	53950	87500	19.0	26800
T5B	#4	53850	88530	18.8	28450
T6A	M15	55900	88750	17.0	25950
T6B	M15	53750	89200	17.0	25950
T7A	#4	54150	87850	18.5	28800
T7B	#4	53850	87700	19.0	27350
T8A	M15	54200	89600	18.5	26600
T8B	M15	54000	89350	17.3	27600
T9A	#6	62250	108850	13.5	26850
T9B	#6	64200	111250	10.8	26550

TABLE 3.3 REINFORCING STEEL PROPERTIES

```
SPECIMEN NO.=T3A

CONCRETE COVER(IN)=   0.500

CONCRETE THICKNESS(IN)=   5.000             SPECIMEN WIDTH(IN.) =  11.000             SPECIMEN LENTH(IN.) =  30.000

NO. OF REBARS IN THE LOADING DIRECTION =8

SPACING BET. REBARS IN THE LOADING DIRECTION(IN)= 3.0

SIZE OF REBAR IN THE LOADING DIRECTION(IN.) = 0.50000

SPACING BET. REBARS IN THE TRANSVERSE DIRECTION(IN.) = 3.0

INITIAL LOAD(KIPS)=     3.00             FIRST CRACK LOAD(KIPS)=    28.40             YIELD LOAD(KIPS)=    85.20
```

Table T3A.T1 Major Variables for Segment T3A

CONCRETE STRAIN

LOAD(KIPS)	DEMICS ALIGNED ON REBAR TOP	DEMICS ALIGNED ON REBAR MIDDLE	DEMICS ALIGNED ON REBAR BOTTOM	DEMICS ALIGNED BETWEEN REBAR TOP	DEMICS ALIGNED BETWEEN REBAR MIDDLE	DEMICS ALIGNED BETWEEN REBAR BOTTOM
5.0000	0.0000100	0.0000100	0.0000000	0.0000100	0.0000000	0.0000100
10.0000	0.0000300	0.0000200	0.0000200	0.0000200	0.0000200	0.0000200
15.0000	0.0000300	0.0000200	0.0000100	0.0000300	0.0000300	0.0000200
20.0000	0.0000500	0.0000300	0.0000500	0.0000400	0.0000500	0.0000500
25.0000	0.0000800	0.0000700	0.0000600	0.0000700	0.0000600	0.0000700
29.0000	0.0002500	0.0002800	0.0002100	0.0002700	0.0003000	0.0002200
30.0000	0.0003100	0.0003600	0.0002700	0.0003200	0.0003000	0.0003200
35.0000	0.0005600	0.0004500	0.0005400	0.0005800	0.0004200	0.0005600
40.0000	0.0006900	0.0005500	0.0007700	0.0007000	0.0005100	0.0008300
45.0000	0.0008100	0.0006900	0.0009100	0.0008200	0.0006500	0.0009700
50.0000	0.0009300	0.0008000	0.0010400	0.0009700	0.0007900	0.0011200
55.0000	0.0010600	0.0009000	0.0011800	0.0011000	0.0009000	0.0012800
60.0000	0.0012000	0.0010000	0.0013100	0.0012200	0.0010100	0.0014400
65.0000	0.0013200	0.0011000	0.0014400	0.0013300	0.0011000	0.0015500
70.0000	0.0014400	0.0012100	0.0016000	0.0014600	0.0012000	0.0016900
75.0000	0.0015500	0.0011500	0.0017600	0.0015500	0.0013300	0.0018700
80.0000	0.0016800	0.0014200	0.0018300	0.0017000	0.0013800	0.0020100
85.0000	0.0019300	0.0015600	0.0020900	0.0018600	0.0014700	0.0022100
89.0000	0.0027000	0.0016500	0.0023600	0.0028700	0.0016200	0.0025000
91.0000	0.0051500	0.0031900	0.0067600	0.0053100	0.0032700	0.0071900
93.0000	0.0072200	0.0066100	0.0097500	0.0073800	0.0066600	0.0093500

Table T3A.T2 Concrete Strain on Both Lines at Face A

CONCRETE STRAIN

LOAD(KIPS)	AVE.(ON REBAR)	AVE.(BET.REBARS)	AVE.(TOTAL)	LVDT1(STRAIN)	LVDT2(STRAIN)	LVDT(AVE)
5.0000	0.0000067	0.0000067	0.0000067	0.0000000	0.0000100	0.0000050
10.0000	0.0000233	0.0000200	0.0000217	0.0000100	0.0000233	0.0000167
15.0000	0.0000267	0.0000267	0.0000267	0.0000233	0.0000400	0.0000317
20.0000	0.0000433	0.0000467	0.0000450	0.0000367	0.0000500	0.0000433
25.0000	0.0000700	0.0000667	0.0000683	0.0000500	0.0001033	0.0000767
28.4000	0.0002533	0.0002633	0.0002583	0.0002100	0.0002933	0.0002517
30.0000	0.0003133	0.0003133	0.0003133	0.0002333	0.0003367	0.0002850
35.0000	0.0005167	0.0005200	0.0005183	0.0003967	0.0005300	0.0004633
40.0000	0.0005667	0.0006800	0.0006233	0.0005400	0.0006467	0.0005933
45.0000	0.0008033	0.0008133	0.0008083	0.0006467	0.0007533	0.0007000
50.0000	0.0009233	0.0009600	0.0009417	0.0007633	0.0008833	0.0008233
55.0000	0.0010467	0.0010933	0.0010700	0.0009700	0.0010000	0.0009850
60.0000	0.0011700	0.0012233	0.0011967	0.0009633	0.0011133	0.0010383
65.0000	0.0012967	0.0013267	0.0013117	0.0010633	0.0012267	0.0011450
70.0000	0.0014167	0.0014500	0.0014333	0.0011633	0.0013433	0.0012533
75.0000	0.0015533	0.0015833	0.0015683	0.0012833	0.0014733	0.0013783
80.0000	0.0016633	0.0016967	0.0016800	0.0013967	0.0015900	0.0014933
85.0000	0.0018267	0.0018467	0.0018367	0.0015733	0.0016800	0.0016267
89.0000	0.0022367	0.0023300	0.0022833	0.0017067	0.0018933	0.0018000
91.0000	0.0051333	0.0052533	0.0051933	0.0036767	0.0049667	0.0043217
93.0000	0.0078600	0.0077967	0.0078283	0.0062367	0.0071333	0.0066850

Table T3A.T3 Average Concrete Strain

STEEL STRAIN

LOAD(KIPS)	LINE NO. (1) TOP	LINE NO. (1) MIDDLE	LINE NO. (1) BOTTOM	LINE NO. (2) TOP	LINE NO. (2) BOTTOM
5.0000	0.0000100	0.0000100	0.0000000	0.0000100	0.0000000
10.0000	0.0000300	0.0000300	0.0000100	0.0000300	0.0000200
15.0000	0.0000400	0.0000500	0.0000300	0.0000300	0.0000300
20.0000	0.0000700	0.0000900	0.0000600	0.0001500	0.0000800
25.0000	0.0001100	0.0001400	0.0001800	0.0001600	0.0001000
28.0000	0.0003600	0.0003700	0.0003900	0.0004700	0.0002700
30.0000	0.0004300	0.0005200	0.0004800	0.0005300	0.0004100
35.0000	0.0005900	0.0006300	0.0005900	0.0006700	0.0005800
40.0000	0.0007700	0.0007500	0.0007900	0.0007800	0.0007100
45.0000	0.0009100	0.0009000	0.0009300	0.0009200	0.0008900
50.0000	0.0011200	0.0010600	0.0010200	0.0010000	0.0010200
55.0000	0.0011400	0.0011700	0.0015500	0.0011800	0.0010800
60.0000	0.0012700	0.0012900	0.0012600	0.0012800	0.0011900
65.0000	0.0013900	0.0014000	0.0013700	0.0014100	0.0013300
70.0000	0.0015100	0.0015100	0.0015100	0.0014800	0.0014200
75.0000	0.0016400	0.0016400	0.0016000	0.0016500	0.0015700
80.0000	0.0017500	0.0017300	0.0017100	0.0016900	0.0015900
85.0000	0.0018300	0.0017900	0.0017500	0.0018100	0.0016700
90.0000	0.0025900	0.0019000	0.0018900	0.0021500	0.0019100
91.0000	0.0056100	0.0046300	0.0052300	0.0054100	0.0043200
93.0000	0.0073100	0.0082500	0.0079900	0.0070700	0.0076900

Table T3A.T4 Steel Strains

STEEL STRAIN

LOAD(KIPS)	AVE.(LINE(1)	AVE.(LINE(2)	AVE.(TOTAL)
5.0000	0.0000067	0.0000050	0.0000058
10.0000	0.0000233	0.0000250	0.0000242
15.0000	0.0000400	0.0000300	0.0000350
20.0000	0.0000733	0.0001150	0.0000942
25.0000	0.0001433	0.0001300	0.0001367
29.4000	0.0003733	0.0003700	0.0003717
30.0000	0.0004600	0.0004700	0.0004650
35.0000	0.0006367	0.0006250	0.0006308
40.0000	0.0007700	0.0007450	0.0007575
45.0000	0.0009033	0.0009000	0.0009017
50.0000	0.0010333	0.0010500	0.0010417
55.0000	0.0012330	0.0011890	0.0012110
60.0000	0.0012733	0.0012350	0.0012542
65.0000	0.0013967	0.0013700	0.0013783
70.0000	0.0015100	0.0014500	0.0014900
75.0000	0.0016267	0.0016100	0.0016183
80.0000	0.0017300	0.0016400	0.0016850
85.0000	0.0017900	0.0017400	0.0017650
89.0000	0.0021267	0.0020800	0.0021033
91.0000	0.0054967	0.0048650	0.0051808
93.0000	0.0080167	0.0073800	0.0076983

Table T3A.T5 Average Steel Strain

CRACK WIDTH (IN.)

LOAD(KIPS)	TOTAL(ON REBAR)	TOTAL(BET.REBARS)	AVE.(TOTAL)	AV1.(ON REBAR)	AV2.(BET.REBARS)	AVE.(1,2)
25.0000	0.002362	0.003937	0.003150	0.000787	0.001312	0.001050
30.0000	0.002362	0.003937	0.003150	0.000787	0.001312	0.001050
35.0000	0.003937	0.004724	0.004331	0.001312	0.001575	0.001444
40.0000	0.006299	0.007087	0.006693	0.001260	0.001417	0.001339
45.0000	0.007874	0.007874	0.007874	0.001312	0.001312	0.001312
50.0000	0.009449	0.011811	0.010630	0.001350	0.001687	0.001519
55.0000	0.011024	0.013386	0.012205	0.001575	0.001912	0.001744
60.0000	0.012598	0.018898	0.015748	0.001800	0.002362	0.002081
65.0000	0.014961	0.022047	0.018504	0.002137	0.002756	0.002447
70.0000	0.017323	0.022835	0.020079	0.002475	0.002854	0.002665
75.0000	0.025197	0.024409	0.024803	0.002100	0.002712	0.002406
80.0000	0.029134	0.027559	0.028346	0.002428	0.003062	0.002745
85.0000	0.030709	0.033071	0.031890	0.002559	0.003675	0.003117
89.0000	0.042520	0.047244	0.044882	0.003271	0.004724	0.003998
91.0000	0.105512	0.114961	0.110236	0.007537	0.010451	0.008994
93.0000	0.151181	0.199213	0.175197	0.010079	0.016601	0.013340

Table T3A.T6 Total and Average Crack Width Measured on Two lines in Face A

STEEL RATIO (p)	CONC. THICKNESS t(in)	AVERAGE CRACK SPACING GROUP A C = 0.50 in	GROUP B C = 0.75 in
0.0147	5.00	3.15	3.20
	7.00	3.51	3.50
	10.00	6.00	6.00
0.0207	5.00	3.25	3.35
	7.00	3.70	3.77
	10.00	5.70	6.00
0.0294	5.00	3.88	3.24
	7.00	3.70	3.80
	10.00	4.80	5.30

TABLE 5.1 EFFECT OF CONCRETE COVER ON THE AVERAGE CRACK SPACING AT THE STABILIZED CRACK PATTERN

CONCRETE THICKNESS t	SPECIMEN NUMBER	S_{exp} (in)
5.0"	T1A	3.15
	T1B	3.20
	T2A	3.25
	T2B	3.35
	T3A	3.88
	T3B	3.24
7.0"	T4A	3.51
	T4B	3.50
	T5A	3.70
	T5B	3.77
	T6A	3.70
	T6B	3.80
10.0"	T7A	6.0
	T7B	6.0
	T8A	6.05
	T8B	6.00
	T9A	4.80
	T9B	5.30

TABLE 5.2 AVERAGE CRACK SPACING AT THE FINAL CRACK PATTERN FOR ALL THE SPECIMENS

SPECIMEN NUMBER	d_b/p	S_b	S_{exp}	S_b/S_{exp}	S_L	S_L/S_{exp}
T1A	25.50	2.70	3.15	0.857	4.57	1.450
T2A	21.50	2.38	3.25	0.732	4.02	1.236
T3A	17.00	2.03	3.88	0.523	3.60	0.928
T4A	30.30	3.09	3.51	0.880	4.87	1.387
T5A	24.15	2.60	3.70	0.702	4.39	1.186
T6A	21.40	2.38	3.70	0.643	4.01	1.084
T7A	34.00	3.39	6.00	0.565	5.67	0.945
T8A	30.40	3.10	6.05	0.512	4.84	0.800
T9A	25.50	2.70	4.80	0.562	4.41	0.919
T1B	25.50	3.04	3.20	0.950	4.81	1.503
T2B	21.50	2.72	3.35	0.811	4.23	1.263
T3B	17.00	2.36	3.24	0.728	3.67	1.133
T4B	30.30	3.42	3.50	0.977	5.20	1.486
T5B	24.15	2.93	3.77	0.777	4.66	1.236
T6B	21.40	2.71	3.80	0.713	4.23	1.113
T7B	34.00	3.72	6.00	0.620	5.70	0.950
T8B	30.40	3.43	6.00	0.572	5.03	0.838
T9B	25.50	3.04	5.30	0.573	4.72	0.890

TABLE 5.3 COMPARISON BETWEEN MEASURED AND COMPUTED CRACK SPACING BASED ON BOTH LEONHARDT AND BEEBY

Sp. No.	A_s	p	d_b	n	C	P_{cr}	$f_{s1,cr}$	$1+\frac{1}{pn}$	$f_{s2,cr}$	ℓ_o	ℓ_t	S_L
T1A	0.88	0.0147	0.375	7.18	0.50	25.00	2.700	10.49	28.41	1.64	3.75	4.57
T1B	0.88	0.0147	"	6.57	0.75	27.80	2.78	11.37	31.59	1.82	3.90	4.81
T2A	1.24	0.0207	0.445	5.51	0.50	27.60	2.27	9.78	22.25	1.34	3.35	4.02
T2B	1.24	0.0207	"	5.50	0.75	29.70	2.44	9.79	23.95	1.45	3.50	4.23
T3A	1.60	0.0291	0.500	5.41	0.50	28.40	2.41	7.35	1.7.75	1.36	2.92	3.60
T3B	1.60	0.0291	"	6.45	0.75	25.00	2.47	6.32	15.62	1.20	3.07	3.67
T4A	1.24	0.0148	0.445	5.08	0.50	27.80	1.56	14.33	22.42	1.35	4.20	4.87
T4B	1.24	0.0148	"	5.14	0.75	35.00	1.99	14.18	28.22	1.71	4.35	5.20
T5A	1.60	0.0207	0.500	5.89	0.50	32.50	2.21	9.20	20.31	1.56	3.61	4.39
T5B	1.60	0.0207	"	5.08	0.75	37.50	2.62	8.94	23.44	1.80	3.76	4.66
T6A	2.48	0.0295	0.630	5.12	0.50	37.50	1.98	7.62	15.12	1.37	3.33	4.01
T6B	2.48	0.0295	"	5.17	0.75	41.00	2.19	7.55	16.53	1.50	3.48	4.23
T7A	1.60	0.0145	0.500	6.27	0.50	42.50	2.21	12.00	26.56	2.04	4.65	5.67
T7B	1.60	0.0145	"	5.94	0.75	37.50	1.86	12.61	23.44	1.80	4.80	5.70
T8A	2.48	0.0206	0.63	5.14	0.50	32.00	1.23	10.44	12.90	1.17	4.26	4.84
T8B	2.48	0.0206	"	5.44	0.75	34.00	1.38	9.92	13.71	1.24	4.41	5.03
T9A	3.52	0.0293	0.75	5.39	0.50	40.00	1.55	7.33	11.36	1.31	3.76	4.41
T9B	3.52	0.0293	"	5.14	0.75	50.00	1.86	7.64	14.20	1.63	3.91	4.72

TABLE 5.4 AVERAGE CRACK SPACING BASED ON EQUATION (2.31)

SPECIMEN NUMBER	CONCRETE COVER (C) (in)	BAR DIAMETER d_b (in)	A_s	REINFORCED RATIO p	1.33C (in)	d_b/p	S_b (in)	S_{exp} (in)	ℓ (in)
T1A	0.50	0.375	0.88	0.0147	0.665	25.50	2.70	3.15	0.45
T2A		0.445	1.24	0.0207		21.50	2.38	3.25	0.87
T3A		0.500	1.60	0.0294		17.00	2.03	3.88	1.85
T4A		0.445	1.24	0.0147		30.30	3.09	3.51	0.42
T5A		0.500	1.60	0.0207		24.15	2.60	3.70	1.10
T6A		0.63	2.48	0.0294		21.40	2.38	3.70	1.32
T7A		0.50	1.60	0.0147		34.00	3.39	6.00	2.61
T8A		0.63	2.48	0.0207		30.40	3.10	6.05	2.95
T9A		0.75	3.52	0.0294		25.50	2.70	4.80	2.10
T1B	0.75"	0.375	0.88	0.0147	0.997	25.50	3.04	3.20	0.16
T2B		0.445	1.24	0.0207		21.50	2.72	3.35	0.63
T3B		0.500	1.60	0.0299		17.00	2.36	3.24	0.88
T4B		0.445	1.24	0.0147		30.30	3.42	3.50	0.08
T5B		0.500	1.60	0.0207		24.15	2.93	3.77	0.84
T6B		0.630	2.48	0.0294		21.40	2.71	3.80	1.09
T7B		0.500	1.60	0.0147		34.00	3.72	6.00	2.28
T8B		0.630	2.48	0.0207		30.40	3.43	6.00	2.57
T9B		0.750	3.52	0.0294		25.50	3.04	5.30	2.26

S_b : THE MINIMUM CRACK SPACING BASED ON BEEBY'S EQUATION

$$S_b = 1.33C + 0.08\ d_b/p$$

S_{exp}: THE MINIMUM CRACK SPACING BASED ON OUR TEST RESULTS

$$\ell = S_{exp} - S_b$$

TABLE 5.5 VALUE OF THE "ALMOST LOST BOND" LENGTH BASED ON BEEBY' EQUATION

SPECIMEN NUMBER	ℓ_t	ℓ_{m1}	CALCULATED S_{mb}	TEST RESULTS S_{exp}
T1A	2.70	1.02	3.21	3.15
T2A	2.38	1.78	3.59	3.25
T3A	2.03	2.37	3.21	3.88
T4A	3.09	1.78	3.98	3.51
T5A	2.60	2.37	3.78	3.70
T6A	2.38	3.78	4.27	3.70
T7A	3.39	2.37	4.57	6.00
T8A	3.10	3.78	4.99	6.05
T9A	2.70	5.07	5.23	4.80
T1B	3.04	1.02	3.55	3.20
T2B	2.72	1.78	3.61	3.35
T3B	2.36	2.37	3.54	3.24
T4B	3.42	1.78	4.31	3.50
T5B	2.93	2.37	4.11	3.77
T6B	2.71	3.78	4.60	3.80
T7B	3.72	2.37	4.90	6.00
T8B	3.43	3.78	5.32	6.00
T9B	3.04	5.07	5.60	5.30

TABLE 5.6 AVERAGE CRACK SPACING BASED ON EQUATION (5.2)

SPECIMEN NUMBER	d_b/p	ℓ_t	ℓ_{m2}	S_{mL}	S_{exp}	S_{mL}/S_{exp}
T1A	25.50	3.75	1.593	4.546	3.15	1.443
T2A	21.50	3.35	1.528	4.114	3.25	1.265
T3A	17.00	2.92	1.493	3.666	3.88	0.945
T4A	30.30	4.20	1.528	4.964	3.51	1.414
T5A	24.15	3.61	1.493	4.356	3.70	1.177
T6A	21.40	3.33	1.426	4.043	3.70	1.092
T7A	34.00	4.65	1.493	5.396	6.00	0.899
T8A	30.40	4.26	1.426	4.973	6.05	0.821
T9A	25.50	3.76	1.377	4.448	4.80	0.926
T1B	25.50	3.90	1.593	4.696	3.20	1.467
T2B	21.50	3.50	1.528	4.264	3.35	1.272
T3B	17.00	3.07	1.493	3.816	3.24	1.177
T4B	30.30	4.35	1.528	5.114	3.50	1.461
T5B	24.15	3.76	1.493	4.506	3.77	1.195
T6B	21.40	3.48	1.426	4.193	3.80	1.103
T7B	3.40	4.80	1.493	5.546	6.00	0.924
T8B	30.40	4.41	1.426	5.123	6.00	0.853
T9B	2.55	3.91	1.377	4.598	5.30	0.867

TABLE 5.7 COMPARISON BETWEEN MEASURED AND COMPUTED CRACK SPACING BASED ON EQUATION 5.4

SPECIMEN NUMBER	P_s (kips)	$\varepsilon_{s2} \times 10^{-3}$	$\varepsilon_{mL} \times 10^{-3}$	$W_{mL} \times 10^{-3}$	$W_{exp} \times 10^{-3}$	W_{mL}/W_{exp}
T1A	40.0	1.3609	0.64636	4.645	2.187	2.12
T1B	45.0	1.7188	1.0628	7.113	3.407	2.09
T2A	50.0	1.5508	1.0786	6.435	1.772	3.63
T2B	50.0	1.5273	0.9885	5.674	3.206	1.77
T3A	55.0	1.2778	0.9370	4.473	1.744	2.56
T3B	55.0	1.1477	0.9107	4.173	2.559	1.63
T4A	55.0	1.7706	1.1023	6.821	3.248	2.10
T4B	60.0	1.8190	1.2000	8.330	3.631	2.29
T5A	62.5	1.4575	1.0634	6.112	1.941	3.14
T5B	60.0	1.3181	0.8031	5.392	2.608	2.06
T6A	82.5	1.2819	1.0170	5.142	1.909	2.69
T6B	78.5	1.2197	0.8870	4.916	2.313	2.12
T7A	65.0	1.4105	0.8076	6.632	2.215	2.99
T7B	67.5	1.5425	1.0663	7.894	3.712	2.12
T8A	80.0	1.2127	1.0187	5.758	1.782	3.23
T8B	82.0	1.1979	0.9919	5.859	2.953	1.98
T9A	140.0	1.4812	1.3603	7.055	3.037	2.32
T9B	110.0	1.1770	0.9397	5.592	2.657	2.10

TABLE 5.8 COMPARISON BETWEEN MEASURED AND COMPUTED CRACK WIDTH BASED ON LEONHARDT'S EXPRESSION

SPECIMEN NUMBER	A_s	P_s	p	$\varepsilon_{s2} \times 10^{-3}$	$\varepsilon_{mb} \times 10^{-3}$	S_b	$W_{mb} \times 10^{-3}$
T1A	0.88	40.0	0.00147	1.3609	0.79131	2.70	2.1365
T1B	0.88	45.0	.001470	1.7188	1.17460	3.04	3.5710
T2A	1.24	50.0	0.02070	1.5508	1.15580	2.38	2.7509
T2B	1.24	50.0	0.02070	1.5273	1.11080	2.72	3.0154
T3A	1.60	55.0	0.02910	1.2778	1.02370	2.03	2.0781
T3B	1.60	55.0	0.02910	1.1477	0.94680	2.36	2.2340
T4A	1.24	55.0	0.01480	1.7706	1.13220	3.09	3.4980
T4B	1.24	60.0	0.01480	1.8190	1.24830	3.42	4.2690
T5A	1.60	62.5	0.02070	1.4575	1.09640	2.60	2.8500
T5B	1.60	60.0	0.02070	1.3181	0.90925	2.93	2.6640
T6A	2.48	82.50	0.02950	1.2819	1.05320	2.38	2.5060
T6B	2.48	78.50	0.02950	1.2197	0.94992	2.71	2.5740
T7A	1.60	65.0	0.01450	1.4105	0.81960	3.39	2.7780
T7B	1.60	67.5	0.01450	1.5425	1.00280	3.72	3.7304
T8A	2.48	80.0	0.02060	1.2127	0.93150	3.10	2.8879
T8B	2.48	82.0	0.02060	1.1979	0.91690	3.43	3.1450
T9A	3.52	140.0	0.02930	1.4812	1.34100	2.70	3.6210
T9B	3.52	110.0	0.02930	1.1770	0.95190	3.04	2.8940

TABLE 5.9 AVERAGE CRACK WIDTH AT FINAL CRACK PATTERN BASED ON BEEBY'S EXPRESSION

SPECIMEN NUMBER	$W_{mb} \times 10^{-3}$	$W_{exp} \times 10^{-3}$	W_{mb}/W_{exp}
T1A	2.136	2.187	0.97
T1B	3.571	3.407	1.05
T2A	2.751	1.772	1.55
T2B	3.015	3.206	0.94
T3A	2.078	1.744	1.19
T3B	2.234	2.559	0.87
T4A	3.498	3.248	1.07
T4B	4.269	3.631	1.17
T5A	2.850	1.941	1.46
T5B	2.664	2.608	1.02
T6A	2.506	1.909	1.31
T6B	2.574	2.313	1.11
T7A	2.778	2.215	1.25
T7B	3.730	3.712	1.00
T8A	2.888	1.782	1.62
T8B	3.145	2.953	1.06
T9A	3.621	3.037	1.19
T9B	2.894	2.657	1.08

TABLE 5.10 COMPARISON BETWEEN MEASURED AND COMPUTED CRACK WIDTHS BASED ON BEEBY'S EXPRESSION

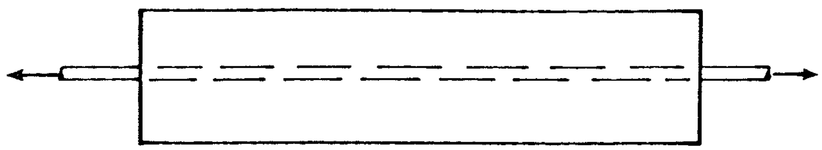

(a) Prism

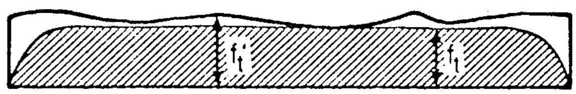

(b) Variation of Tensile Strength and Stress Along Prism

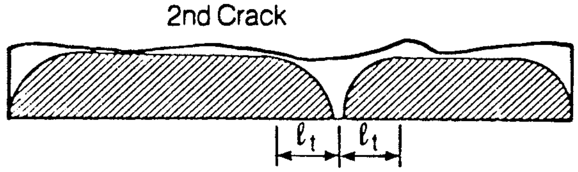

(c) Tensile Stresses after First Crack

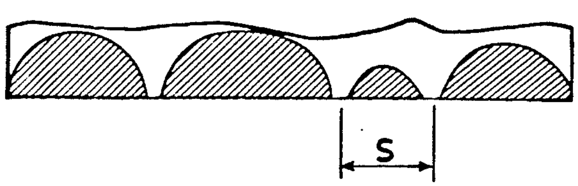

(d) Tensile Stresses after Three Cracks

Figure 2.1 Cracking of an Axially Loaded Prism

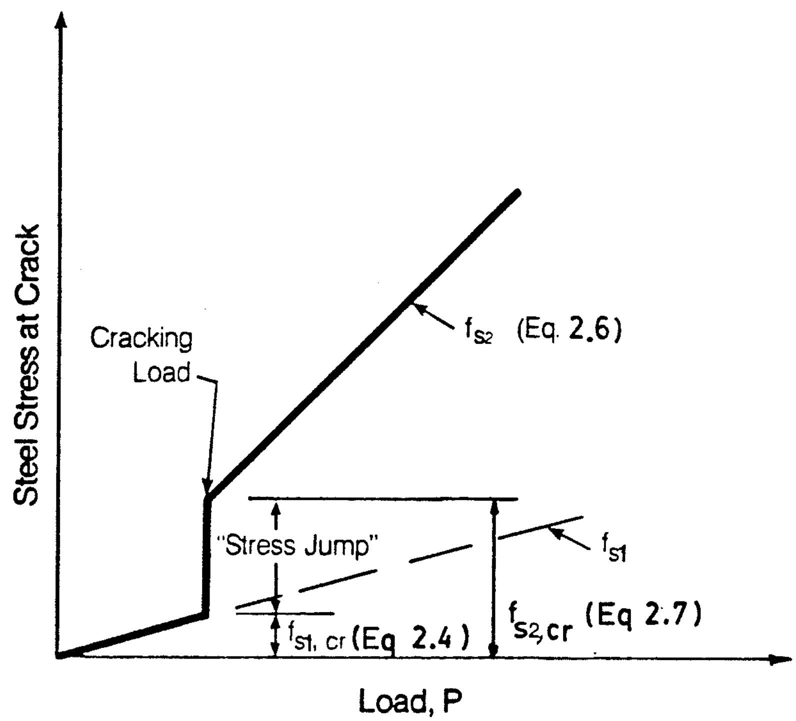

Figure 2.2 Jump in Steel Stress at Cracking

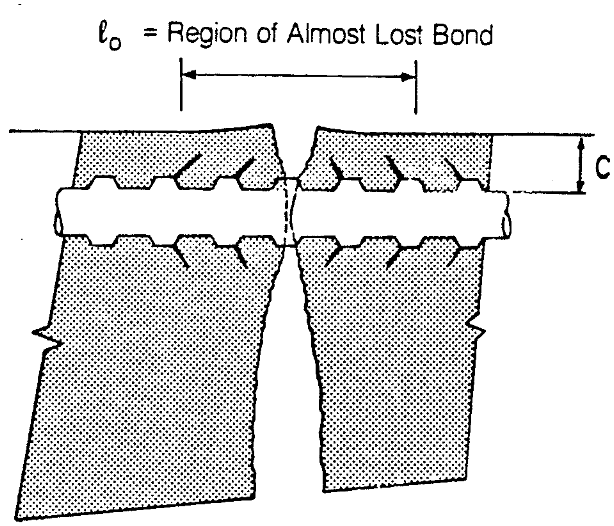

Figure 2.3 Internal Cracks at Bar Deformations

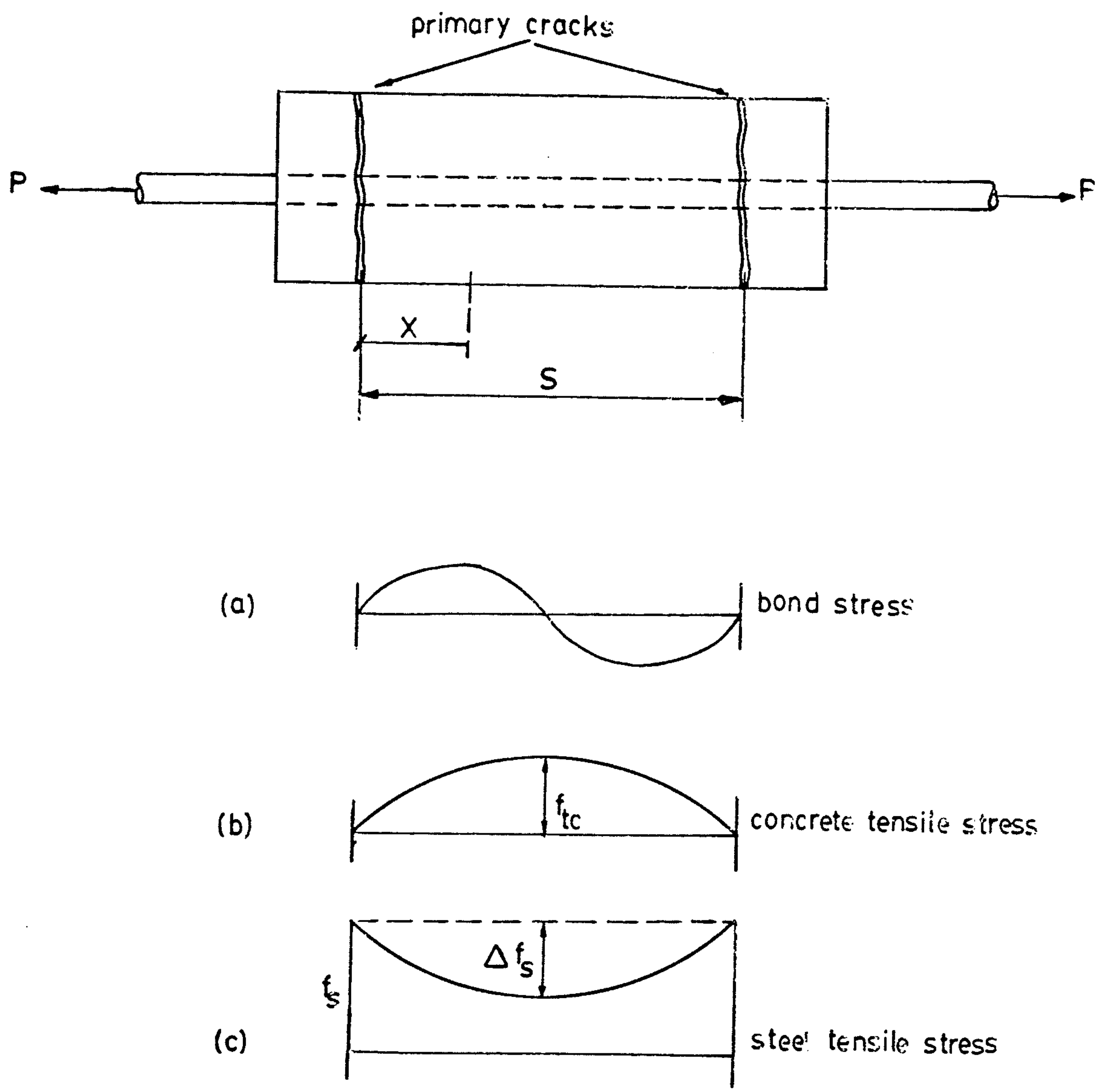

Figure 2.4 Stresses in Concrete and Steel in a Cracked Prism

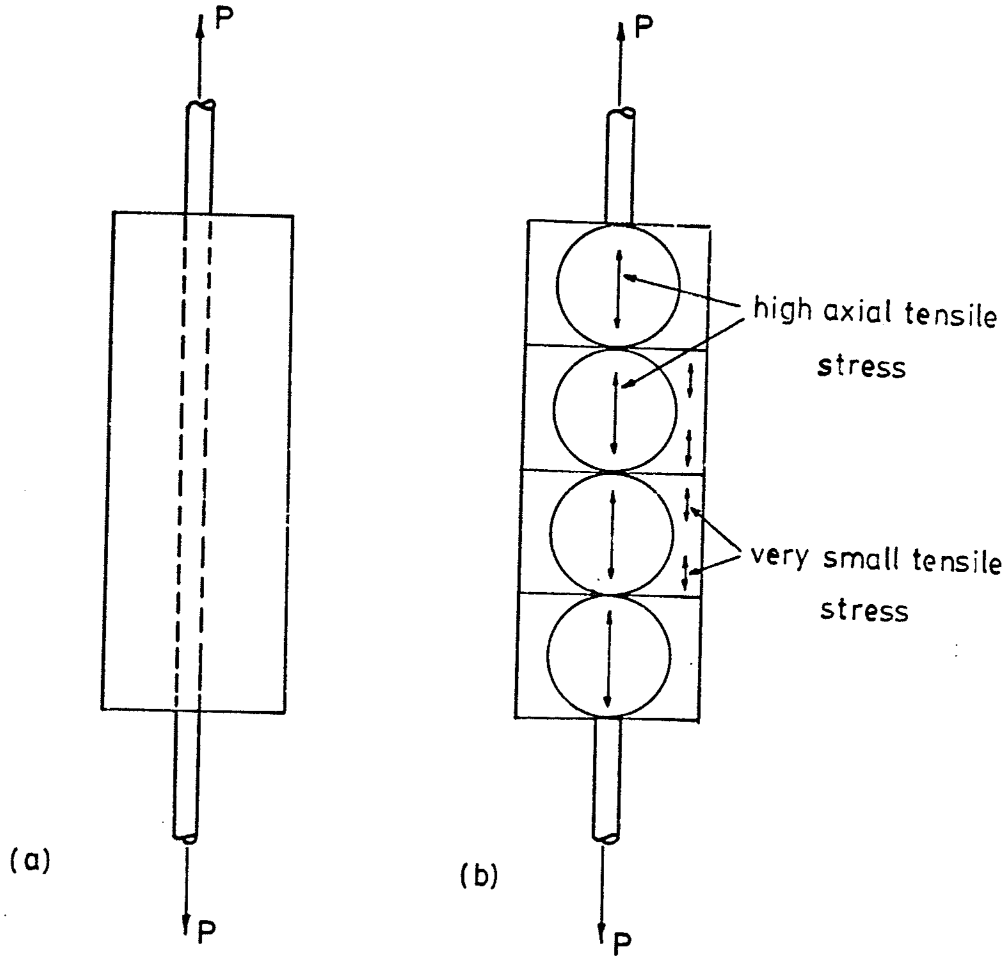

Figure 2.5 Brom's Stress Circle Method

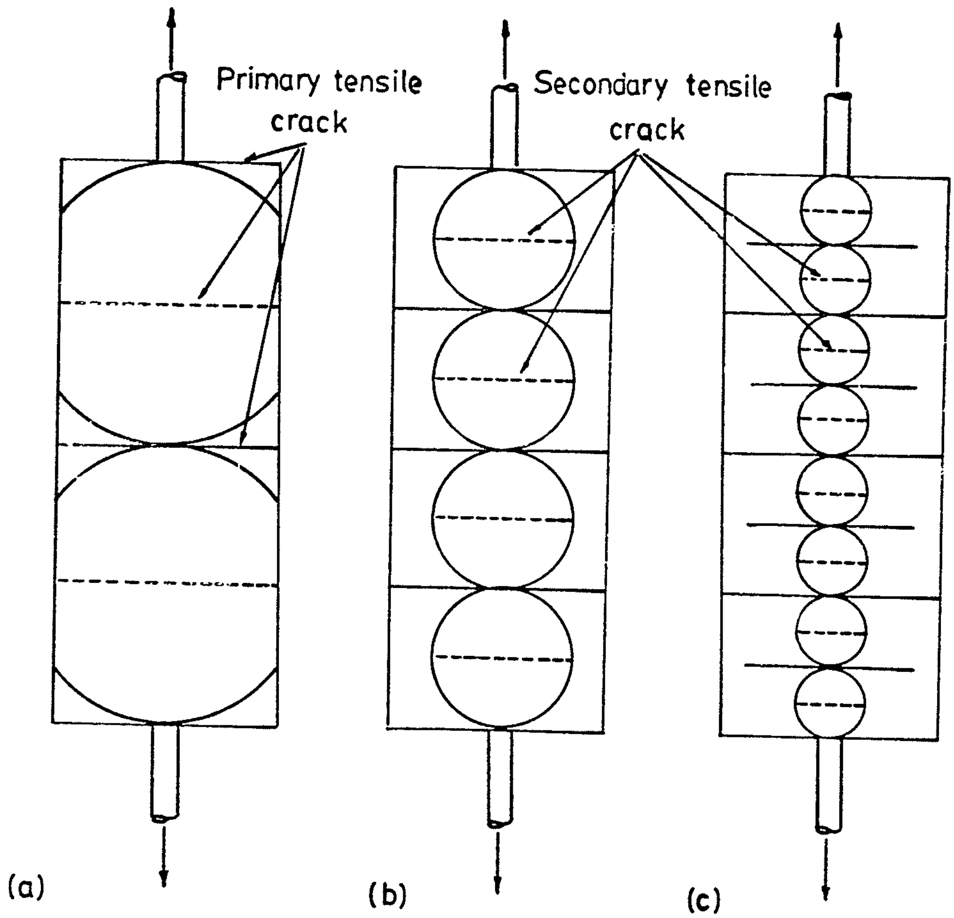

Figure 2.6 Mechanism of Tension Cracking (member reinforced with single bar)

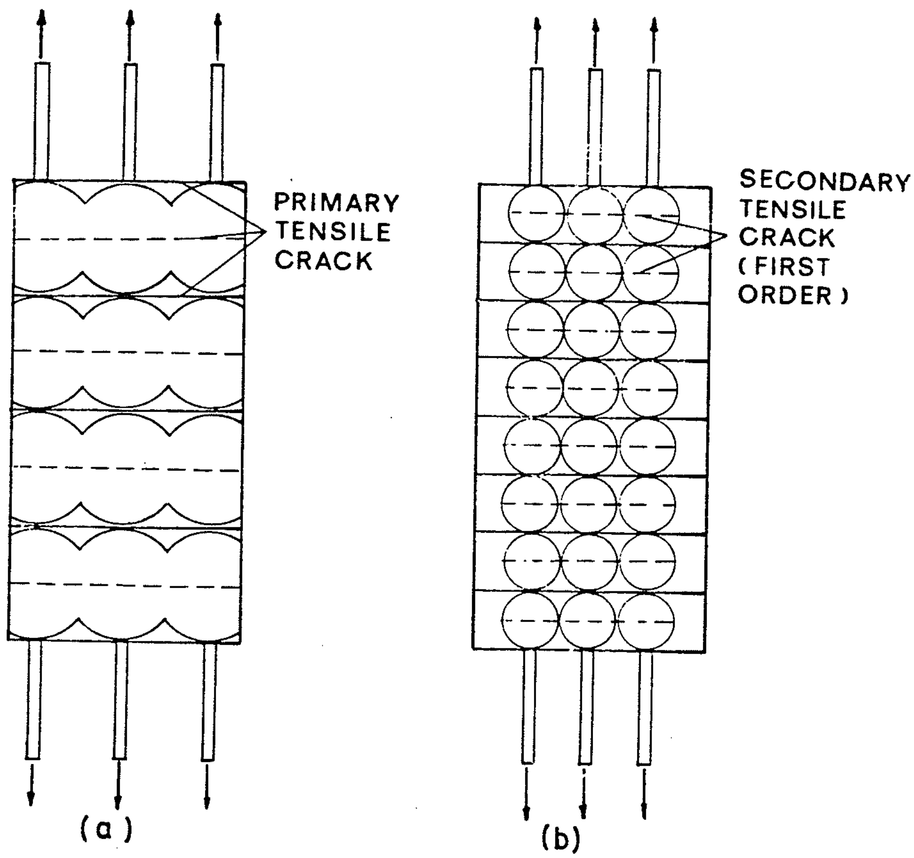

Figure 2.7 Mechanism of Tension Cracking
(member reinforced with several bars)

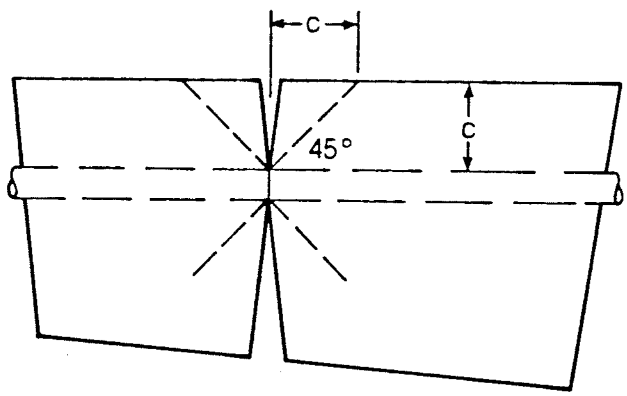

Figure 2.8 Spread of Tensile Stresses
Adjacent to a Crack

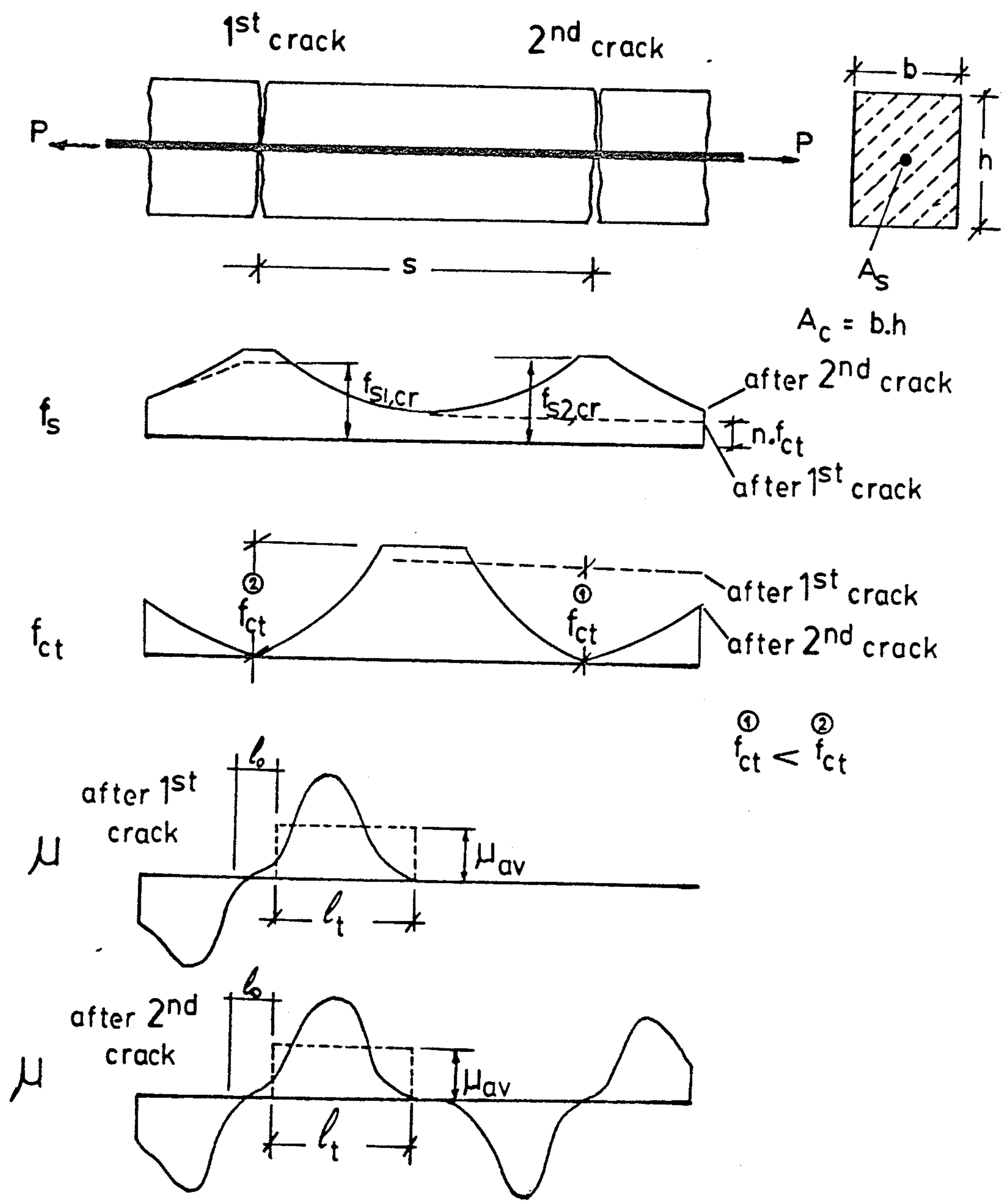

Figure 2.9 Stresses in Concrete and Steel in a R.C. Prism Under Axial Tension

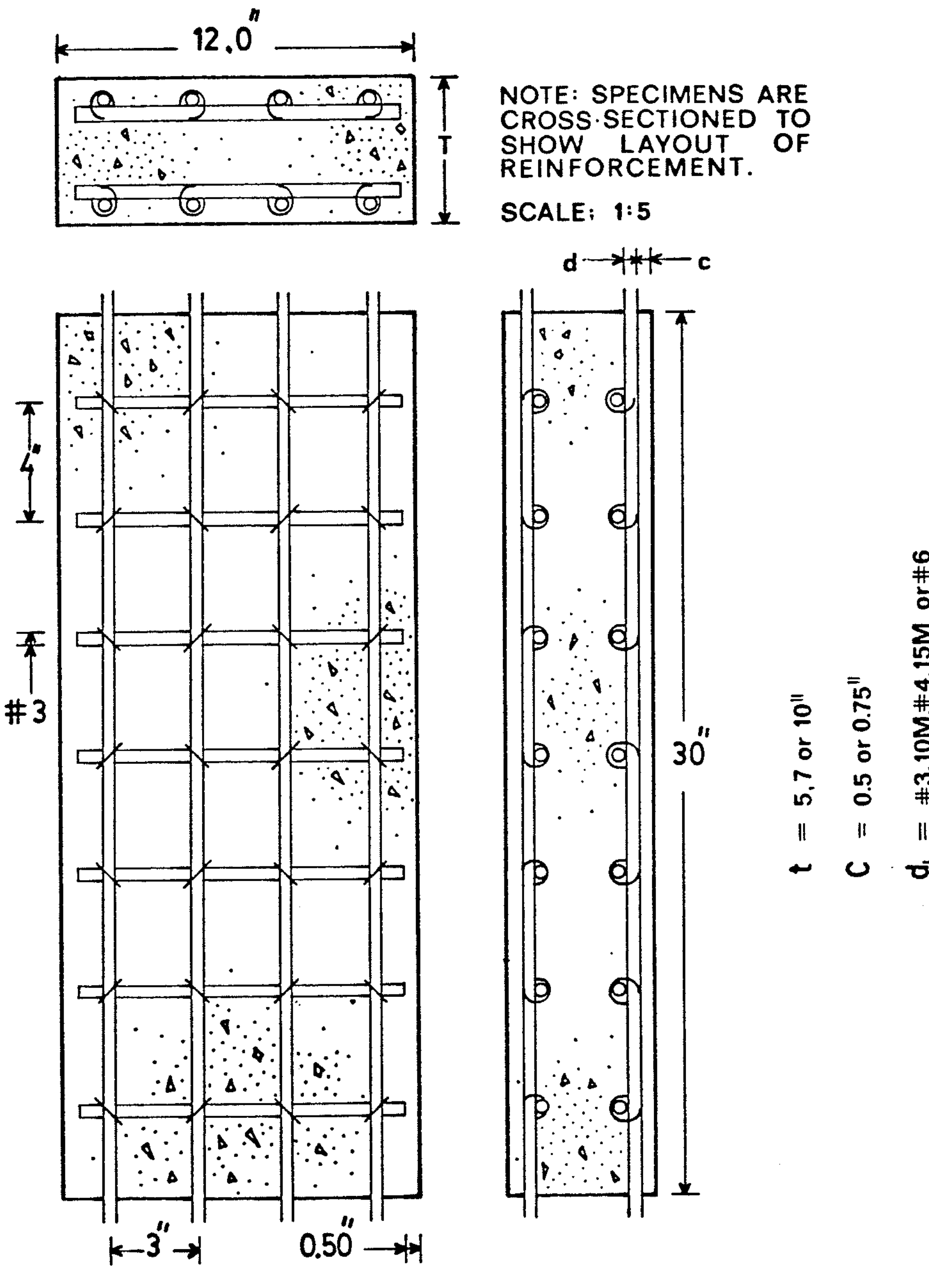

Figure 3.1 Side View of Typical Segment

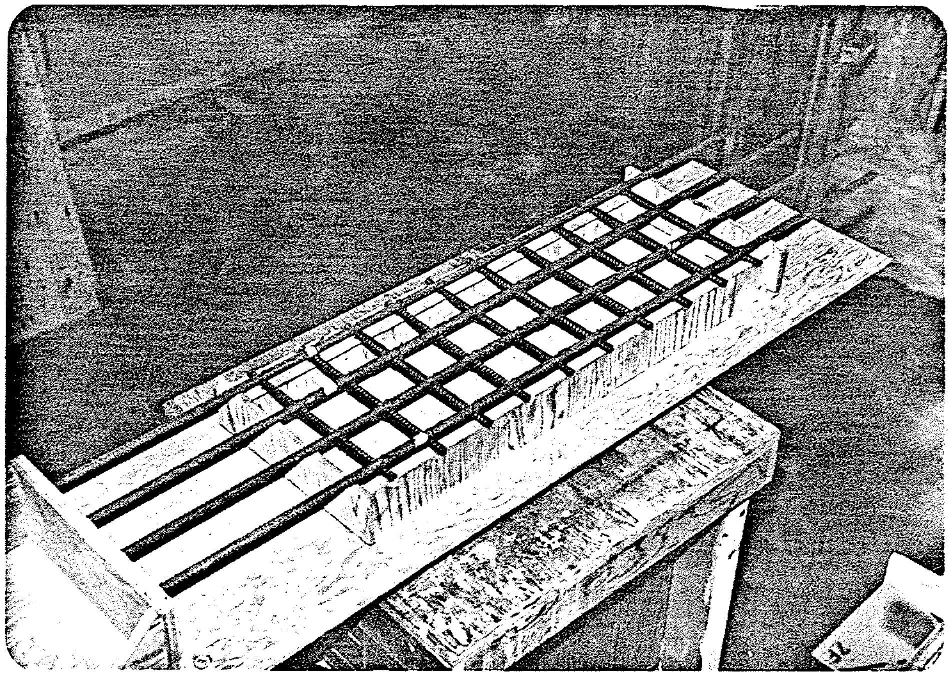

Figure 3.2 Initial Design of the Formwork

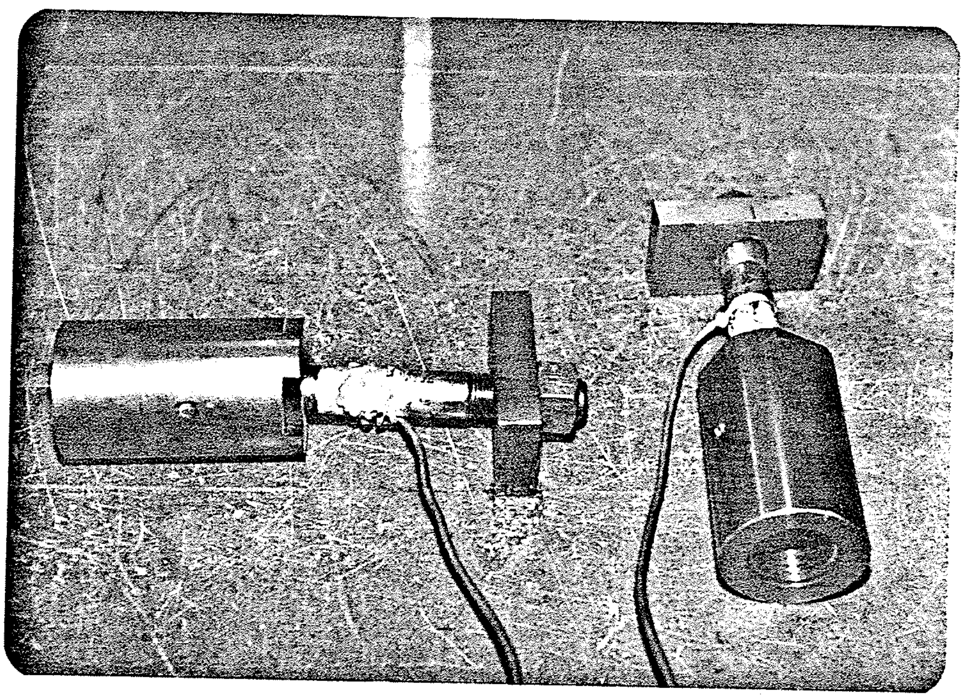

Figure 3.3 Load Cell

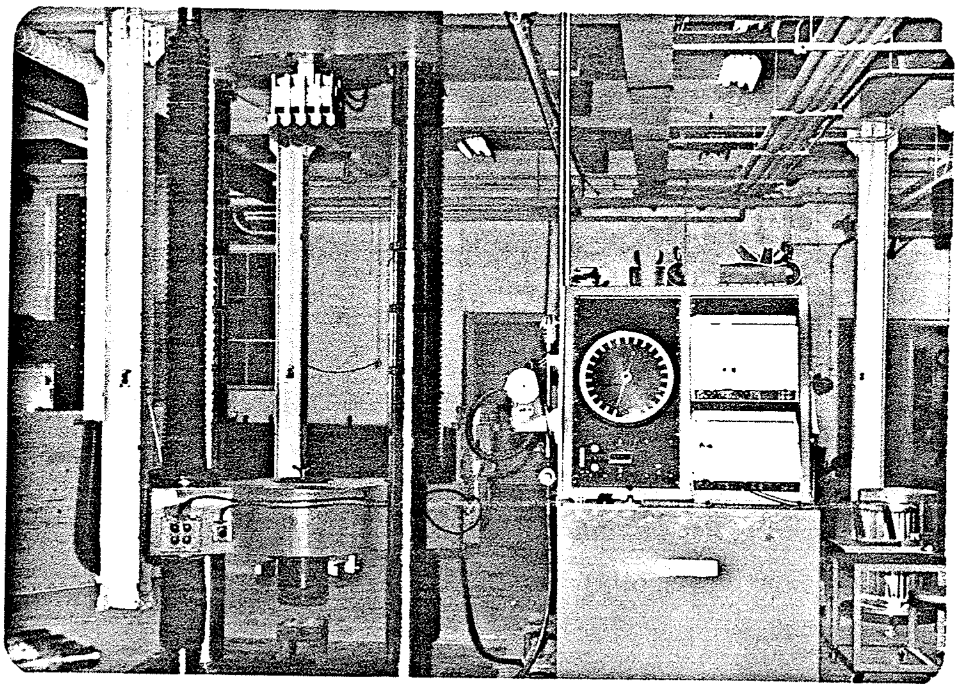

Figure 3.4 Testing Machine

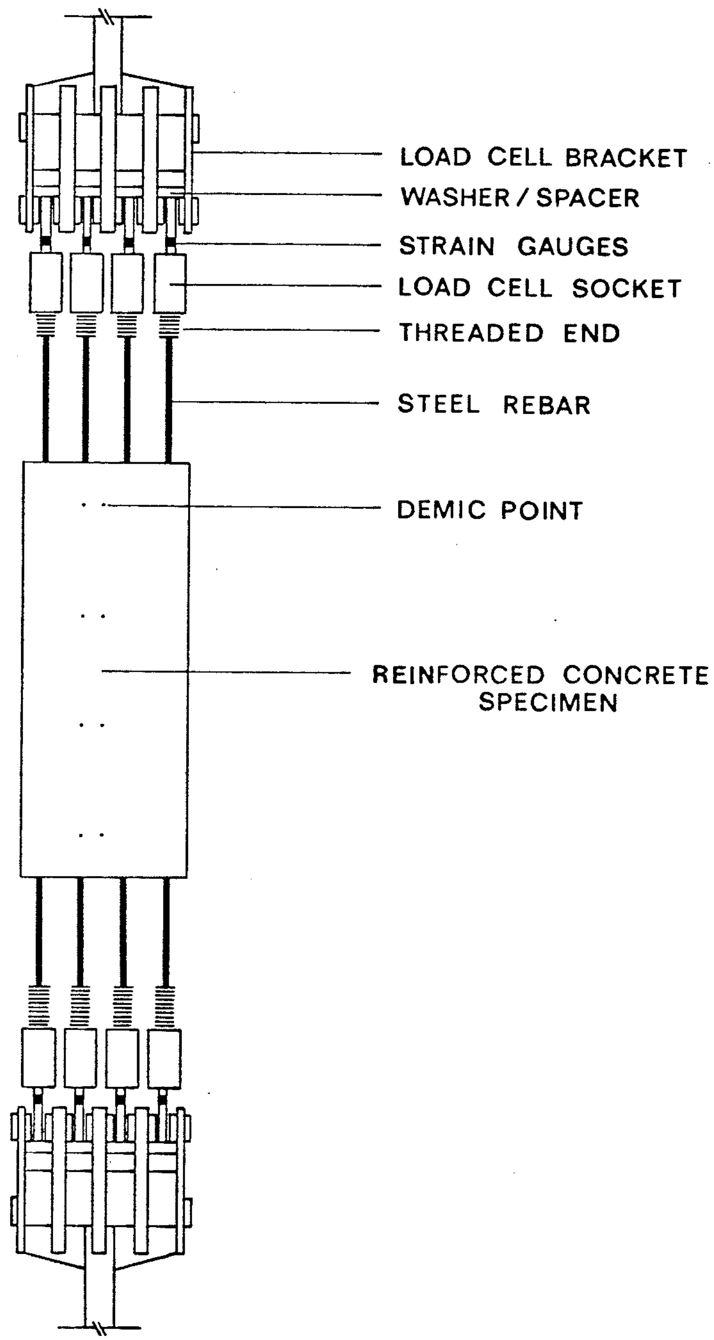

Figure 3.5 Specimen and Apparatus

SCALE: 1:3
ALL DIMENSIONS IN INCHES

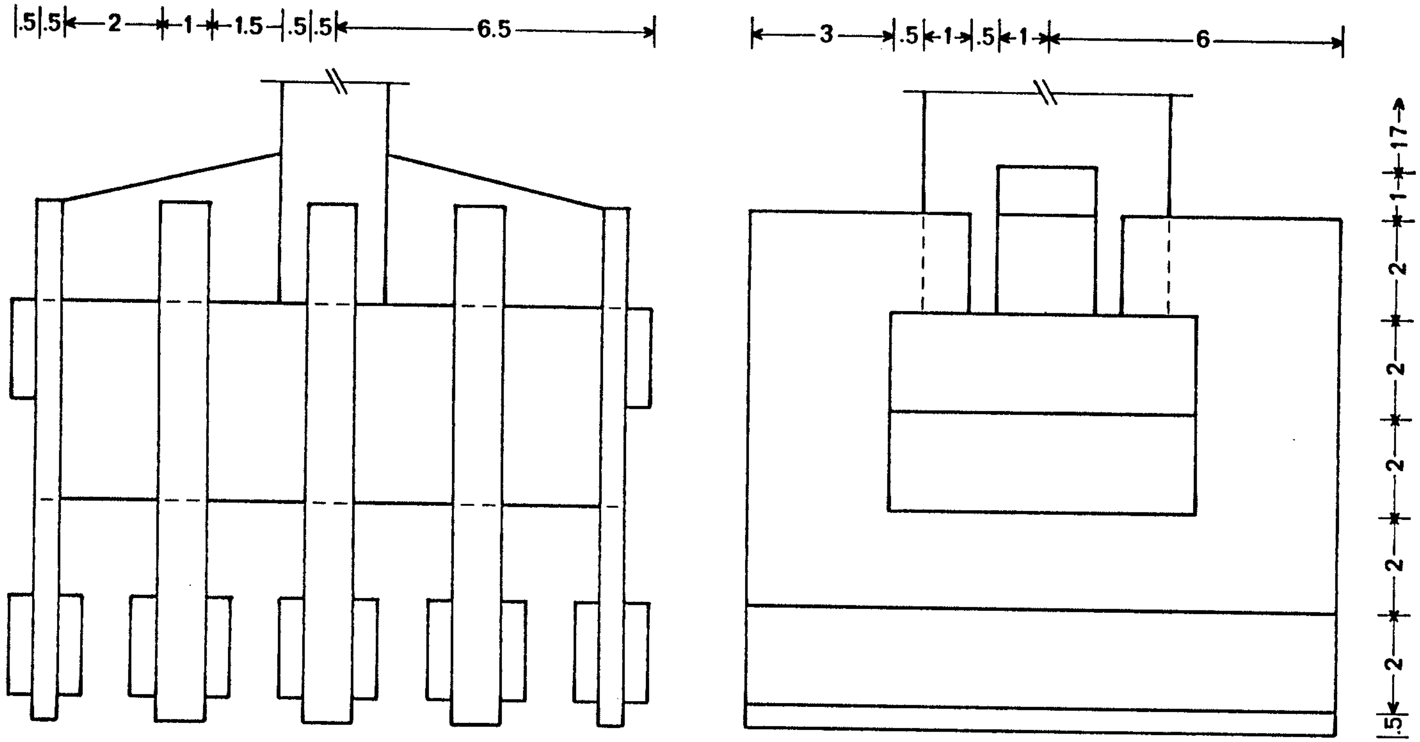

Figure 3.6 End Fitting

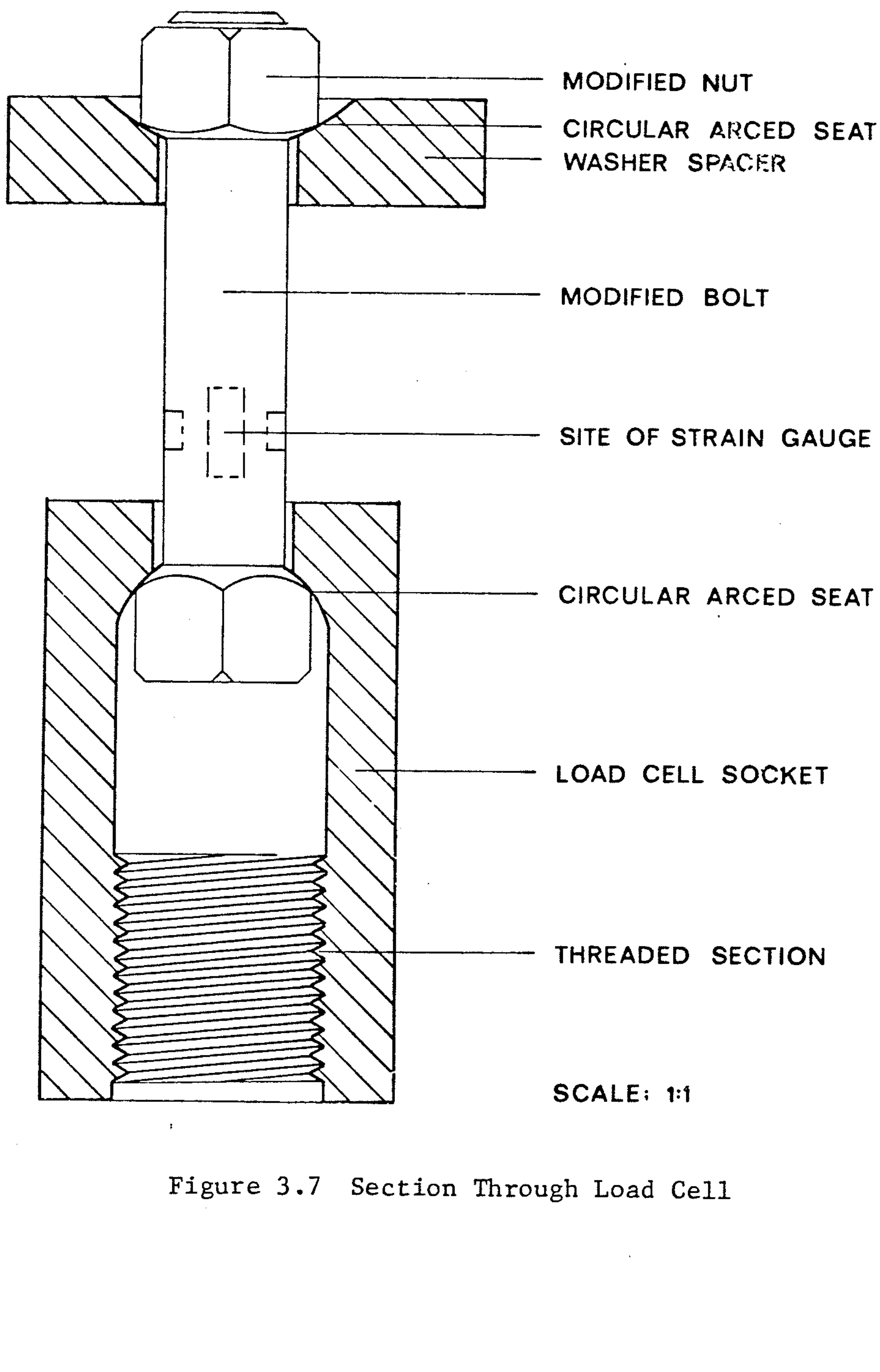

Figure 3.7 Section Through Load Cell

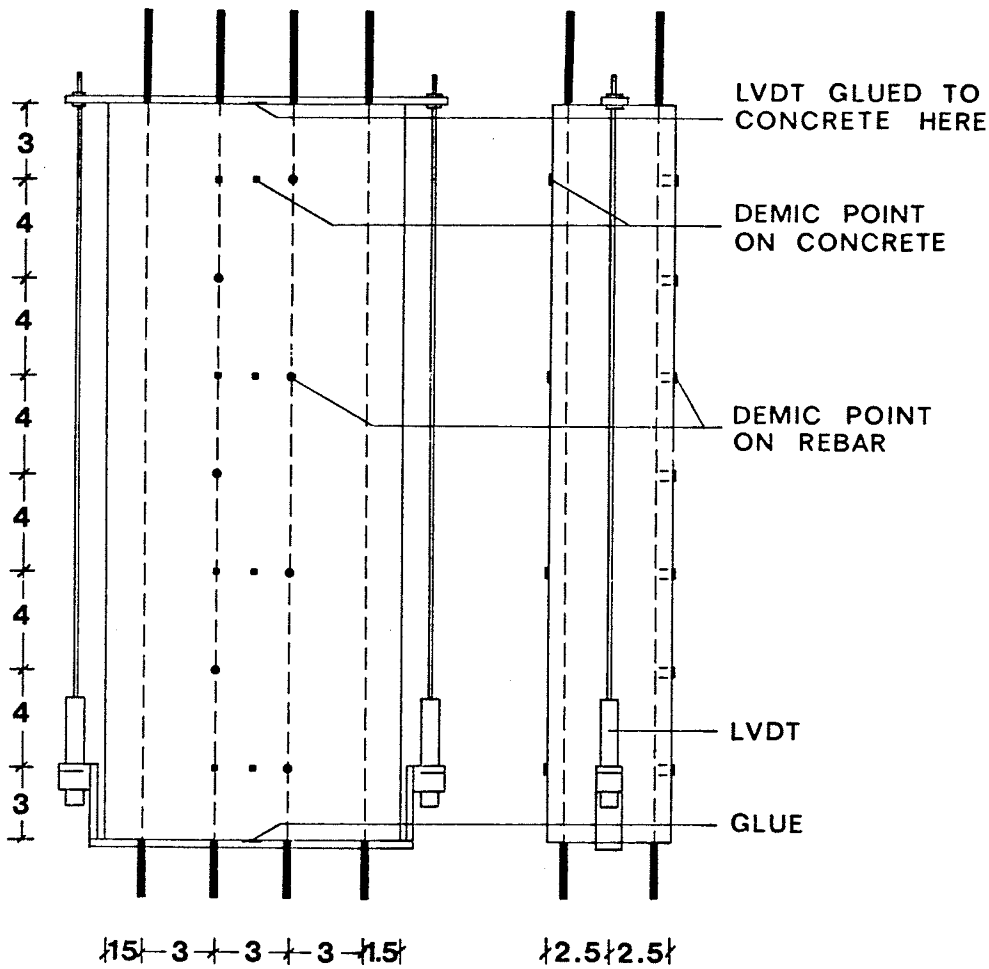

Figure 3.8 Positions of Demic Points and LVDT's

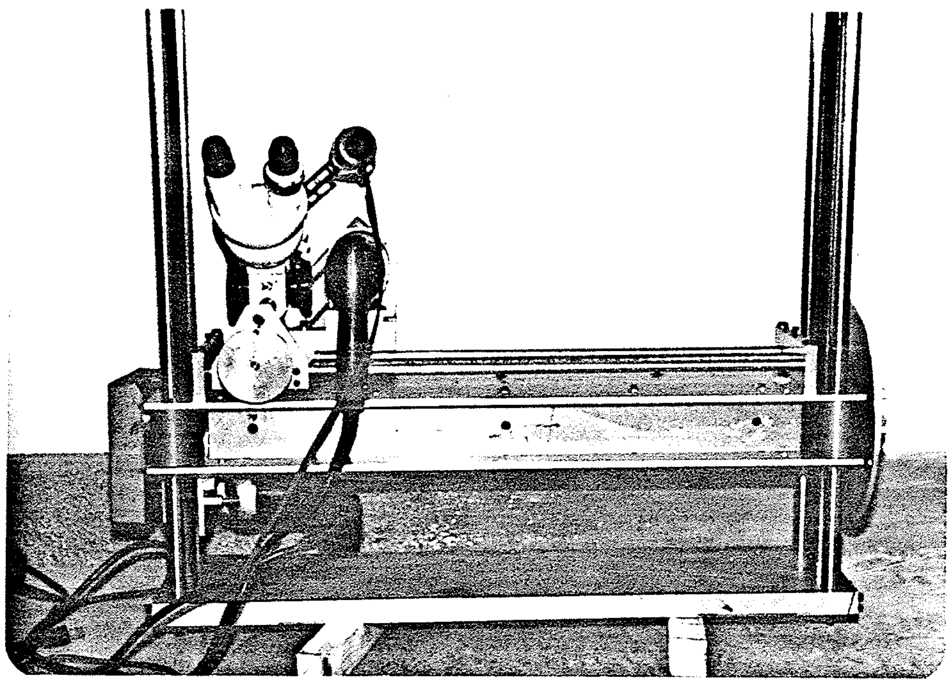

Figure 3.9 Microscope and Frame

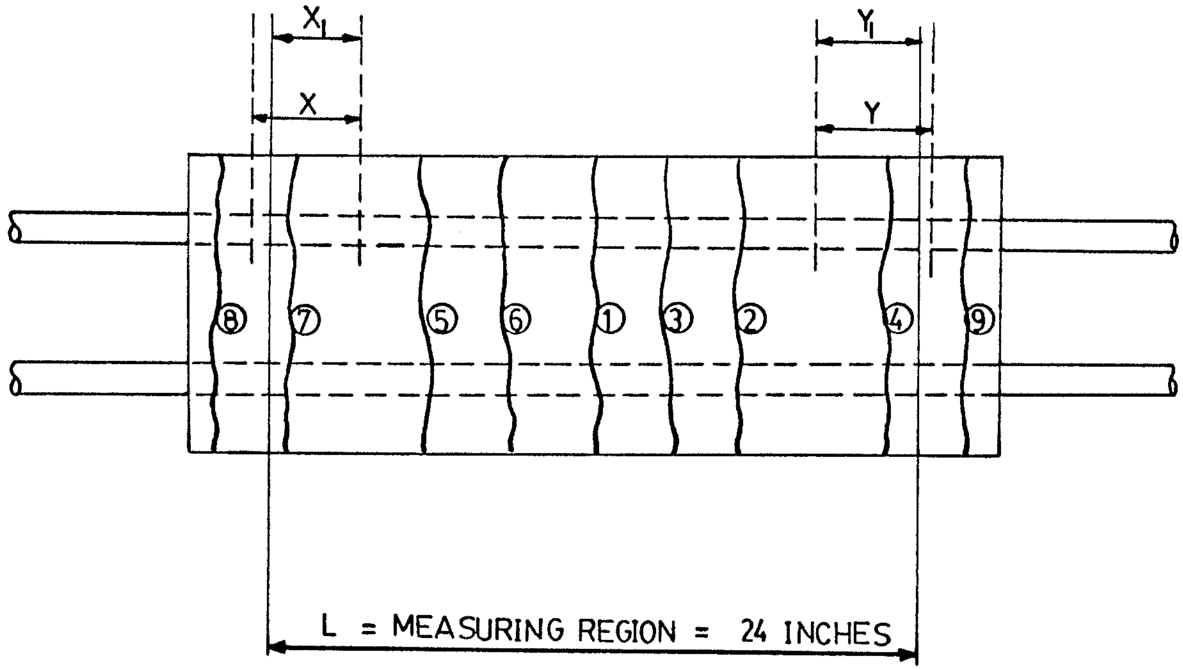

$$N = \text{NUMBER OF CRACKS} = \frac{X_1}{X} + 5 + \frac{Y_1}{Y}$$

$$\text{AVERAGE SPACING} = \frac{L}{N}$$

Figure 4.1 Method and Location of Crack Measurement

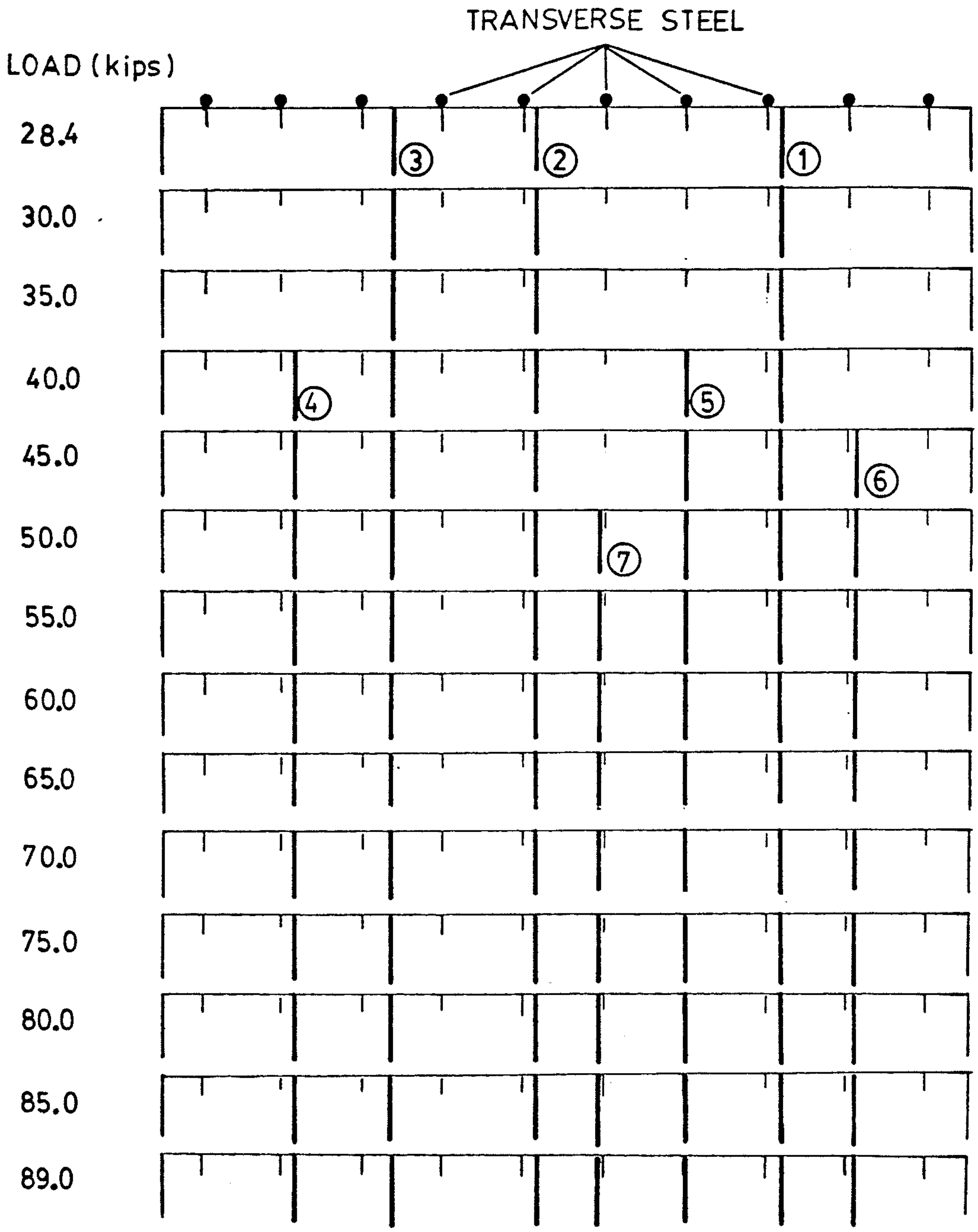

Figure T3A.P1 Sequence of Crack Formation

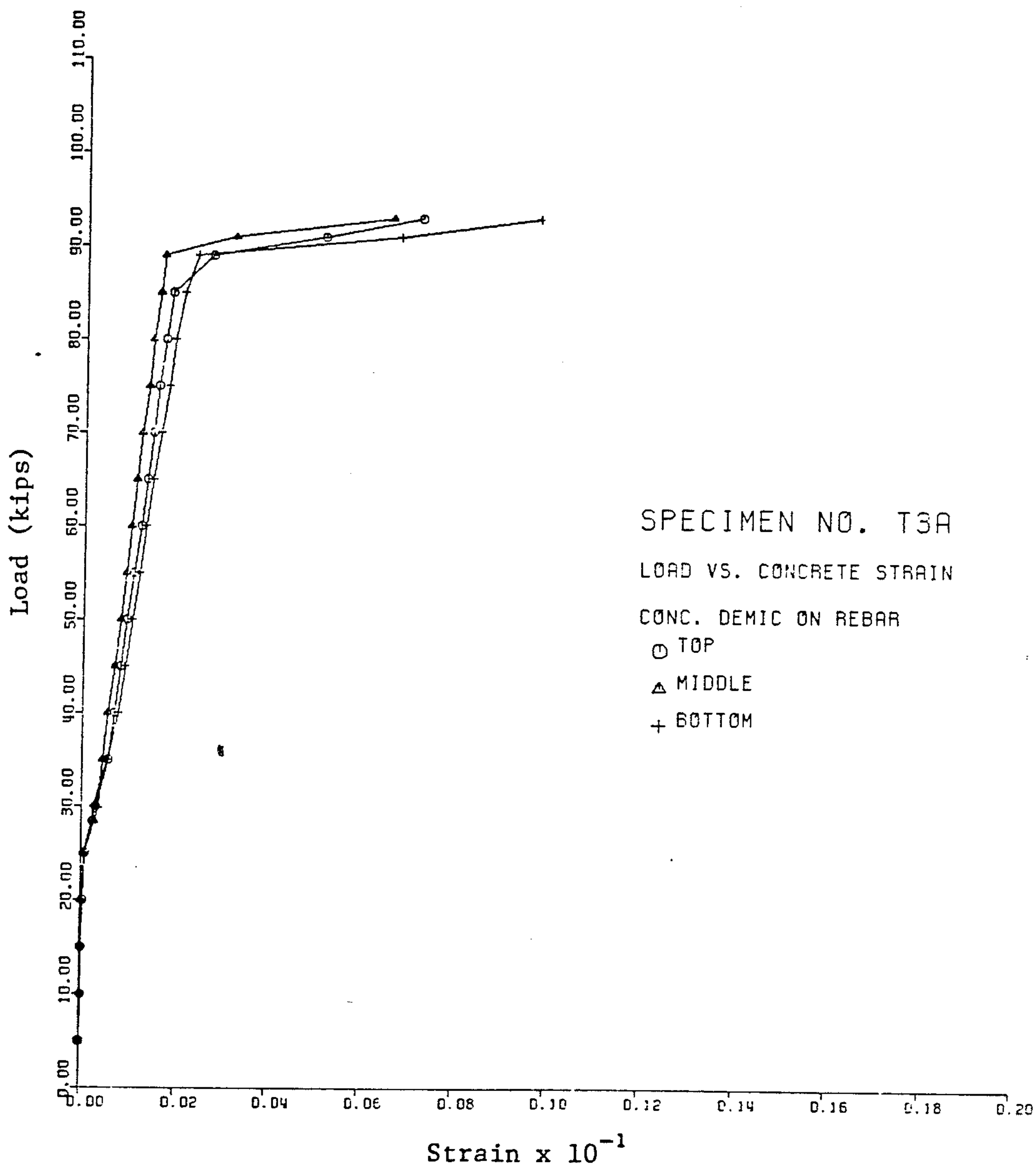

Figure T3A.P2 Load-Concrete STrain, Demic on Rebar for Segment T3A

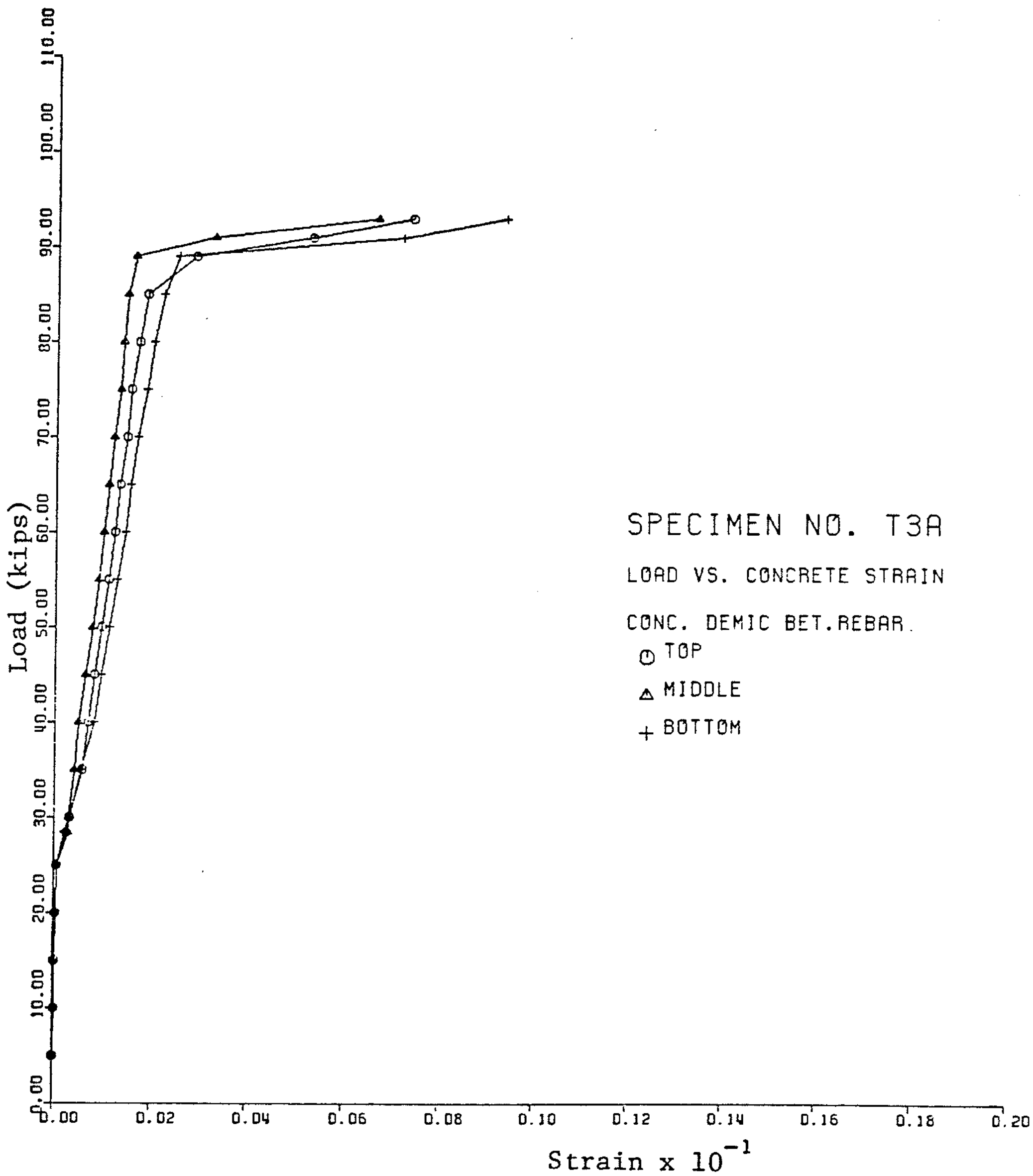

Figure T3A.P3 Load-Concrete STrain, Demic Between Rebar for Segment T3A

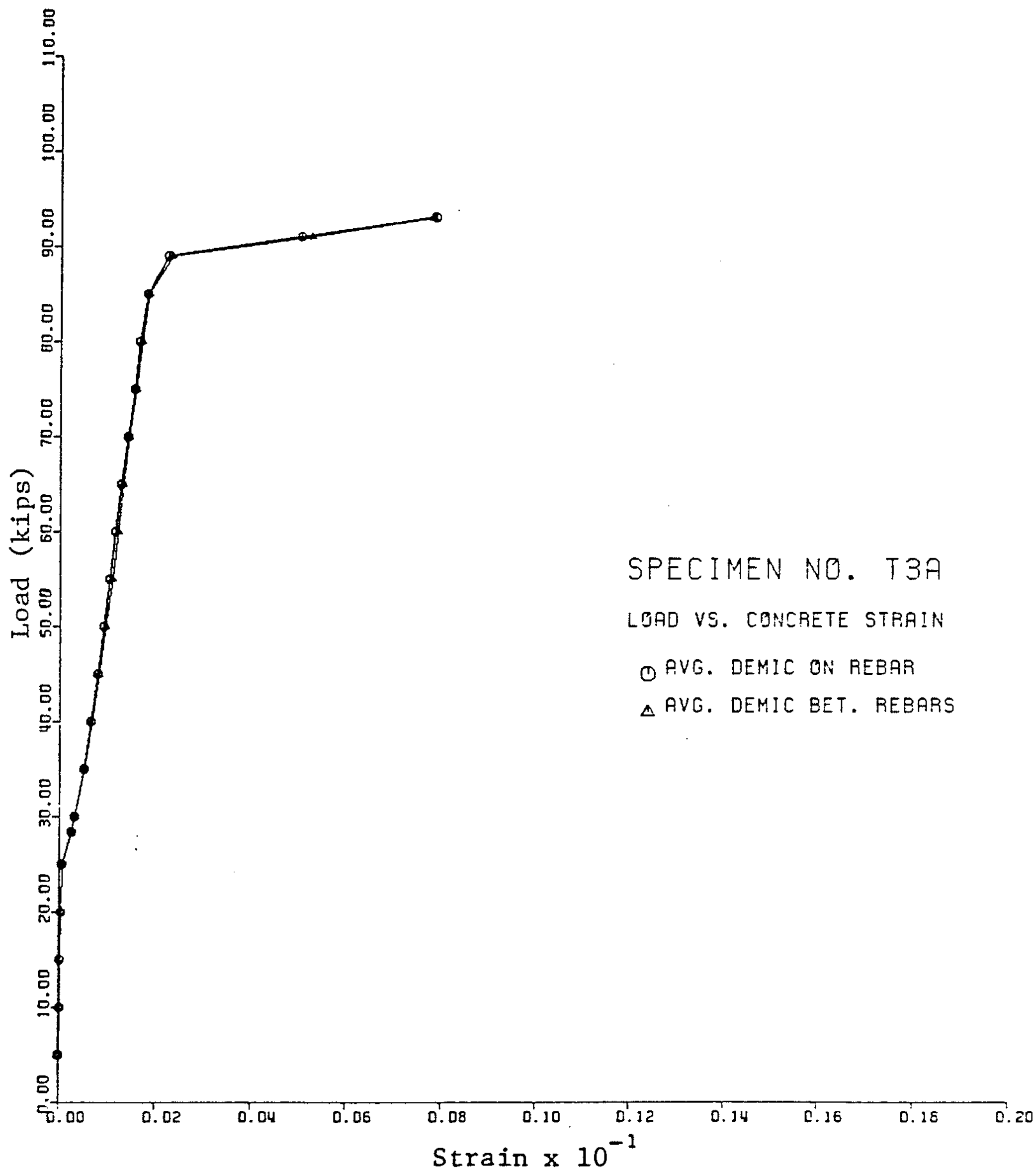

Figure T3A.P4 Load-Average Concrete Strain,
Segment T3A

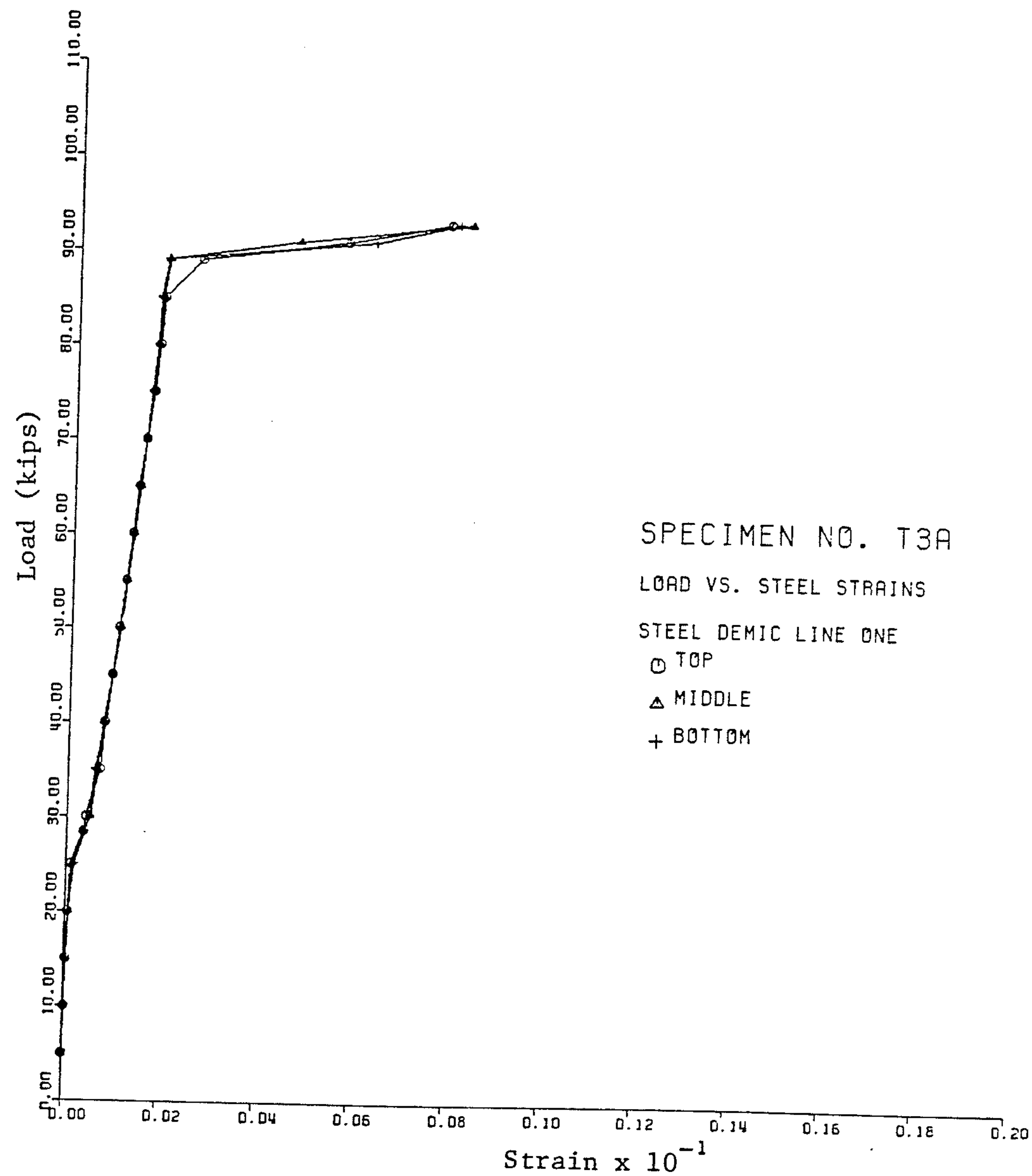

Figure T3A.P5 Load-Steel Strains, Demic on Line One for Segment T3A

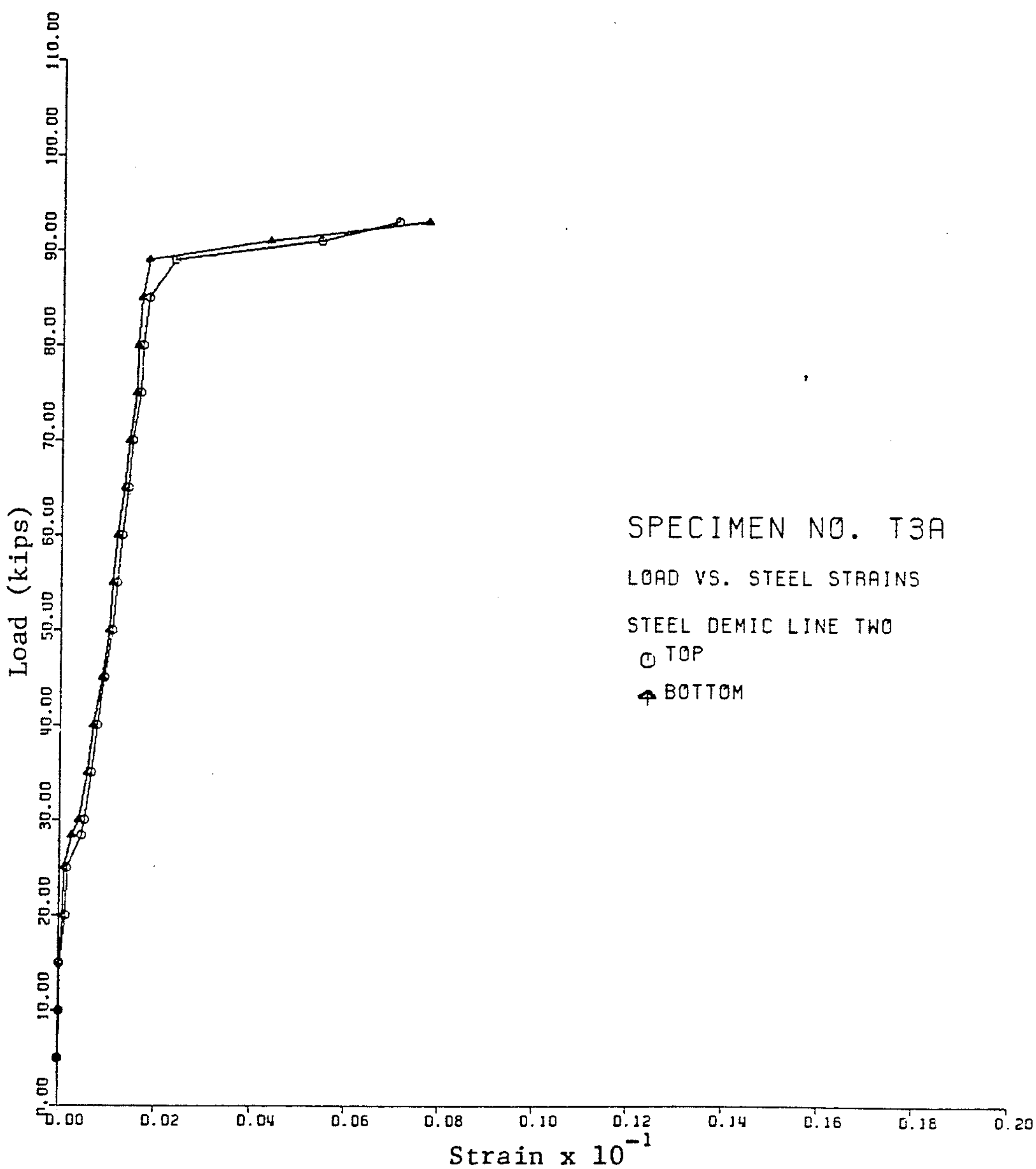

Figure T3A.P6 Load-Steel Strains, Demic on Line Two for Segment T3A

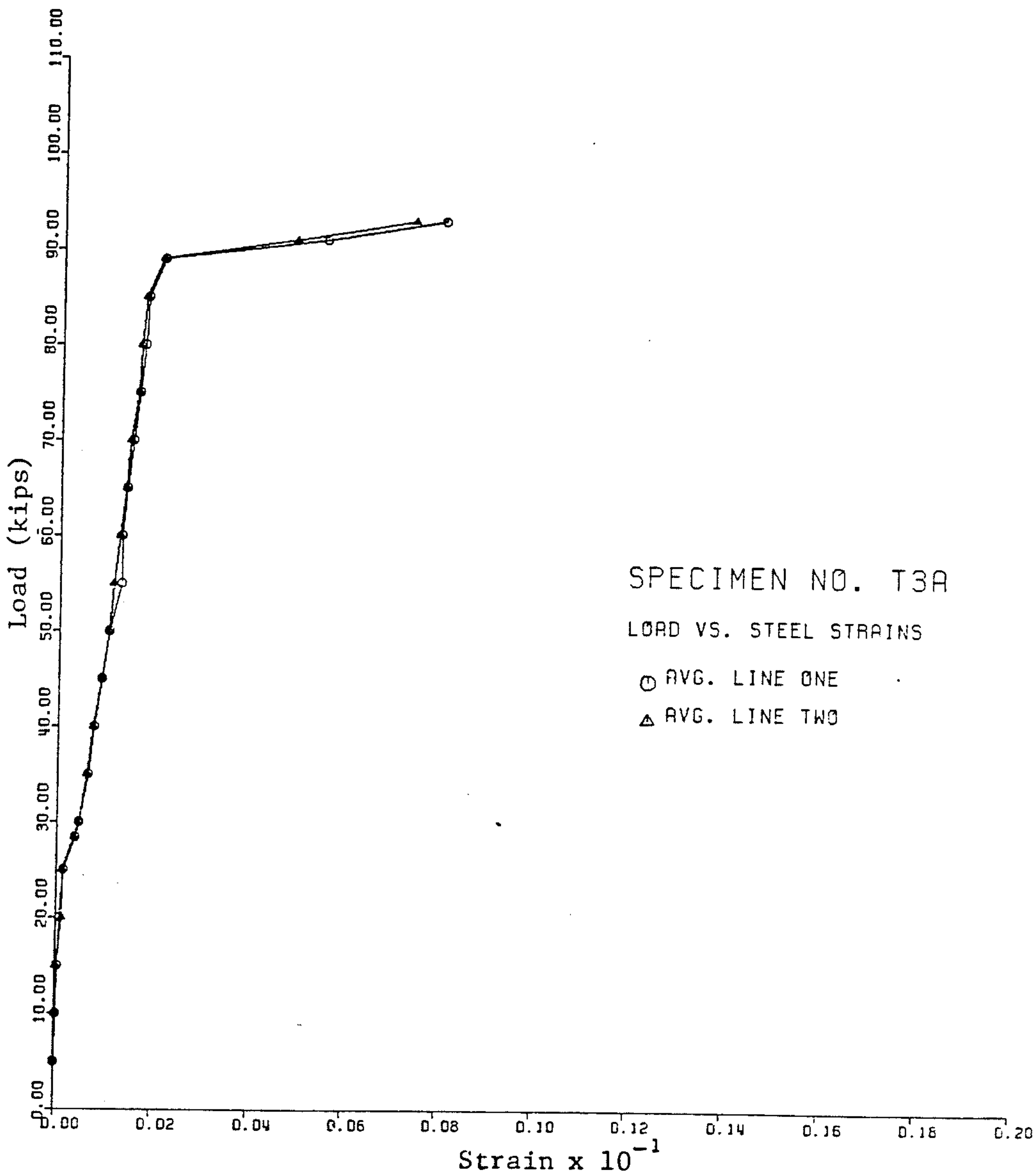

Figure T3A.P7 Load-Average Steel Strains

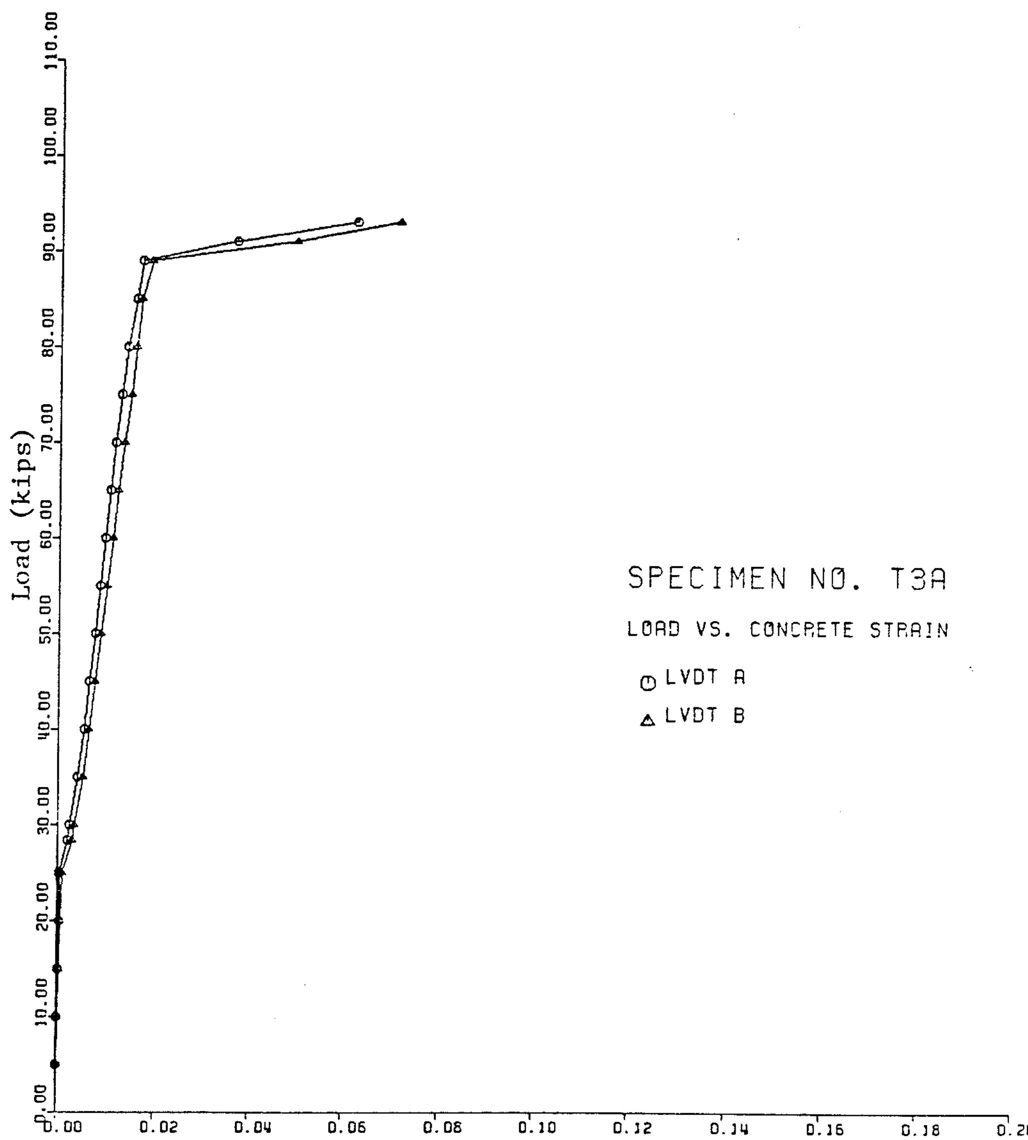

Strain x 10^{-1}

Figure T3A.P8 Load-Gross Strain

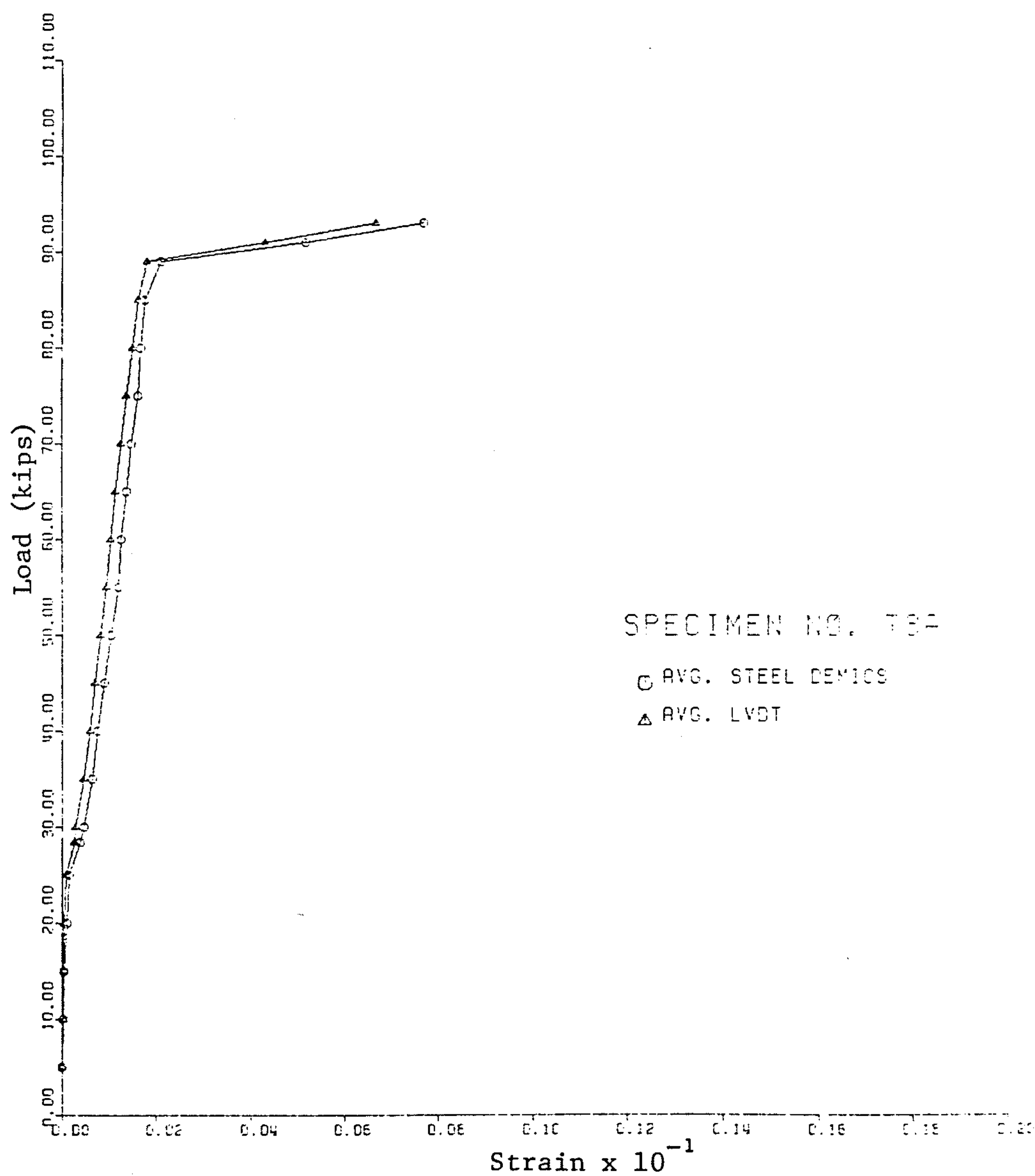

Figure T3A.P9 Load-Average Steel Strains and Gross Strain for Segment T3A

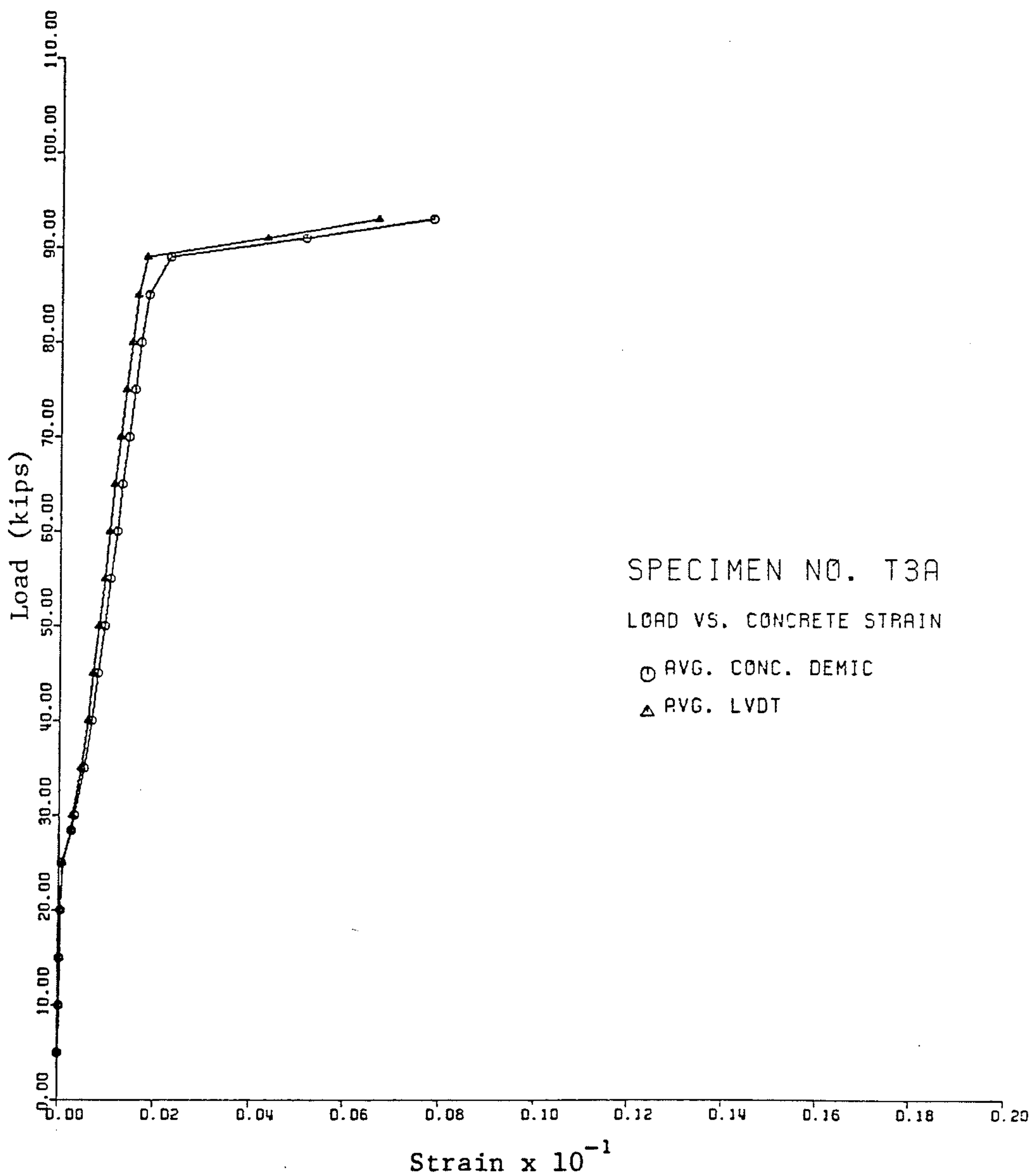

Figure T3A.P10 Load-Average Concrete Strain, Segment T3A

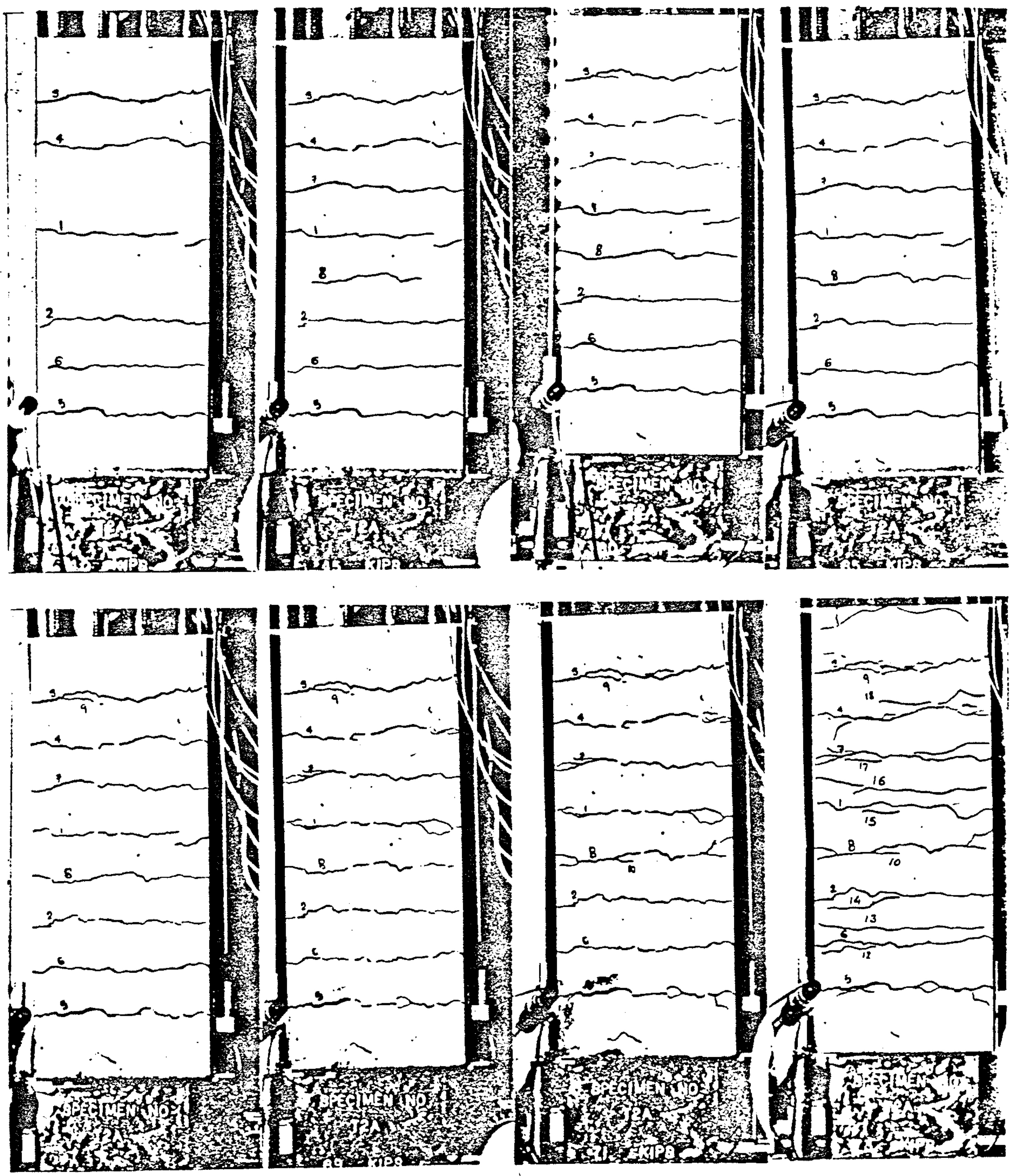

Figure 5.1 Cracking Sequence - Specimen T2A (Side A)

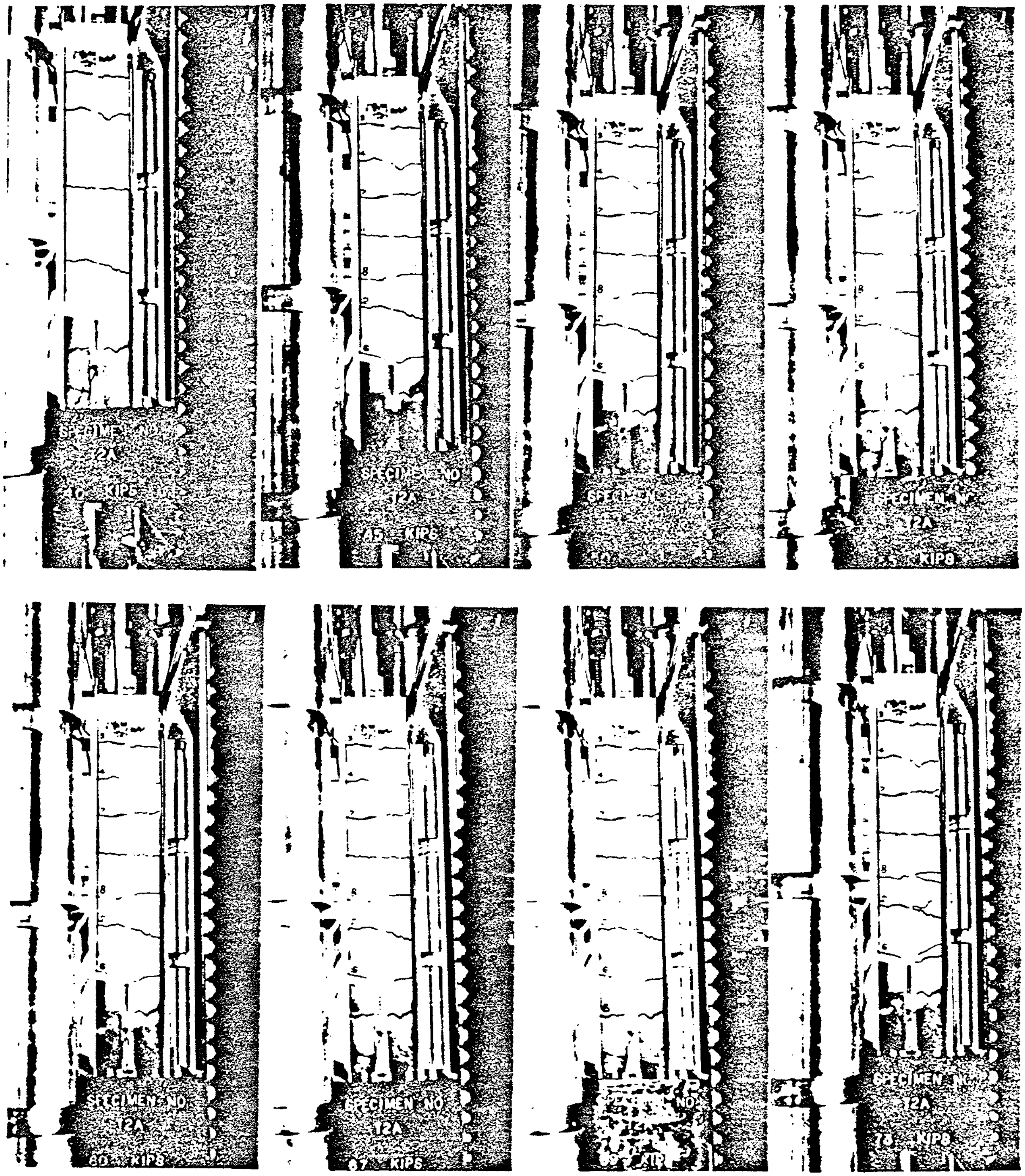

Figure 5.2 Cracking Sequence - Specimen T2A (Edge A)

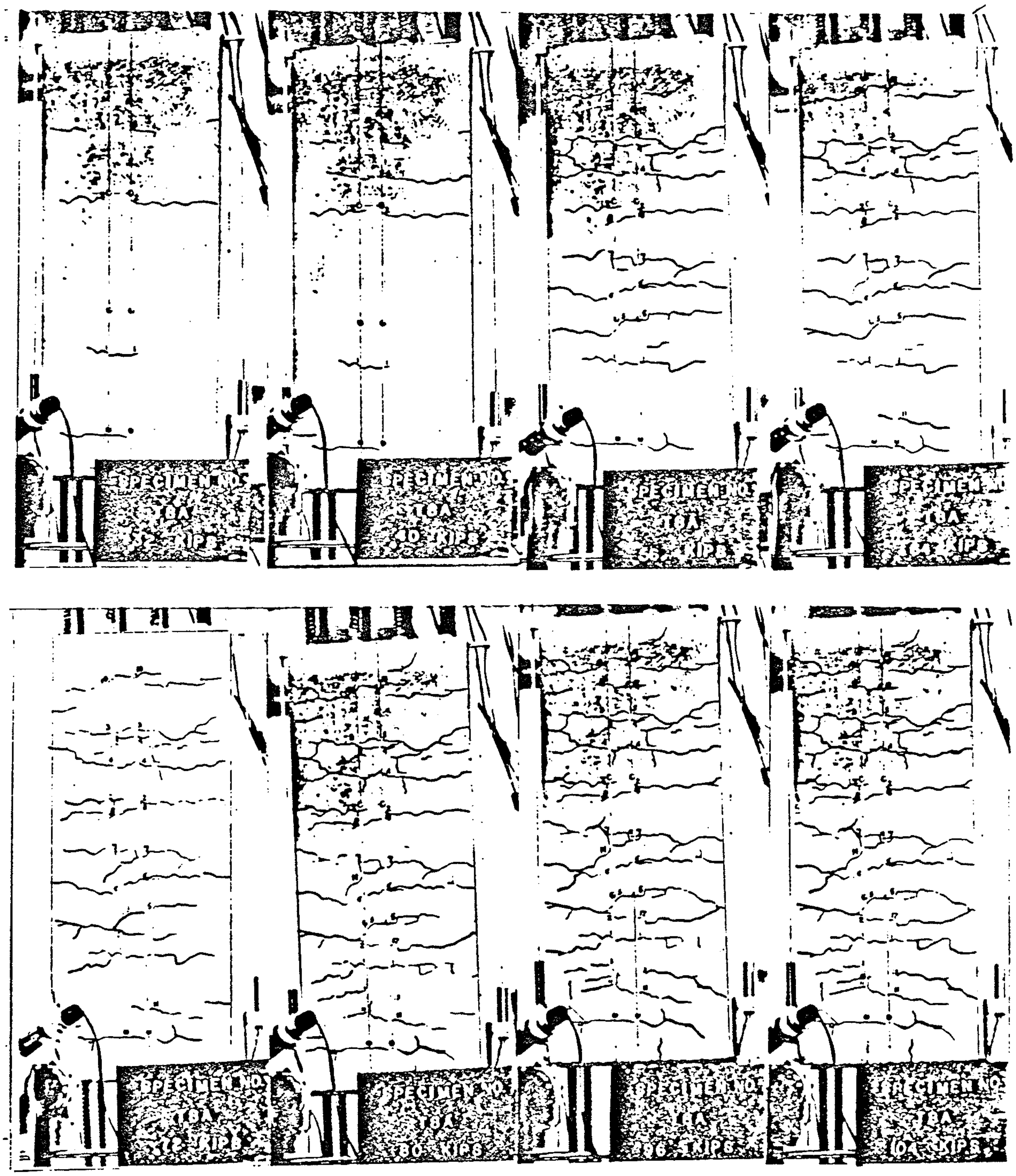

Figure 5.3 Cracking Sequence - Specimen T8A (Side A)

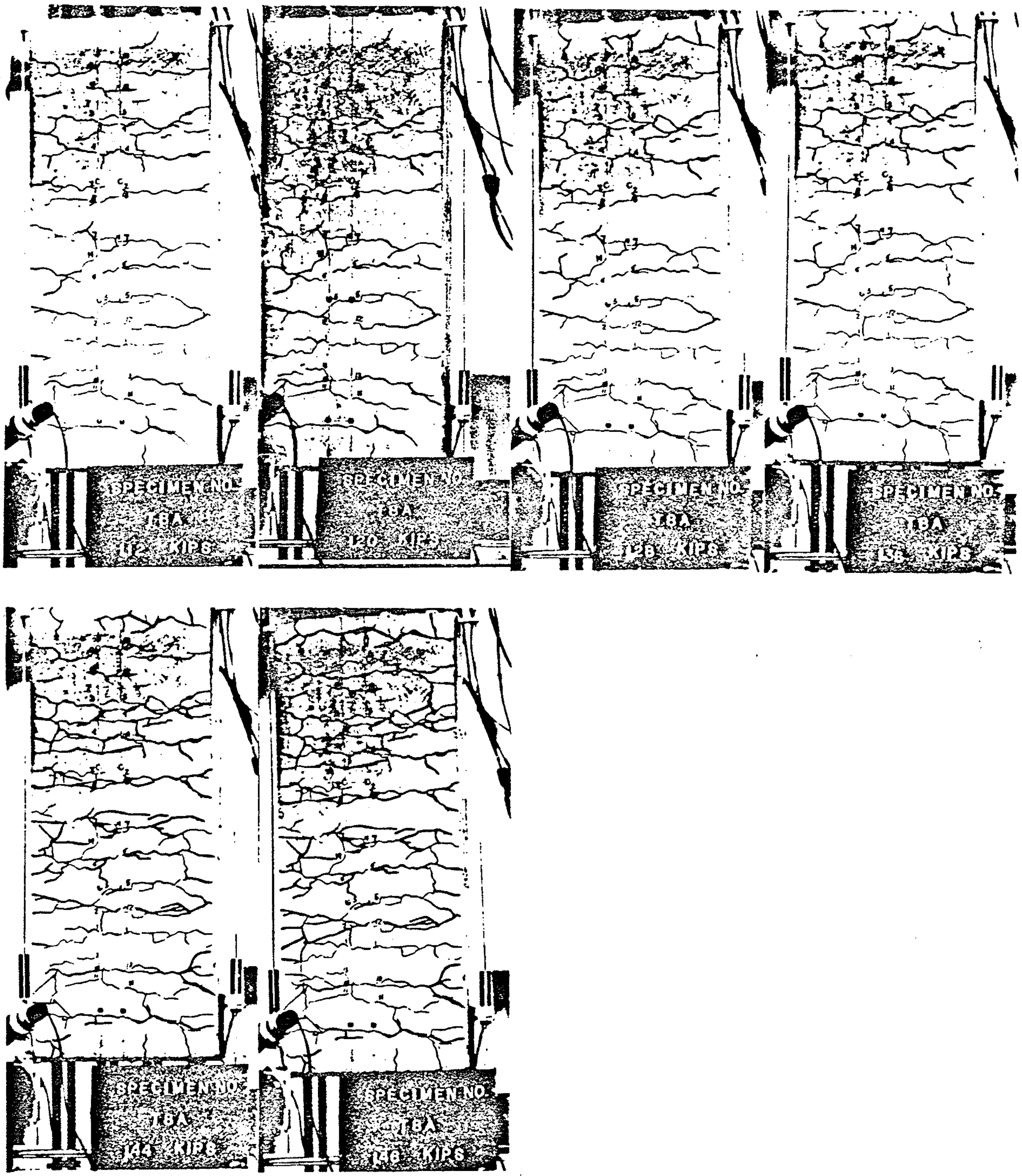

Figure 5.3 Cracking Sequence - Specimen T8A (Side A)

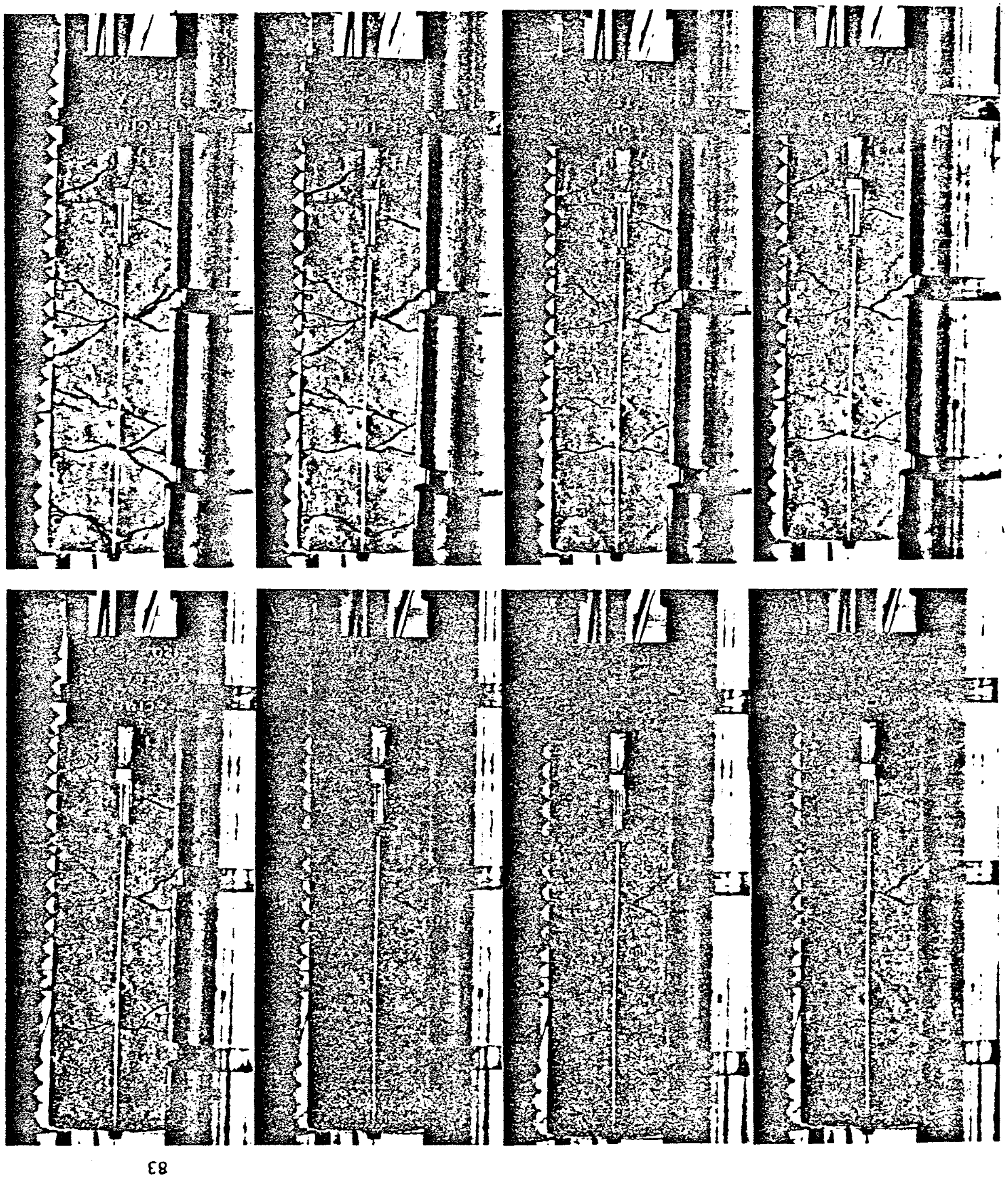

Figure 5.4 Cracking Sequence - Specimen T8A (Edge A)

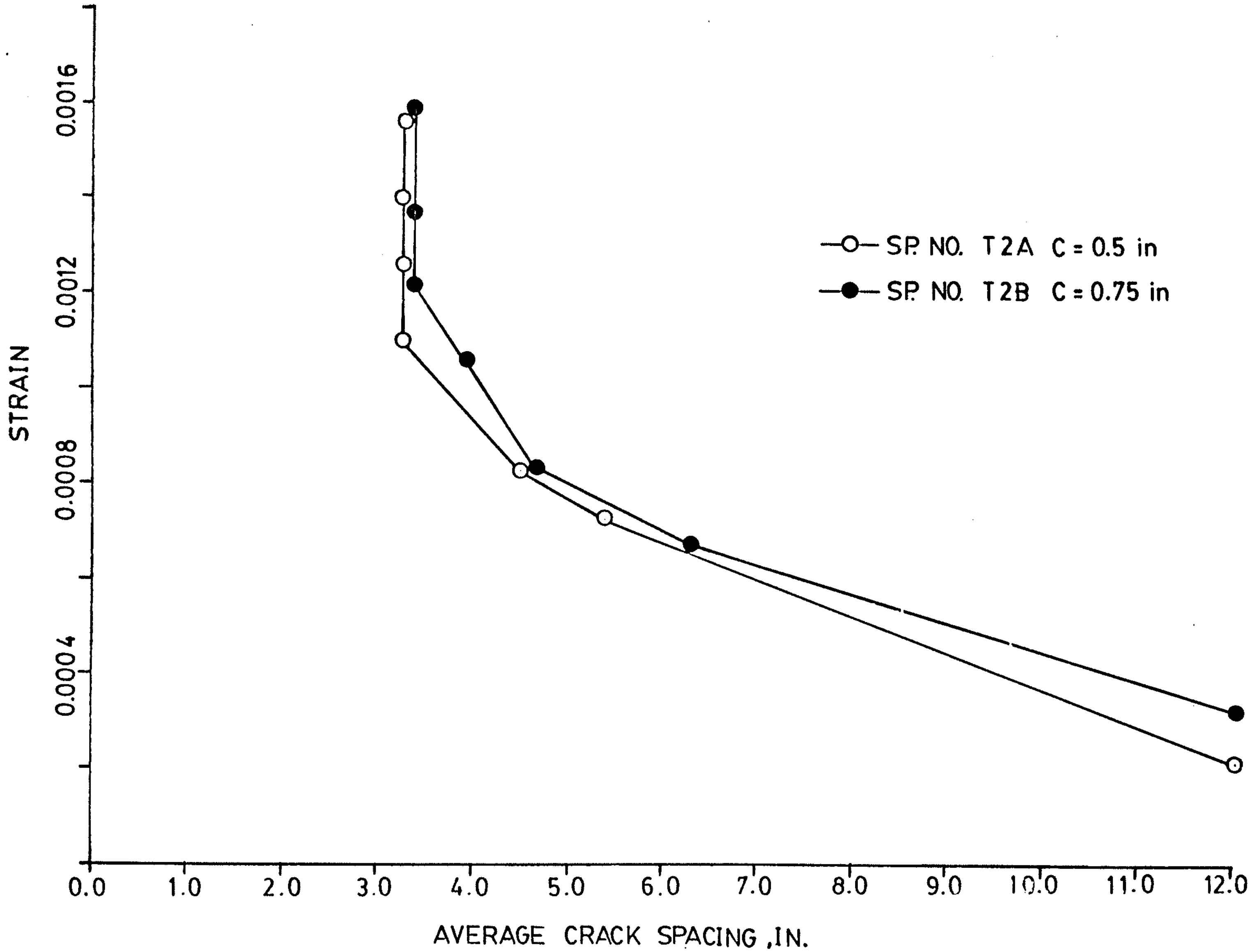

Figure 5.5 Effect of Concrete Cover on Crack Spacing

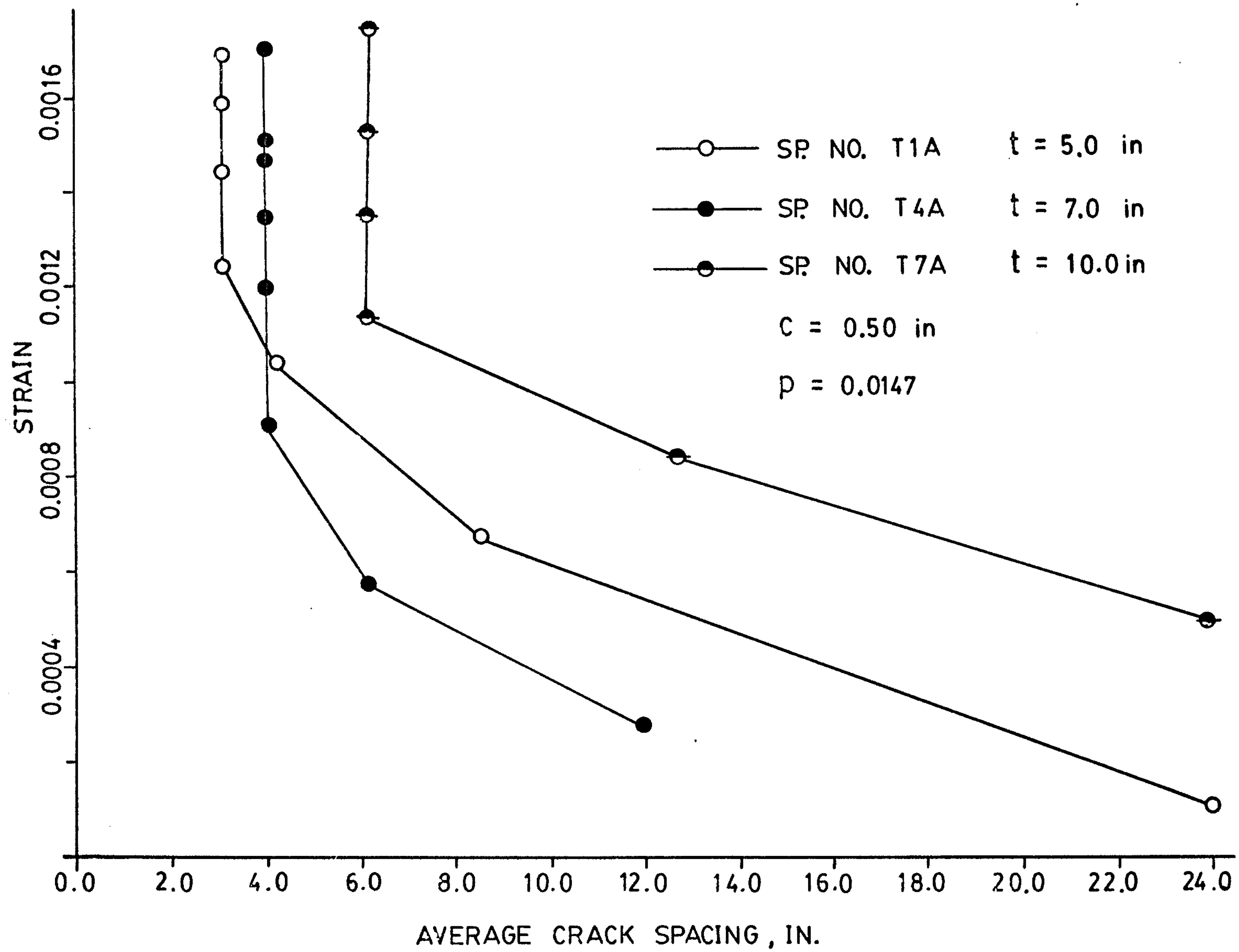

Figure 5.6 Effect of Concrete Thickness on Crack Spacing

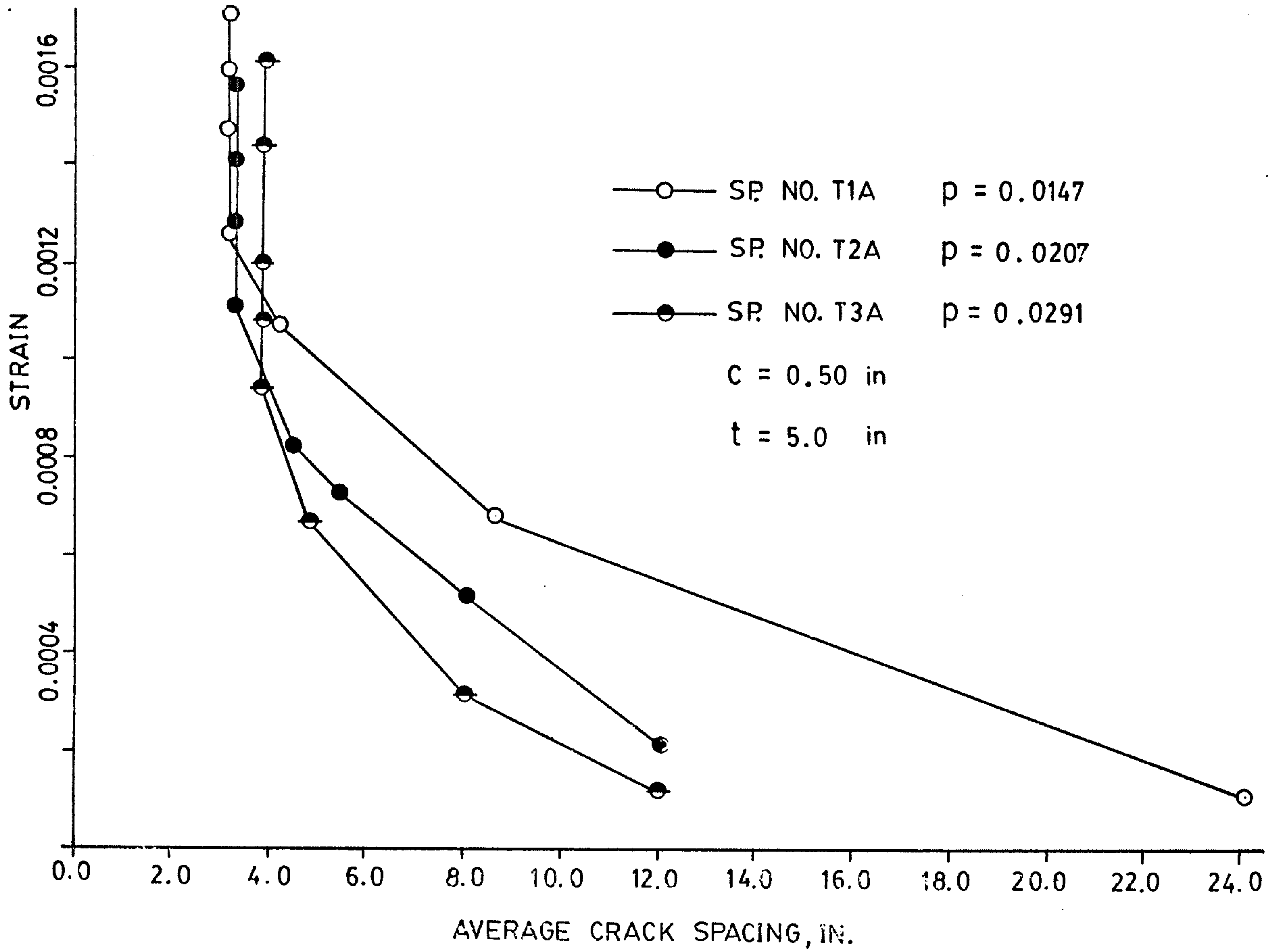

Figure 5.7(a) Effect of Steel Ratio on Crack Spacing

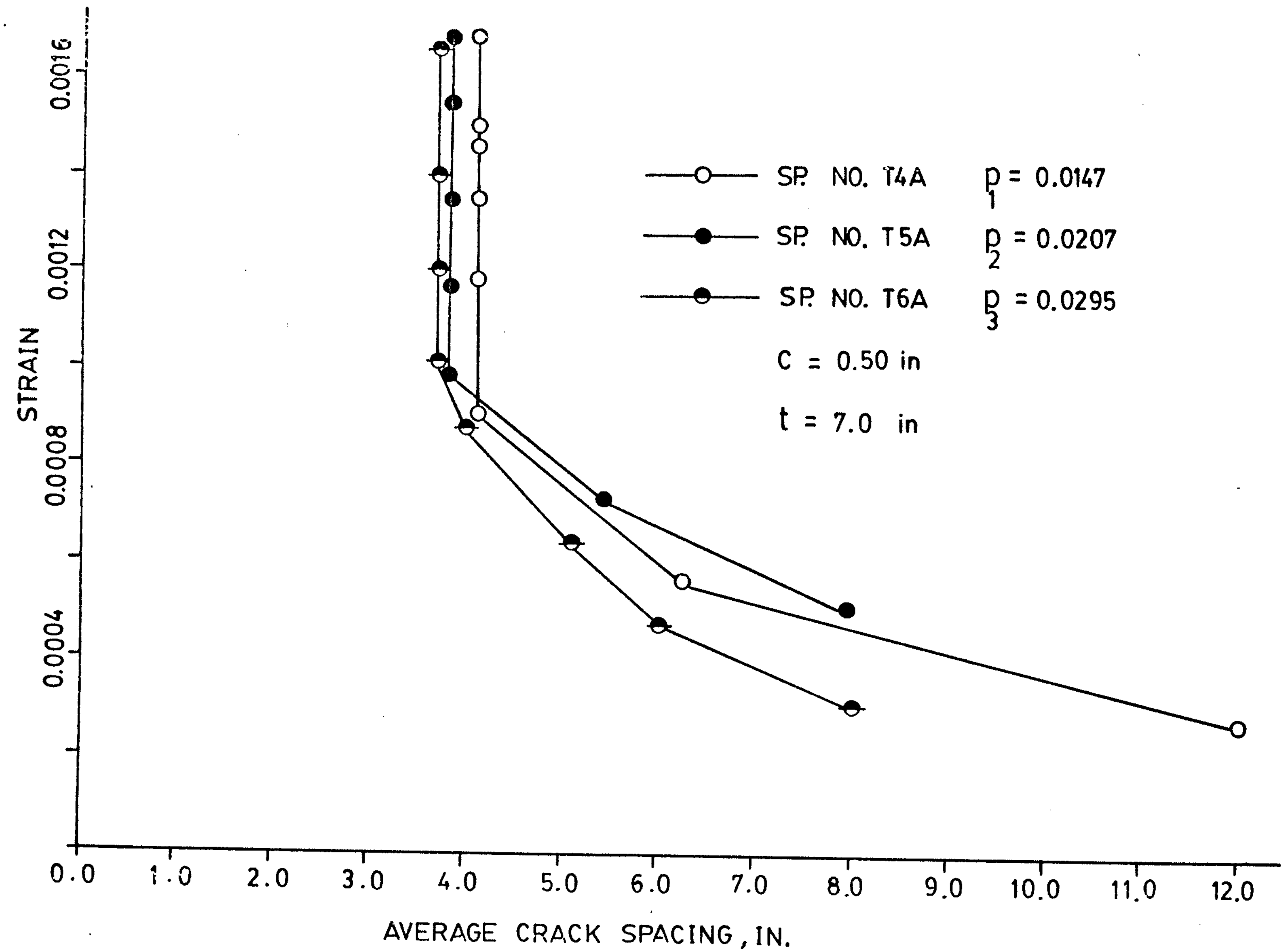

Figure 5.7(b) Effect of Steel Ratio on Crack Spacing

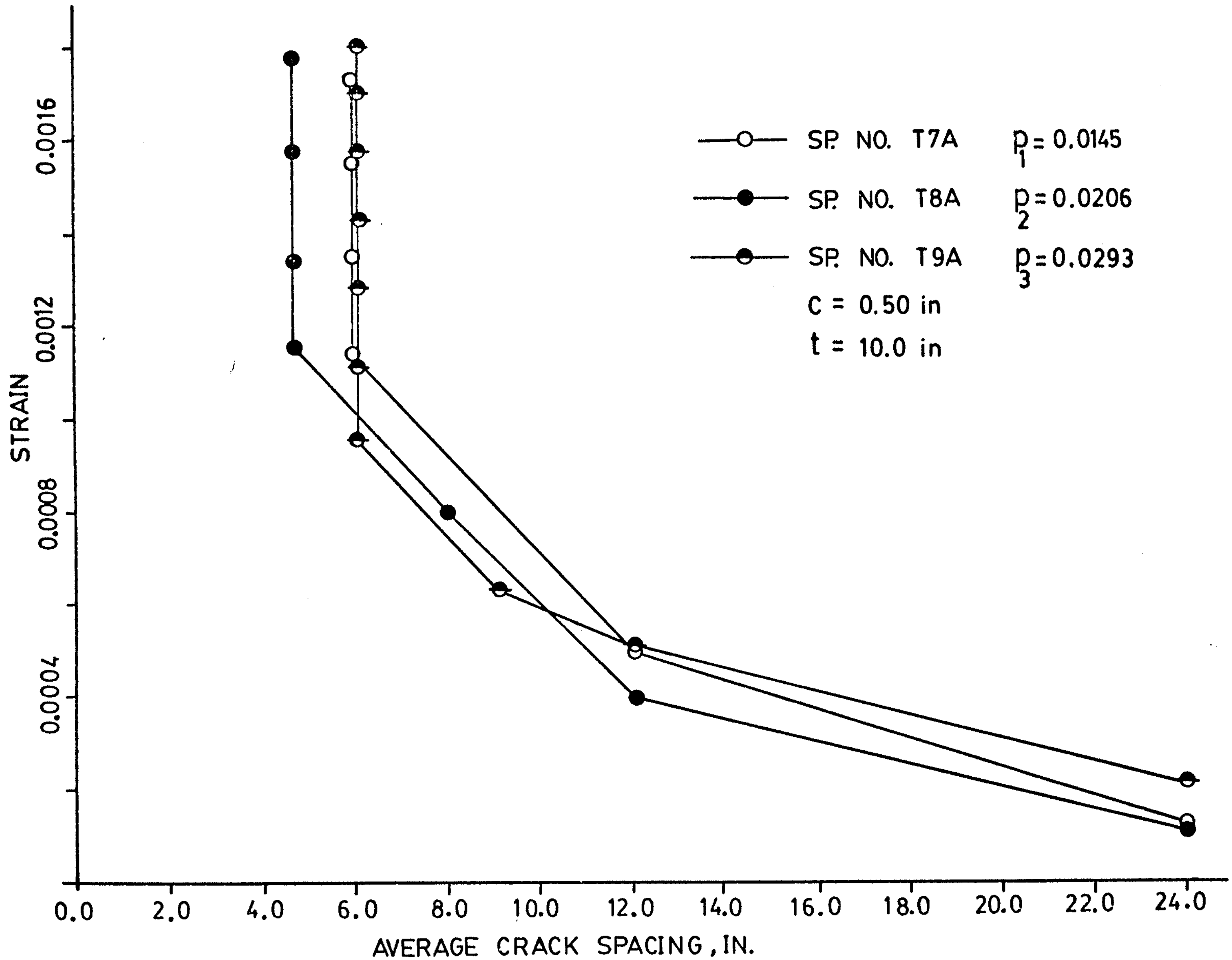

Figure 5.7(c) Effect of Steel Ratio on Crack Spacing

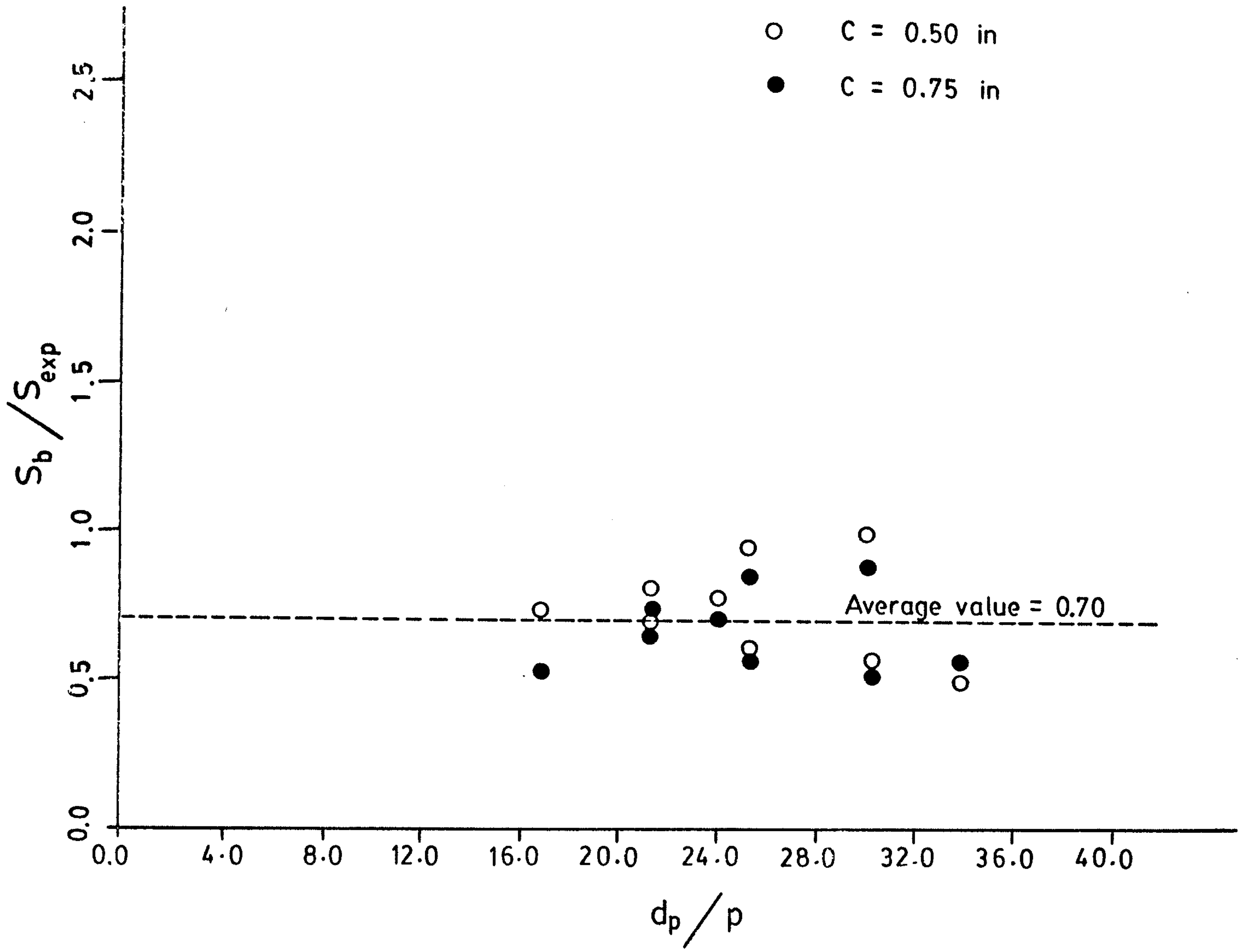

Figure 5.8 Comparison of Measured and Computed Crack Spacing Based on Beeby's Equation

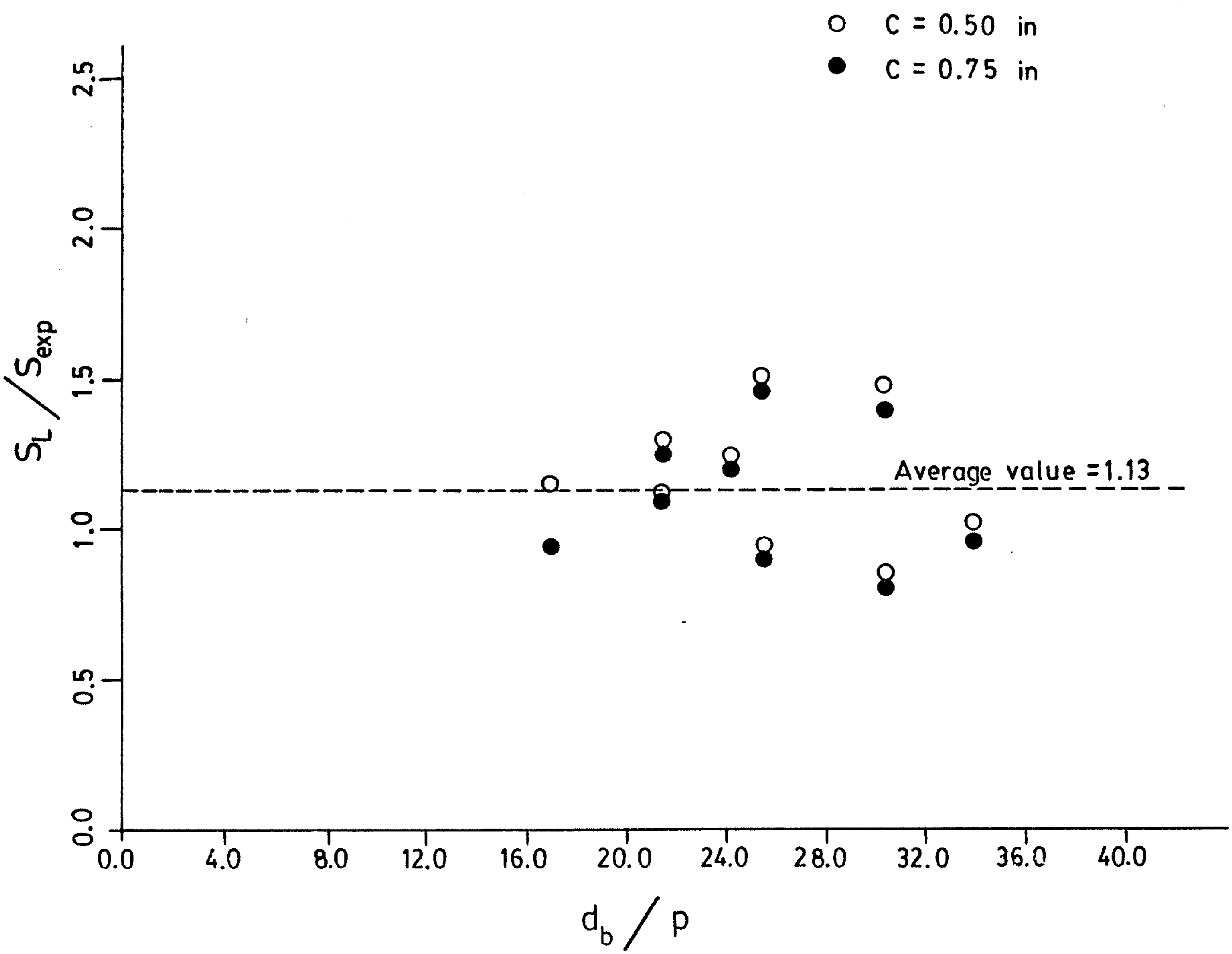

Figure 5.9 Comparison of Measured and Computed Crack Spacing Based on Leonhardt's Equation

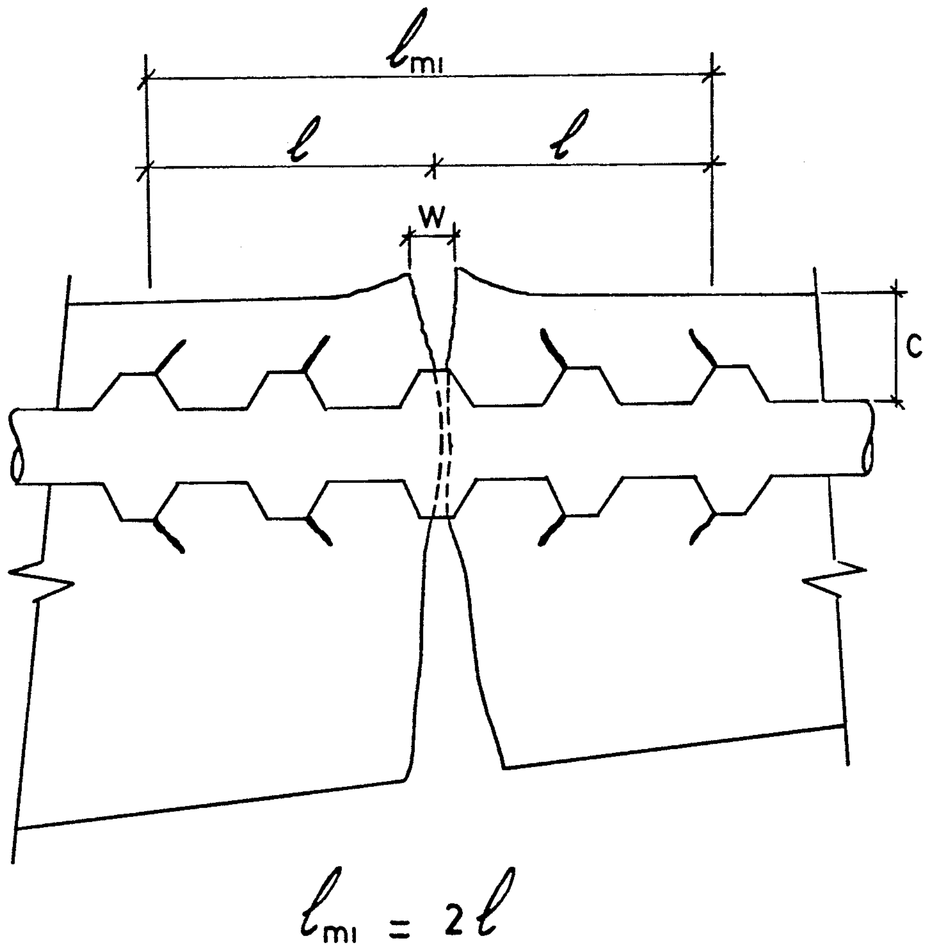

Figure 5.10 Region of "Almost Lost Bond"

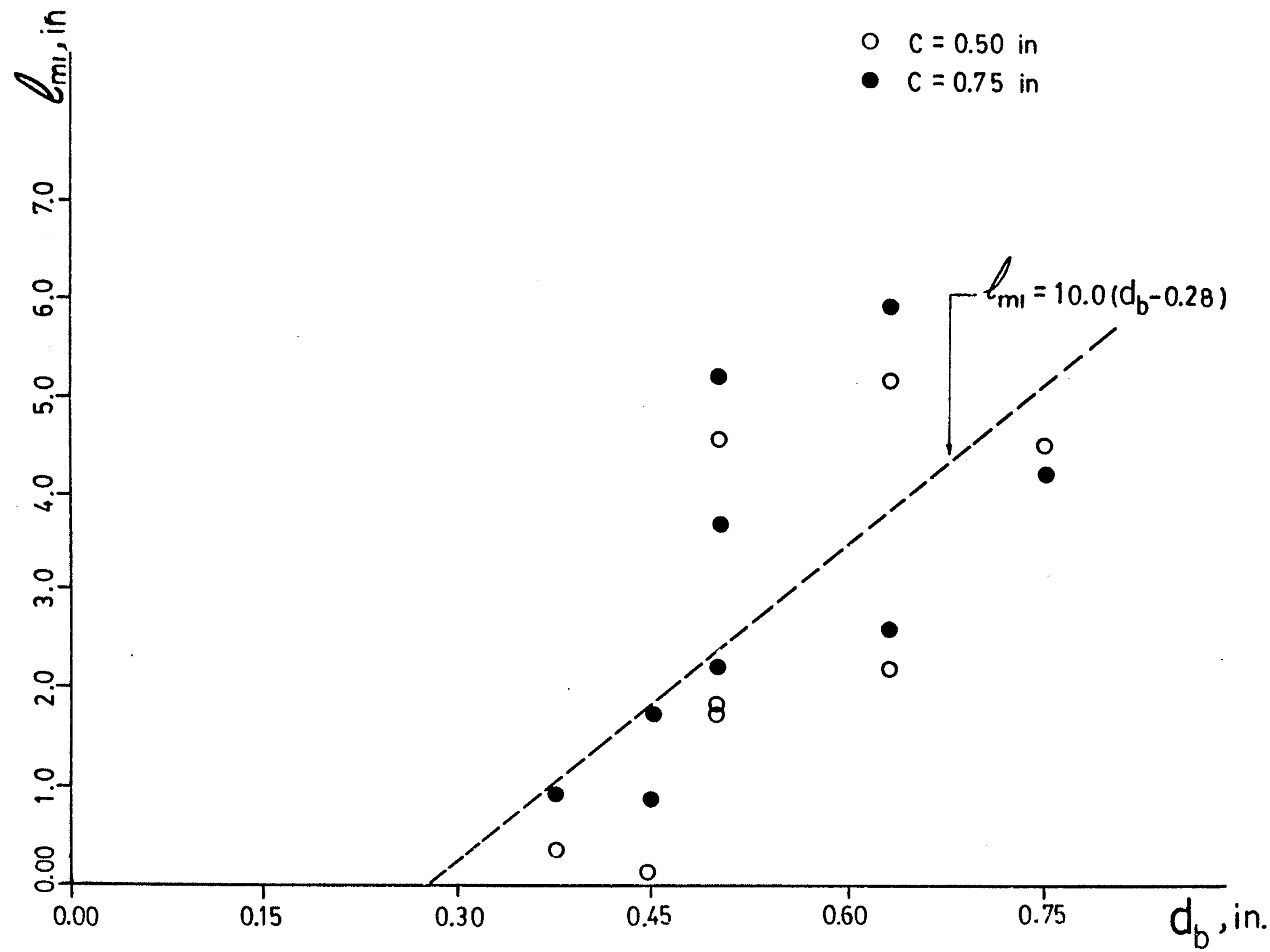

Figure 5.11 Relationship Between the Length of the "Almost Lost Bond" Based on Beeby and Bar Diameter

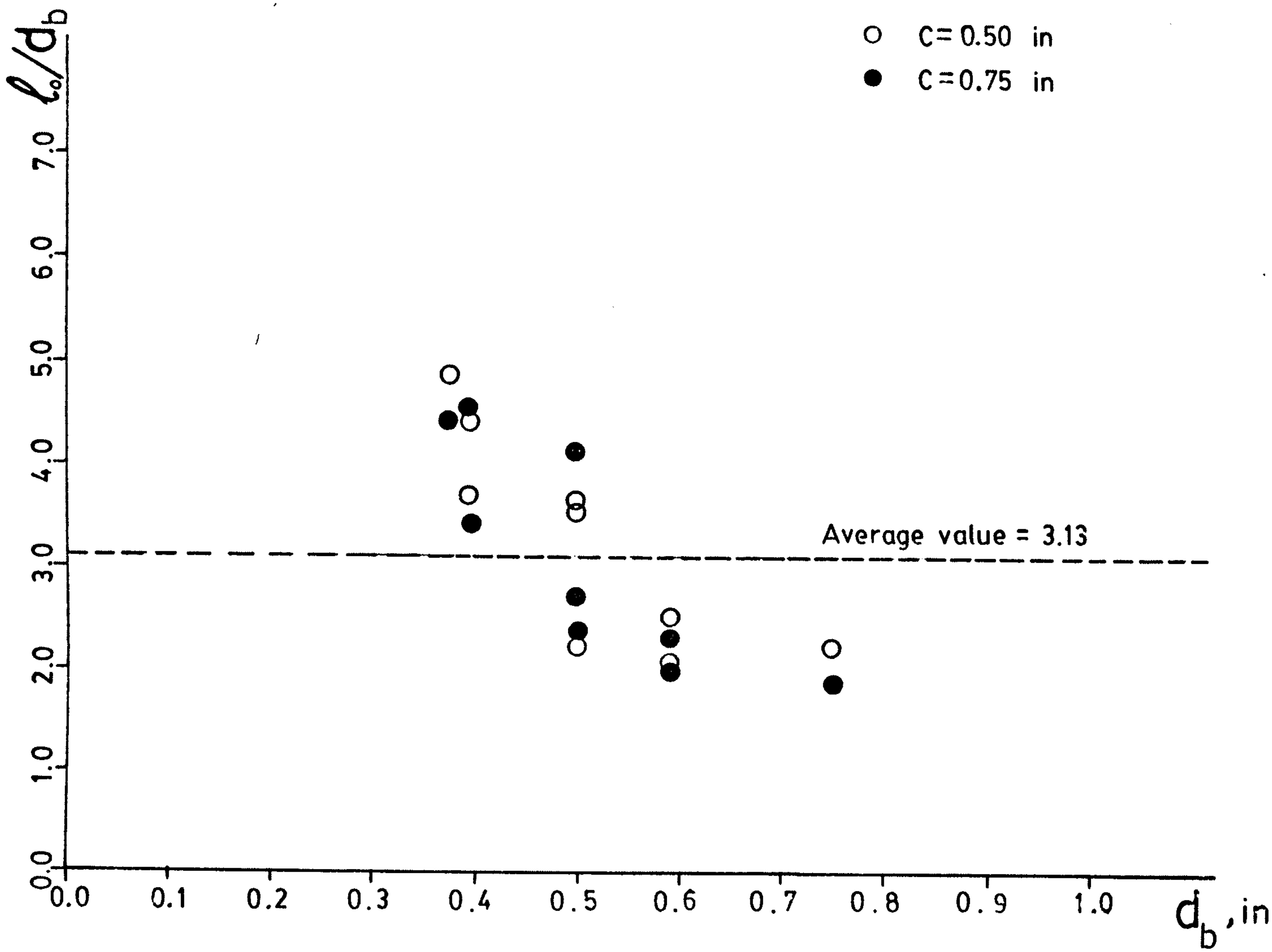

Figure 5.12 Relationship Between the "Almost Lost Bond" Length Based on Leonhardt's Equation and Bar Diameter

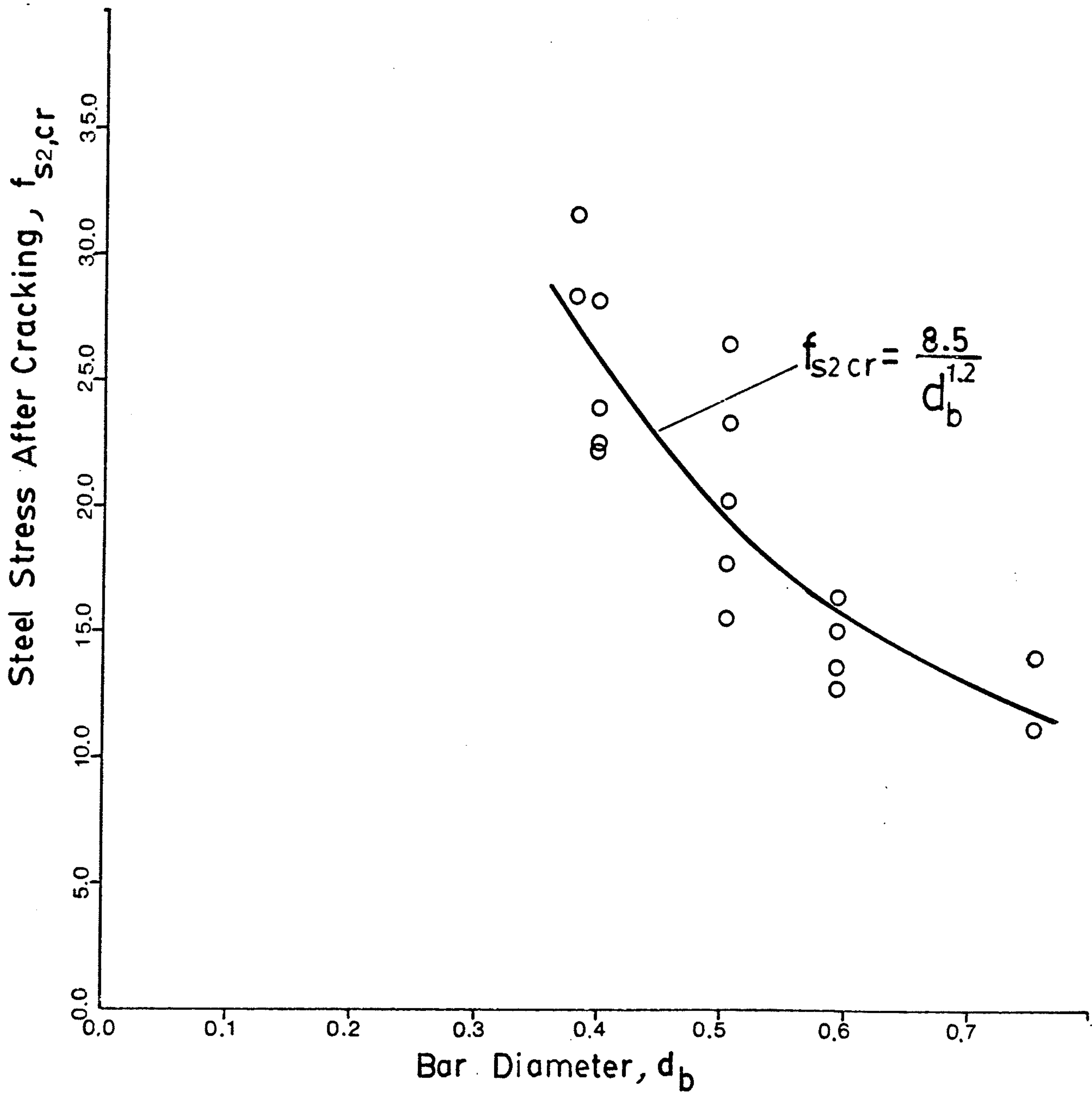

Figure 5.13 Relation Between the Steel Stress Immediately After Cracking and Bar Diameter

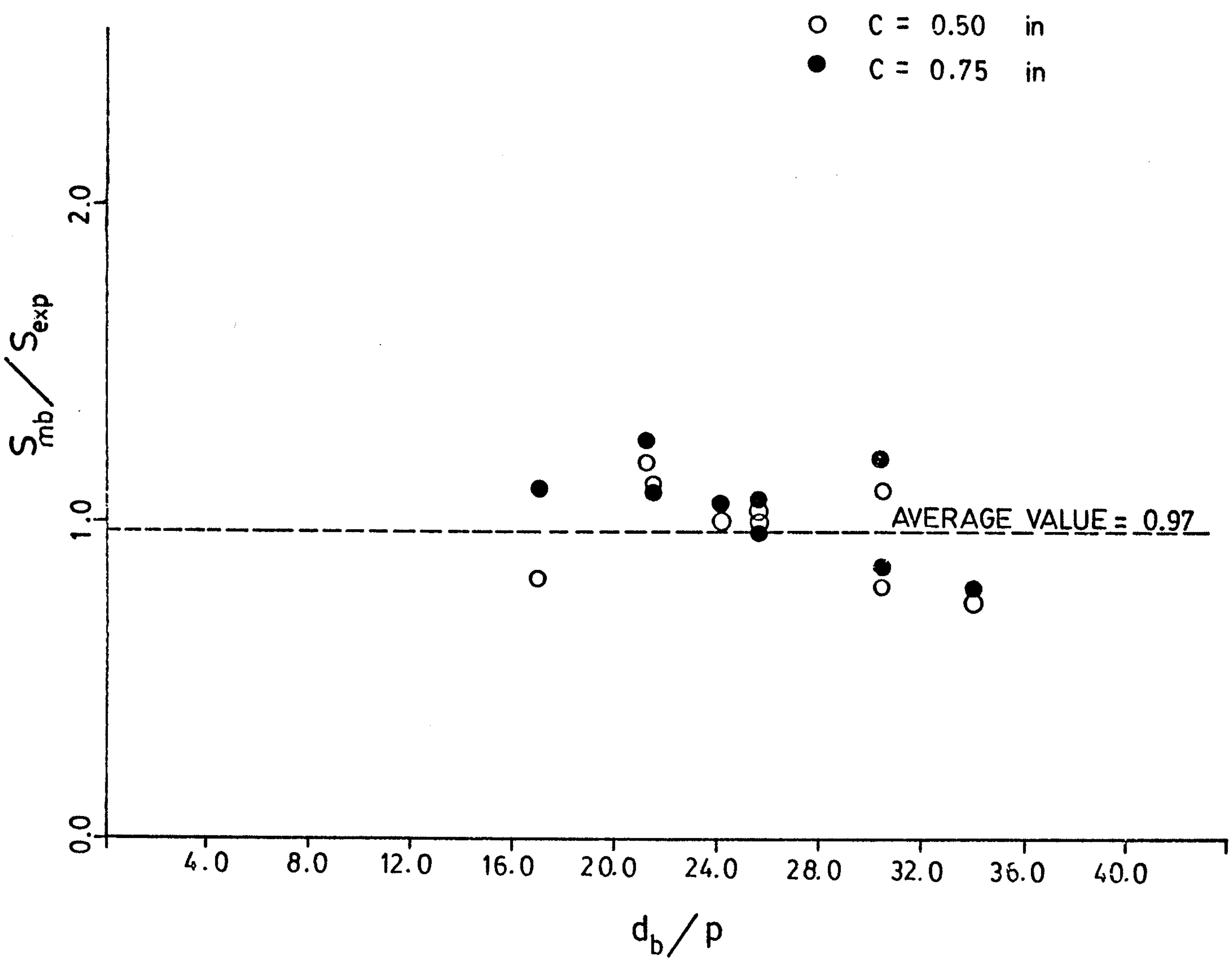

Figure 5.14 Comparison of Measured and Computed Crack Spacing Based on Equation 5.2

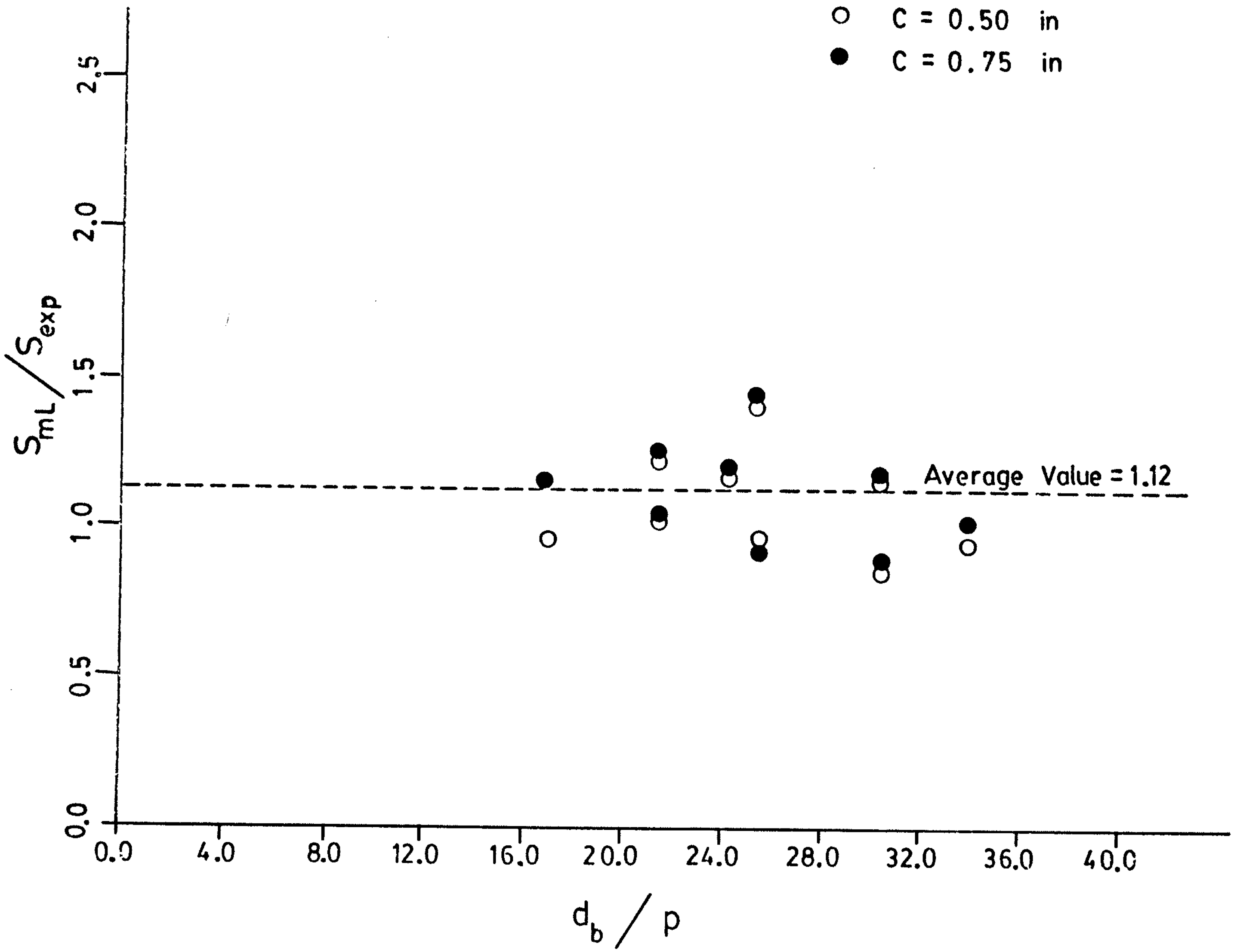

Figure 5.15 Comparison of Measured and Computed Crack Spacing Based on Equation 5.4

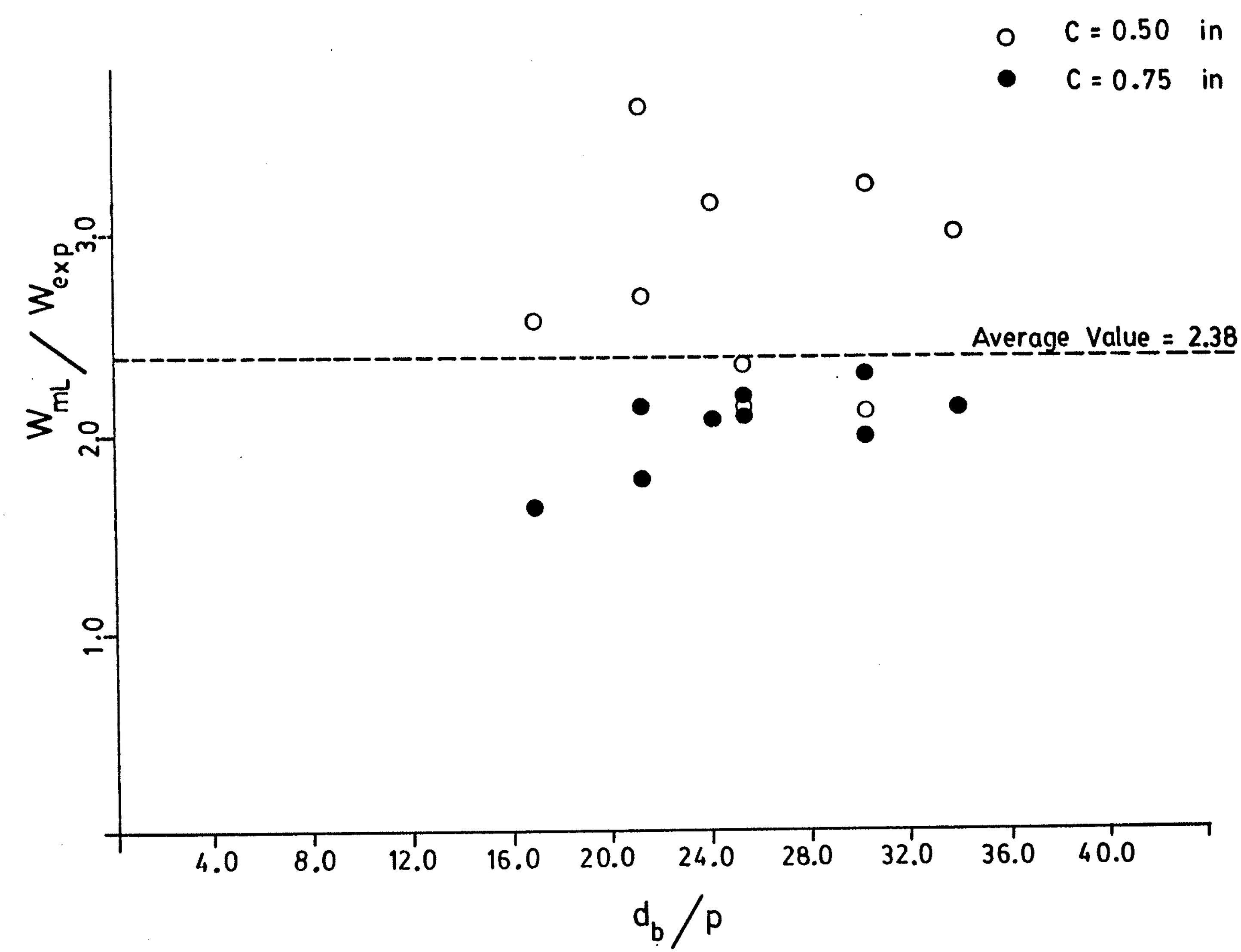

Figure 5.16 Comparison of Measured and Computed Crack Widths Based on Loeonhard't Expression

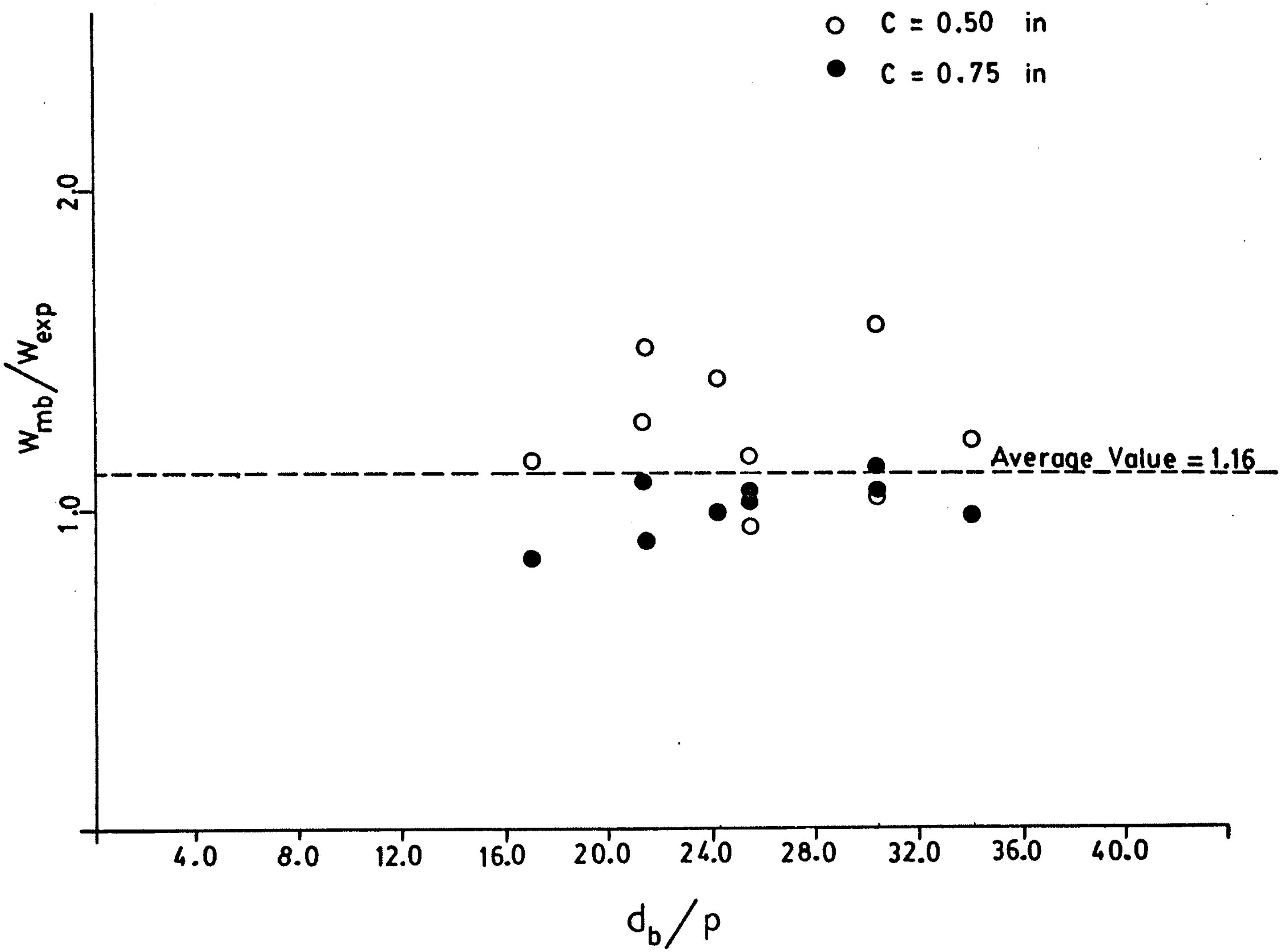

Figure 5.17 Comparison of Measured and Computed Crack Widths Based on Beeby's Expression